



Università
Ca'Foscari
Venezia

PhD in Science and Management of Climate Change
Research Dissertation

**Reconstruction of human-environment interactions
through multi-proxy characterization in
lake sediments from Easter Island/ Rapa Nui
SSD: CHIM/01**

Erhenhi Evans Osayuki: 860427

PhD Program Coordinator

Prof. Enrica De Cian

Supervisor

Prof. Dario Battistel

Co-Supervisors

Prof. Carlo Barbante

“The farther backward you can look, the farther forward you are likely to see.”

- Winston Churchill -

“Our age is not more dangerous – not more risky – than those of earlier generations, but the balance of risks and dangers has shifted. We live in a world where hazards created by ourselves are as, or more, threatening than those that come from the outside.”

- Anthony Giddens -

Table of Contents

List of figures	iv
List of Tables	vi
INTRODUCTION	1
1.0 Background	1
CHAPTER ONE: EASTER ISLAND	3
1.1 The Origin of Easter Island	3
1.2. Rapa Nui colonization	3
<i>The Rapanui oral tradition</i>	4
<i>Heyerdahl's "South American Origin" Hypothesis</i>	4
<i>Flenley and Bahn's Polynesian Origins</i>	5
1.3. The Rapa Nui Civilization	6
<i>The Moai Cult</i>	7
<i>The Birdman Cult</i>	8
1.4 The demise of the Rapa Nui civilization	10
<i>Inter-tribal warfare</i>	11
<i>European Contact</i>	12
<i>Ecocide hypothesis</i>	13
<i>A New Scenario</i>	14
CHAPTER TWO: RAPA NUI CLIMATE AND ENVIRONMENT	18
2.1 Rapa Nui Climate	18
2.2 Modern vegetation.....	19
Prehistoric agriculture.....	20
2.3 Rapa Nui Sedimentary records.....	20
Earlier sedimentary records	20
Recent Records	22
2.4 Research objective.....	25
CHAPTER THREE: PALEOENVIRONMENTAL AND	32
PALEOCLIMATE PROXIES	32
3.1 Paleoclimatology	32
3.2 Climate archives.....	32

3.3 Lake sediment as a climate archive.....	33
3.4 Proxies.....	34
Charcoal.....	35
Polycyclic aromatic hydrocarbon.....	37
Monosaccharide anhydrides.....	40
n-Alkanes.....	42
Fecal sterols.....	44
Geochemical composition.....	45
CHAPTER FOUR: MATERIALS AND METHODS.....	55
4.1 Sediment core and water samples.....	55
<i>Rano Aroi sediment and water sampling.....</i>	<i>55</i>
<i>Rano Raraku sediment and water sampling.....</i>	<i>56</i>
4.2 Instrumental equipment and Sample preparation.....	58
4.3 Biomarker analytical process.....	58
<i>Sample preparation.....</i>	<i>58</i>
<i>Extraction.....</i>	<i>58</i>
<i>Volume reduction.....</i>	<i>59</i>
<i>Sample cleanup and concentration.....</i>	<i>59</i>
<i>Derivatization.....</i>	<i>59</i>
<i>Gas chromatography-mass spectrometry.....</i>	<i>60</i>
<i>Ion chromatography-mass spectrometry.....</i>	<i>60</i>
<i>Quantification.....</i>	<i>61</i>
4.4 Charcoal analytical process.....	63
4.5 multi-elemental analysis.....	63
4.6 Rano Raraku water sample preparation and analysis.....	64
CHAPTER FIVE: RANO RARAKU.....	67
5.1 Rano Raraku age model.....	67
5.2 Results.....	68
<i>Major elements and ions.....</i>	<i>68</i>
<i>Trace Elements.....</i>	<i>70</i>
<i>Rare Earth Elements.....</i>	<i>71</i>
<i>Water isotopic composition.....</i>	<i>73</i>
<i>The Marine Origin of Rano Raraku Water.....</i>	<i>74</i>
<i>Lake level oscillations.....</i>	<i>75</i>
<i>Chloride mass balance.....</i>	<i>76</i>

CHAPTER SIX: RANO AROI.....	78
6.2 Rano Aroi age model.....	78
6.3 Biomarkers and Charcoal	81
<i>Coprostanol (Cop)</i>	81
6.4 Geochemical composition Results	86
Trace and major elemental	86
Rare earth elements	90
Elemental ratios	93
6.5 Geochemical composition Record	95
<i>Phase 1 (1st century - 1090 CE)</i>	95
<i>Phase 2 (1090 -1400 CE)</i>	96
<i>Phase 3 (1400 -1520 CE)</i>	97
<i>Phase 4 (1520 - 1710 CE)</i>	98
<i>Phase 5 (1710 -1790 CE)</i>	98
<i>Phase 6 (1790 - 1900 CE)</i>	99
<i>Phase 7 (1900 CE - Present)</i>	99
6.6 DISCUSSION	101
Conclusions:.....	104
ABSTRACT.....	109
ABSTRACT (ITALIAN VERSION).....	110

List of figures

Figure 1.1: Satellite image of Easter Island, position, and coordinate (source: European space agency)

Figure 1.2: Satellite image of Easter Island, position, and coordinate (source: European space agency)

Figure 1.3 : (A) skeletal sketch of the hare paenga, foundation blocks, and paved terrace without the thatched roof. (B) the foundation of the Peanga (C) agricultural protection structure (D) hara moa, a structure where chickens were kept (E) Curbstones

Figure 1.4: (A) Ahu Nau Nau with a topknot, (B) Ahu Ko Te Riku, with open pupils with a facial expression, (D) Fallen Moai topknots (Pukao) in the foreground; behind, moai are overthrown face-down. (E) Ahu Tongariki, one of the largest Ahu, with 15 Moai

Figure 1.5: View of the three islets (Motu Nui, Motu Iti, and Motu Kau Kau) where the athletes should obtain the eggs of the sooty tern (Photo: Rull 2016)

Figure 1.6: The ceremonial City of Orongo at the southwest rim of the Kao crater (photo: Rull 2018)

Figure 1.7: Images of mata'a from Easter Island (from collections at the P. Sebastian Englert Museum, Rapa Nui) (photo: Lipo 2016)

Figure 2.1: different pollen types from Easter Island, (Rano Aroi) pollen 1 to 6) while (pollen 7 and 8 (Rano Raraku) (1) Unknown species, (2) Poaceae, (3) Cyperaceae, (4) Compositae, (5) Polygonum, (6) Triumfetta, (7) and (8) Verbena litoralis [22].

Figure 3.1: Temporal resolution and time span of marine and continental climate archives (in a geologic time plotted in log scale by the power of 10)

Figure 3.2: Figure 3.1: Formation of lacustrine sediments: controlling factors and processes (figure: Zolitschka 2015)

Figure 3.3. Diagram demonstrating the sources of primary and secondary charcoal (Figure: Whitlock and Larsen (2001)

Figure 3.4. Macroscopic charcoal particles (arrow) left after washing sediment through a 250µm screen (figure: Whitlock and Larsen (2001))

Figure 3.5 Cellulose, hemicellulose, and lignin structures (figure: Rubin 2008)

Figure 3.6. Structures of monosaccharide anhydride; Levoglucosan (1), mannosan (2), and galactosan (3).

Figure 3.7. Formation of levoglucosan through decomposition of cellulose (figure: Simoneit (1999))

Figure 3.8. structure of coprostanol and epicoprostanol

Figure 3.9 Microbial reduction of fecal in the intestinal and environment (figure: Sistiaga 2014)

Figure 4.1. Present day images of the lake Rano Raraku (a), and Rano Aroi (b)

Figure 5.1 Images of the Rano Raraku sediment core showing a mixture between old and young sediment (reservoir effect) between 0.2 m and 0.6 m 1

Figure 5.2. Ce/Ce* and LREE/HREE mean ratios with standard deviation in the considered matrices

Figure 5.3 Isotopic composition of rainfalls in Easter Island (black dots; from Herrera and Custodio 2008) and Rano Raraku water in 2007 (red dot). Mean meteoric water line (blue), rainfalls best fit (black line), and straight-line derived from evaporation mode

Figure 5.4 Rano Raraku water level, from 1 m to almost completely dry in few months. (a) 7 September 2017, (b) 25 January 2018, (c) 3 March 2018

Figure 6.1. Rano Aroi age-depth chronology based on ^{14}C ages (A) MCMC iterations showing distribution of stationary; (B) green curve and grey histogram for the accumulation rate; (C) green curve and grey histogram for memory distribution; (D) Calibrated ^{14}C dates (transparent blue) and the depth-age model (darker greys indicate more likely calendar ages, grey stippled lines indicates 95% confidence intervals) (figure: Roman 2021)

Figure 6.2 Rano Aroi sediment core (LTS-AROI17-1A and parts LTS-AROI17-1B (bottom)) with Depth (right) and calibrated radiocarbon ages (right)

Figure 6.3 Coprostanol flux in Rano Aroi with moving average (lowess smoothing 5 points)

Figure 6.4. Levoglucosan fluxes ($\text{ng cm}^{-2} \text{ yr}^{-1}$) in Rano Aroi core with moving average (lowess smoothing 5 points)

Figure 6.5. charcoal fluxes ($\text{cm}^{-2} \text{ yr}^{-1}$) in Rano Aroi core with moving average (lowess smoothing 5 points)

6.6 n-alkane indices indicating change in vegetation with moving average (lowess smoothing 5 points)

Figure 6.7 biomarkers and charcoal flux from Rano Aroi sedimentary core, showing 4 phase of phase of environmental changes in the island

Figure 6.8 (A) Dendrogram obtained by hierarchical cluster analysis using the Euclidean distance and Ward's method. Principal component bi-plot: PC1 vs PC2 (B) and PC3 vs PC4 (C) [8] 12

Figure 6.9. Temporal evolution of the PCA in the Rano Aroi record, reported in Table 6.3 (Roman et al. 2021)

Figure 6.9 (Gd/Yb)_N plotted vs. (La/Sm)_N. Peat samples at different depths are colored dots

Figure 6.11 Rano Aroi record of the environmental and climatic proxies discussed in this paper: principal

Figure 6.11. Summary of the key paleogeochemical trends from trace elements in Rano Aroi covering the last 2000 years, compared to previous local geochemical/vegetational and regional climate reconstructions

List of Tables

Table 3:1 List of the 19 PAHs considered in this research (source: <https://pubchem.ncbi.nlm.nih.gov/>)

Table 4.1 Samples and sampling locations at Rano Raraku

Table 4.2 Mass to charge ratios and response fact of the biomarkers considered in this study

Table 5.1. Major ions, trace and rare earth elements, isotopic composition, and diagnostic element ratios in water samples from Rano Raraku

Table 5.2. Trace elements in filtered water, suspended matter, and soils from Rano Raraku.

Table 5.4. Rare Earth Elements in filtered water suspended matter and soils from Rano Raraku.

Table 6.1 Rano Aroi sediment core conventional Radiocarbon Age in CRA (years before present).

Table 6.2 Trace and major elements determined in the Aroi sedimentary record (mean, maximum and minimum values), water, and suspended particulate matter (SPM) collected in proximity of the outlet (mean \pm standard deviation). W statistics and p-values refer to the Shapiro-Wilk (SW) normality test. H0: the null hypothesis of normal distribution is accepted vs. H1: the null hypothesis is rejected. Missing values mark concentrations lower than their respective detection limits.

Table 6.3 Summary of the trends obtained from the principal component analysis in rrom the geochemical composition and corresponding chronological phases, — not significant, ▲ slightly positive ▼, slightly negative.

INTRODUCTION

1.0 Background

The interaction between human and its immediate environment has mainly been driven by the basic needs for human survival and adaptation to a changing environment. The interaction includes but not limited to burning of fossil fuels, pollution, deforestation, overpopulation and exploitation of ecosystem services, such as food, shelter, land, freshwater, medicinal resources and other raw materials that can be beneficial for human well-being [1–5]. Years of human-environmental interaction often lead to environmental modification, which may directly affect ecosystem diversity, global carbon storage, and atmospheric chemistry [6].

Environmental modification (natural and anthropogenic) may lead to many environmental problems and extreme climate events, which can have several negative effects on human society, such as drought, storm, flood, food security, economic and civilization destabilization [7,8]. Many of the above-mentioned environmental problems can be avoided or managed if humans are able to properly understand and differentiate between natural and anthropogenic environmental changes. But differentiating between these changes has been one of the significant challenges in climate and environmental studies. However, a better understanding can be achieved through the study of past human-environmental interaction, and how humans responded and managed past ecological and climate changes [9].

Easter Island (Rapa Nui) has been an ideal location for the study of past human-environment interaction, due to its isolation and puzzling history of the Polynesian civilization. Several archaeological and ecological studies has been carried out on the island for decades and it has been generally agreed by the scientific community that humans migrated to the Easter Island, settled and grew in population to an equilibrium point, and later experienced social-ecological collapsed [10,11]. However, the timing of the migration and the cause of the collapse has been a major debate for decades. An expedition led by a Norwegian explorer Thor Heyerdahl in 1947, established human settlement on the island to be ca 400 CE [12]. In 2006, Lipo and Hunt challenged the early human settlement theory by Thor Heyerdahl, stating that radiocarbon dates retrieved from archeological finds suggest initial human arrival to be ~ 1200 CE [13]. Flenley, however assumed the initial human settlement to be between 800 CE to 1200 CE on the ground of radiocarbon dates obtained from fossil pollen core [14].

Different theories have also been proposed relating to the supposed social-ecological collapse of Rapa Nui, own civilization collapse by overexploitation of natura resource, this assumption has been termed the “Ecocide” [15,16]. Others have challenged the overexploitation theory, stating that the collapse was actually a genocide due to the ill treatment suffered by the islanders during the European contact in 1722 CE [17]. The ecocide and the geocide views have been the most popular for decades, and both views suggest that the Rapa Nui social-ecological collapse was caused by anthropogenic activities, while ignoring the potential role of natural climate and environmental change. However, recent Palaeoecological studies have indicated that climate change could have played a significant role in the Rapa Nui civilization collapse [18,19].

Although palaeoecological research on Easter Island has provided a general framework for the deforestation and environmental changes, however, the cause and timing of the deforestation remains inconclusive [20]. This study provides a new look at the environmental evolution of Rapa Nui, through the use multiple proxy analysis from lake sediments to reconstruct different environmental parameters. This method provides information on the timing and possible causes of the social-ecological collapse.

CHAPTER ONE: EASTER ISLAND

1.1 The Origin of Easter Island

Easter Island, hereafter referred to using the indigenous name Rapa Nui is a remote island located in the southern Pacific Ocean about 3700 km from Chile's west coast and 4023 km from east of Tahiti, with coordinate $27^{\circ}09'S$, $109^{\circ}26'W$. The triangular-shaped island (measures at 16, 18, and 22 km respectively, covering roughly 164 km^2 in total) (fig 1.1) was formed by the emergence of three erupted volcanos in 780 kyr, that last erupted between 200 and 110 kyrs ago. *Pito-o-te-Henua* (the end of the world) was the first name of the Island [1], before Tahitian sailors named it Rapa Nui in the nineteenth century, due to its resemblance to a smaller Polynesian island called Rapa (Nui meaning big). In contrast, it was named Easter Island by European explorers who visited the island on easter day in 1722 [2–4].

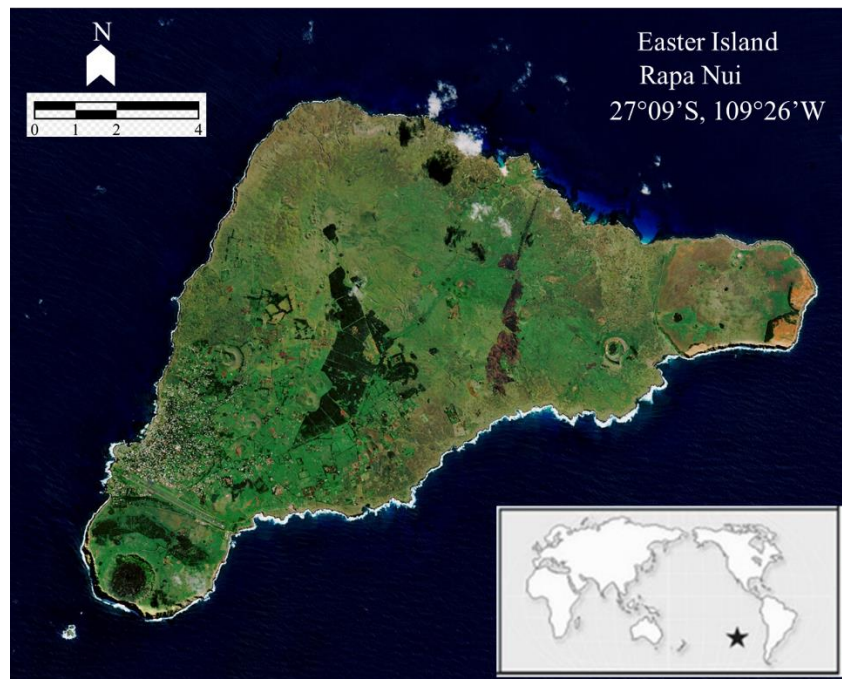


Figure 1.1: Satellite image of Rapa Nui, position, and coordinate (source: European space agency)

1.2. Rapa Nui colonization

The history and geographical origin of the first settlers in Rapa Nui has been extensively debated by scholars, given that the island is positioned between Polynesia to the West, Bolivia and Peru to the East. This debate has been fueled by the mystery of the Rapa Nui culture, which has led to several versions of Rapa Nui colonization, the facts of this debate

are primarily presented through archaeological and ethnological evidences [5]. A brief account of the colonization hypotheses is provided below.

The Rapanui oral tradition

The mystery of the Rapa Nui culture is primarily due to the isolation of the island, which has made the legends and myths of the island very relevant. These myths and Legends that explains the history of the island have been orally conveyed by the natives for thousands of years [6]. However, the Legends may exaggerated by the imagination of the listener or that of the teller, therefore, the historical reconstruction based on these legends falls between fantasy and reality [7,8].

According to the legend of Rapanui, the island was discovered by Hotu Matu'a and a few dozens of companions who migrated from Hiva Island located in East Polynesian [1]. Hotu Matu'a and his passengers emigrated in a boat capable of carrying passengers (between 15 to 20 people) and loads up to 9000 kg, the Polynesians traveled with supplies and domesticated animals such as food, fresh water, dogs, pigs, chickens, and rats. Hotu Matu'a and his passengers landed on *Anakena* beach, located in the northwestern part of the island, before settling near Rano Raraku and began to spread through the island. This colonization history has a different set of details and versions according to whoever tells the story. However, no version of the story has a specific timing of when the Polynesian settlers arrived on the island. But every version of the story agrees on the geographical origin of Hotu Matu'a and his passengers. Hence, the modern Rapanui refer to their culture as that of Polynesian heritage [9].

Heyerdahl's "South American Origin" Hypothesis

A Spanish missionary Joaquín de Zúñiga in 1803 proposed that the wind and the ocean currents favors navigation from South America to Polynesia, and a link between the statues in Rapa Nui and those from South America was established during this period. A Norwegian explorer Thor Heyerdahl used this observation to propose that the prehistoric Native Americans discovered Rapa Nui, before the Polynesians arrived to establish the Rapanui civilization. In 1947, Heyerdahl and five other men launched the famous Kon-Tiki expedition to test Zúñiga's navigation hypothesis. They used only the assistance of the ocean currents

and winds during the expedition, it took them 101 days to navigate from Peru to the Tuamotu Island while using a simple raft with a single sail. After the expedition, Heyerdahl organized a fieldwork to further collect data that supports this theory, during the fieldwork he discovered that some plants in Rapa Nui were of South America origin, such as sweet potato (*Ipomoea batatas*), and bottle gourd [10], he also indicated that some tools found in Rapa Nui is similar to that of South America. With this evidence, Heyerdahl concluded that the natives from South America discovered the island approximately 400 CE before the arrival of the Polynesians [11]. He also connected his hypothesis with the Rapanui legend about a war amongst two groups (short-ear and the long-ears), where short-ear won the war, eliminating their enemies, he depicted the Polynesians as the short-ears [5].

Flenley and Bahn's Polynesian Origins

Flenley and Bahn re-evaluated most evidence presented by Heyerdahl, which supports the discovery of Rapa Nui by the Native American population. They emphasized that the ocean current that supports the navigation from East-West is not constant but seasonal, stating that El Niño phenomenon reverts the ocean circulation every four years [12–14], which indicates an opposite flow that supports West–East navigation, they highlighted that the Polynesians were skilled sailors with high hydrodynamic boats, which is different from the boat used by Heyerdahl for the Kon-Tiki expedition [15]. It was also emphasized that the plants of South America origin found in Rapa Nui could be introduced by the Europeans [16]. Flenley and Bahn stated that Eastern Polynesians from the Marquesas Islands discovered Rapa Nui through Mangareva [12,15]. This observation was made based on pollen reconstructions, using radiocarbon-dating in lake sediments, [1].

1.3. The Rapa Nui Civilization

The structures and buildings erected by the Rapanui represent a significant part of their civilization. These structures comprised shelters (*hare paenga*), agricultural protective walled gardens (*manavai*), a ceremonial platform (*ahu*), ground ovens/cooking pits (*umu*), and a sophisticated chicken coop (*hare moa*). The hares inhabited by the islanders could be used to identify their societal status; a practice similar to the aristocracy commonly associated with Polynesians. In this practice, the nobility lived in shelters called hare Paenga which can house between 5 and 16 people. The paenga had the shape of an upside-down canoe with an average length of 15 m, the foundation was made with an elliptical hard basalt stone base, carved into the ground up to 30 to 100 cm, a woody structure made of Toromiro branches is then inserted in a hole cut in the basalt stones, the poles from the Toromiro wood are then joined and tied together at the top with a long ridge pole to form the shape of an upside-down canoe, then structure of the paenga protects it against strong winds [17,18]. Chickens were an essential asset for the Rapanui, hence chicken coops (*hare moa*) were built all over the Island to monitor the chickens properly [19].

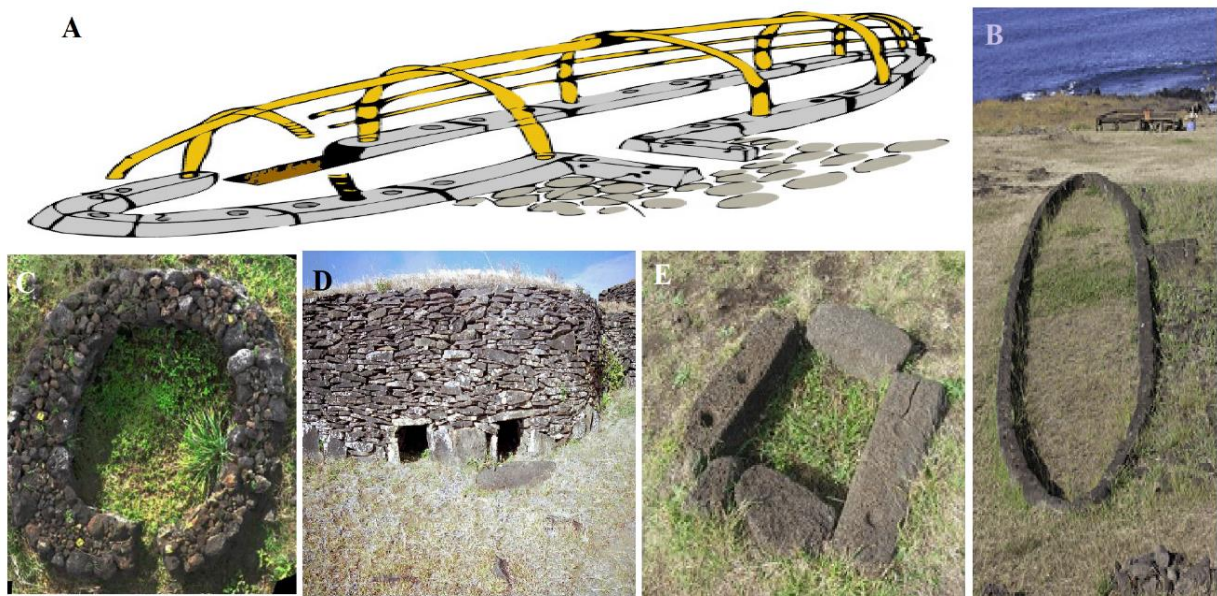


Figure 1.2:(A) skeletal sketch of the hare paenga, foundation blocks, and paved terrace without the thatched roof. (B) the foundation of the *Peanga* (C) agricultural protection structure (D) *hara moa*, a structure where chickens were kept (E) Curbstones (*paenga*) reused to form an earth oven (Melorose 2015) [20]

The Moai Cult

The ancient Rapanui culture is the most interesting feature left in Rapa Nui, it is mainly represented by nearly 1000 documented statues (*Moai*) [21], a carved stone of heads and upper body, primarily in the form of human male. The height of these statues ranges from 2 m to 10 m, the heaviest that was erected in the island stands at 80 metric tons. However, archaeologists found an incomplete *Moai* that would weigh between 145 tons and 165 tons and would have been roughly 21 meters tall if it had been completed. A large amount of *Moai* were made on the Raraku crater from several volcanic stones, they were mainly cut with the bedding of the tuff, while few were cut perpendicular to the bedding, with a carving tool (*Toki*) made from basalt. 17 *Moai* were made from red scoria, 13 from basalt, and 22 from trachyte [22,23]. About 500 were transported across the rough landscape up to 18 km distance, before they were mounted on a raised stone platform (*Ahu*) close to the coast (fig. 1.3 C, E), 62 *Moais* were seen abandoned on the roadway during transportation, some have a unique feature in the form of topknot stone made of red scoria (*Pukao*) (fig. 1.3 A, B), [18,24].

In 1978, archaeologist Sonia Haoa discovered that the *Moais* were initially made with facial expression after fragments of red scoria and white coral were found at the feet of one of the statues during excavation, the red scoria formed the eye of the statue while the white coral formed the pupil, the fixed eyes make it seem like the statue was staring at the sky with a lively facial expression (fig. 1.3 B), Other fragments representing eyes were later found at the foot of some *Moais*, depicting different facial expressions. The carving and transportation of *Moais* required a large population, corresponding labor force, and significant use of natural resources, such as woods and trees utilized as rollers in transportation [25,26]. The main activities and early civilization of the Rapanui revolved around the carving and transporting *Moais*, which is sometimes referred to as the *Moai* industry; as a matter of fact, they made the statues in the image of their ancestors (chiefs and societal leaders that passed), to physically represent a principal god (*make make*), who is the creator of all humankind and responsible for fertility. The Rapanui people worshiped *make make* through *moai* statues, to ensure the protection of all clans, including the fertility of the soil and sea [17,26], they practiced a dynasty system, the highest authority in Rapa Nui during the *Moai* industry is *Ariki Mau*, he was the chief of *Miru* clan and the direct descent of *make make*.

It is assumed that the production of *Moai* ended due to limitation of natural resource, because logs of woods were needed for the transportation of *Moai* across the island. The Rapanui needed to stop the production in order to preserve resources, which led to the end of the *Moai* industry [17].



Figure 1.3: (A) Ahu Nau Nau with a topknot, (B) Ahu Ko Te Riku, with open pupils with a facial expression, (D) Fallen *Moai* topknots (*Pukao*) in the foreground; behind, moai are overturned face-down. (E) Ahu Tongariki, one of the largest *Ahu*, with 15 *Moai* standing on it (photos from Gioncada 2010; and DiNapoli 2019) [19,24].

The Birdman Cult

The disappearance of the *moai* cult was followed by the introduction of the birdman cult, which restructured the religious, social, and political beliefs of the Rapanui people [27]. The cultural center was moved from Rano Raraku to *Orongo*, a city situated on the southwest rim of the Kao crater. The highest authority in the Island was no longer given to the direct descendant of *make make* in the birdman era; instead, the warriors (*matato'a*) from different clans had to compete for the position of the birdman; the event was carried out yearly in the village of *Orongo* during the Austral spring, through an athletic contest including running down the cliffs in Rano Raraku crater, then swim to *Motu Nui* and return to the islet to take the sooty tern's first egg, whoever wins the contest is said to be the physical representation of *make make*, he then becomes the birdman (*Tangata Manu*) also the highest authority in the Rapanui society for a year [9]. The timing at which the Rapa Nui shifted from the *Moai* Cult

to the Birdman Cult has been primarily based on oral tradition, which may have been inaccurate due to biases and historical distortions [28]. radiocarbon ages between 1,540 and 1,576 CE were derived from the first excavation of a house in *Orongo* by Thor Heyerdahl (Norwegian explorer) [11]. This dating refers to the beginning of room construction in *Orongo*. However, the ages have been deemed inaccurate due to the lack of accurate sample descriptions and questionable stratigraphic correlations [3]



Figure 1.4: View of the three islets (Motu Nui, Motu Iti, and Motu Kau Kau) where the athletes should obtain the eggs of the sooty tern (Photo: Rull 2016) [9].



Figure 1.5: The ceremonial City of *Orongo* at the southwest rim of the *Kao crater* (photo: Rull 2018) [3].

1.4 The demise of the Rapa Nui civilization

The elusive history of the Rapa Nui and its supposed social-ecological collapse has been the interest of researchers over the last decades, the researchers interest is mainly to understand cause of the collapse, from the once-thriving society to a treeless landscape. However, the cause of the collapse is not well understood, as the existing knowledge of the island has several controversial interpretations. the most popular interpretations include Ecocide, which represents civilization collapse as a result of overexploitation of natural resource by the islanders. A contrasting interpretation of the Rapa Nui social-ecological collapse has been termed the Genocide, which represents the ill treatment, suffered by the Rapanui when the Europeans visited island in 1722, however studies has suggested that the Rapa Nui already had already experienced population decline before the arrival of Europeans in 1722 [29]. Different models have also been carried out to explains the Rapa Nui.

Below is a brief discussion of Rapanui population and social-ecological dynamics and a list of proposed hypotheses from different research.

Inter-tribal warfare

One of the persistent narratives about the Rapa Nui social-ecological decline is the internal warfare between clans of Rapanui due to scarce resources on the island [30,31]. The warfare hypothesis is only supported by oral records documented in the twentieth century. However, it lacks proper scientific evidence of warfare, such as defensive structures and lethal trauma on human skeletal materials, which is common on the Pacific islands known for traditions of warfare [32,33]. One of the empirical pieces of evidence used to support the prehistoric conflict hypothesis is the abundance of *mata'a* found on the island. *Mata'a* is an obsidian tool with wide blades and narrow stems, like the relics found on other Polynesian islands like Hawai'i, New Zealand, Chatham Island, and Pitcairn. The general 'spearhead' form, combined with historic visitor suppositions has led some researchers to believe that *mata'a* were weapons [31,34]. However, Lipo and Hunt investigated the shapes and variability of the *mata'a* that were found on Rapa Nui and noted that *mata'a* are not fatal as other rocks on Rapa Nui. Lipo and Hunt also stated that rock-throwing was the Rapanui primary lethal weapon, when they had conflict with the Europeans. They concluded that the Rapanui used *mata'a* for cultivation and domestic activities due to the shapes and their reoccurrence in rocks. However this conclusion does not suggest that the Rapanui clans did not experience any form of internal violence, but *mata'a* was not used as a systemic lethal weapon, because there is no evidence that supports the use of *mata'a* as a deadly weapon [33].

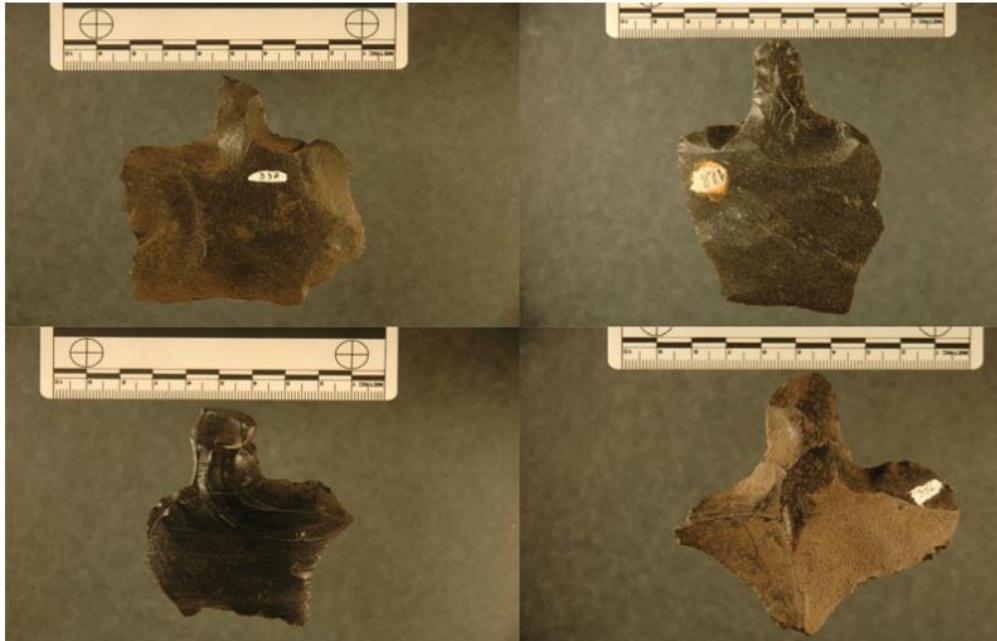


Figure 1.6: Images of mata'a from Rapa Nui (from collections at the P. Sebastian EnglertMuseum, Rapa Nui) (photo: Lipo 2016) [33]

European Contact

An archaeologist, Van Tilburg, who had researched *Moai* for long, indicated that the European visit to Rapa Nui had an adverse effect on the natives. In her report, she stated that the Rapanui were doing fine and still practicing the *Moai* cult at the time Jacob Roggeveen and his crew arrived on the island on Easter Day, on 5th day of April 1722 [35]. Van Tilburg's report coincides with the description of Rapanui by Roggeveen's crew, they described Rapanui as muscular, well-proportioned, tall, and friendly, with a familiar ritual in which the islanders knelt before *Moai* and bowed their heads to offer prayers. The crew also noted that the Rapanui people had an array of agricultural foodstuffs traded with explorers [27]. However, James Cook's observed during his visit to the island in 1774, that the islanders were relatively few and miserable, with poor technological and social-ecological skills [36]. James Cook, in his report, wondered how the islanders were able to develop such advanced civilization represented by *Moai*. He wrote: "*We could hardly conceive how these islanders, wholly unacquainted without any mechanical power, could raise such stupendous figures, and afterward place the large cylindrical stones, upon their heads*" [9]. La Pérouse, who visited Easter Island in 1786, noted a significantly low population, he stated that some islanders were hiding in caves, there was little fresh food on the island, and they were

practicing the birdman culture. La Pérouse also observed that most of the statues on the island have been pushed over. He then proposed the cultural collapse hypothesis represented by deforestation and the disappearance of the *Moai* cult [36–38][14]. Furthermore, a study was carried out on the skeletal remains of almost 500 people dating to late ancient historic, and early historic phases, suggested that a venereal disease, most likely syphilis, was introduced by Europeans to the islanders. The study also stated that some Rapanui were removed from the Island In 1862 and forced into slave labor in Chile which drastically reduced the Rapa Nui population [35]. In 1722, Roggeveen estimated the Rapa Nui population to be thousands, the population was estimated to be about 3000 by Gonzalez in 1770. Forster estimated the population to be 900 with only 50 women in 1774, and the population is said to have been reduced to 110 by 1877 according to McCall [39]. Anderson, who was a hunter, stated that the Europeans also introduced invasive animals such as goats, cows, pigs, horses and rabbits, which contributed to the destruction of the island. he stated that the Rapanui could not protect their valuables from the beasts [35,40]. This hypothesis argued that things changed for the Rapanui shortly after their encounter with the Europeans in 1722.

Ecocide hypothesis

The ecocide hypothesis was proposed by a French explorer La Pérouse and it was popularized by Jared Diamond in 2005, after publishing a book called *collapse*. In the book, Diamond described how the overuse of natural resources by the Rapanui led to the island's social-ecological decline. His hypothesis was primarily based on palaeoecological evidence. And he named it the ecological self-destruction “ecocide”, comparing the ancient Rapanui scenario to the current global climate and environmental crisis [41].

In April 1786, the French explorer La Pérouse visited Rapa Nui for a single day and stated that the Rapanui had the imprudence to cut down all the trees on the island. He indicated that the island became almost uninhabitable as the loss of trees exposed the landscape to direct sunlight, which led to desiccated streams and dilapidation of the island. La Pérouse then proposed the civilization collapse hypothesis by implying that the unfortunate situation of the Rapanui was a direct result of the carelessness of their ancestors [9,41]. Diamond on the other hand, tells a similar story after years of modern-day research, claiming that the Rapanui experienced population growth for hundreds of years and peaked at 15000 [42], until the islanders began to cut down the trees faster than it can grow. He noted that the trees were

used as wood to build houses, canoes, fuel, and transportation of *Moai* across the island from the crater of Raraku to the coast where they were mounted on a raised stone. The islanders eventually ran out of woods and ropes to transport *Moai* across the island due to the disappearance of the forest. Diamond concluded that life became more complex for the islanders, which eventually caused the civilization to collapse [31].

A New Scenario

The ecocide hypothesis is a direct presentation of how a society can experience collapse through overexploitation of natural resources. The hypothesis was based on total exhaustion of natural resource by humans, which eventually led to the demise of the Rapa Nui civilization. However, more records have emerged from recent studies, which led researchers to challenge the 'ecocide' hypothesis. The hypothesis is based on sedimentary record with an extended gap encompassing an important deforestation phase of about 3 millennia. This indicates that the supposed rapid deforestation might be due to lack of continuous records [43]. Studies have indicated that it took about 400 years for the Rapa Nui deforestation to be fully completed (1250 to 1650 AD), this signifies growth in population while resources gradually decrease over 400 years, until the islanders reached unsustainable number [44]. The population size as stated by Diamond [42], is still questionable as there is no evidence that the Rapa Nui population grew to 1500 or more at its peak [29,31,41]. Archeological studies estimated the population size to be between 3000 and 9000 at its peak. Other studies also indicated that the islanders were already experiencing population decline before European contact in 1722. However, the arrival of the Europeans might have worsened the situation of the already declining population which were going through the continuous stress of adaptation [29,45].

Reference

- [1] V. Rull, Human discovery and settlement of the remote easter island (Se pacific), *Quaternary*. 2 (2019). <https://doi.org/10.3390/quat2020015>.
- [2] D. Mann, J. Edwards, J. Chase, W. Beck, R. Reanier, M. Mass, B. Finney, J. Loret, Drought, vegetation change, and human history on Rapa Nui (Isla de Pascua, Easter Island), *Quat. Res.* 69 (2008) 16–28. <https://doi.org/10.1016/j.yqres.2007.10.009>.
- [3] V. Rull, E. Montoya, I. Seco, N. Cañellas-Boltà, S. Giralt, O. Margalef, S. Pla-Rabes, W. D’Andrea, R. Bradley, A. Sáez, CLAFS, a Holistic climatic-ecological-anthropogenic hypothesis on Easter Island’s deforestation and cultural change: Proposals and testing prospects, *Front. Ecol. Evol.* 6 (2018) 1–12. <https://doi.org/10.3389/fevo.2018.00032>.
- [4] J. Flenley, P. Bahn, *The Enigmas of Easter Island*, Oxford University Press, UK, 2003. <https://books.google.com/books?id=PtKSlp4X3oMC>.
- [5] H. Martinsson-Wallin, S.J. Crockford, *Early settlement of Rapa Nui (Easter Island)*, 2001. <https://doi.org/10.1353/asi.2001.0016>.
- [6] Zuzanna Jakubowska-Vorbrich, *Legends and Traditions of Easter Island*, (1975).
- [7] M.A. Mulrooney, C.M. Stevenson, S. Haoa, *The myth of A D. 1680 new evidence from Hanga Ho’onu Rapa Nui (Easter Island)*, (2021).
- [8] S. Rjabchikov, *The Ancient Astronomy of Easter Island : Aldebaran and the Pleiades*, 14 (2015) 1–28.
- [9] V. Rull, Natural and anthropogenic drivers of cultural change on Easter Island: Review and new insights, *Quat. Sci. Rev.* 150 (2016) 31–41. <https://doi.org/10.1016/j.quascirev.2016.08.015>.
- [10] A.G. Ioannidis, J. Blanco-portillo, K. Sandoval, E. Hagelberg, J.F. Miquel-poblete, J.V. Moreno-mayar, J.E. Rodríguez-rodríguez, C.D. Quinto-cortés, K. Auckland, T. Parks, K. Robson, A.V.S. Hill, M.C. Avila-arcos, A. Sockell, J.R. Homburger, Native American gene flow into Polynesia predating Easter Island settlement, *Nature*. 583 (2020). <https://doi.org/10.1038/s41586-020-2487-2>.
- [11] THOR HEYERDAHL, *AMERICAN INDIANS IN THE PACIFIC The Theory behind the Kon-Tiki Expedition*, (1952).
- [12] J.R. Flenley, S.M. King, Late Quaternary pollen records from Easter Island, *Nature*. 307 (1984) 47–50. <https://doi.org/10.1038/307047a0>.
- [13] J.R. Flenley, Further Evidence of Vegetational Change on Easter Island, *South Pacific Stusy*. 16 (1996) 135–141.
- [14] J.R. Flenley, P. Bahn, Conflicting views of Easter Island, *Rapa Nui J.* 21 (2007) 11–13. http://islandheritage.org/wordpress/wp-content/uploads/2010/06/RNJ_21_1_Flenley_Bahn.pdf.
- [15] J. Flenley, K. Butler, P. Bahn, Respect versus contempt for evidence: Reply to Hunt and Lipo, *Rapa Nui J.* 21 (2007) 98–104.

- [16] J.R. Flenley, Further Evidence of Vegetational Change on Easter Island History of Easter Island View project Classifynder View project, 1996. <https://www.researchgate.net/publication/38407638>.
- [17] V. Rull, Contributions of paleoecology to Easter Island's prehistory: A thorough review, *Quat. Sci. Rev.* 252 (2021) 106751. <https://doi.org/10.1016/j.quascirev.2020.106751>.
- [18] C.P. Lipo, T.L. Hunt, Mapping prehistoric statue roads on Easter Island, (2005). <https://doi.org/10.1017/S0003598X00113778>.
- [19] R.J. DiNapoli, C.P. Lipo, T. Brosnan, T.L. Hunt, S. Hixon, A.E. Morrison, M. Becker, Rapa Nui (Easter Island) monument (ahu) locations explained by freshwater sources, *PLoS One.* 14 (2019) 4–6. <https://doi.org/10.1371/journal.pone.0210409>.
- [20] J. Melorose, R. Perroy, S. Careas, An archaeo, *Statew. Agric. L. Use Baseline* 2015. 1 (2015).
- [21] J. Van Tilburg, L. Angeles, A.L. Kaeppler, M.I. Weisler, C. Cristino, Petrographic analysis of thin-sections of samples from two monolithic statues (MOAI), Rapa Nui (Easter Island) PETROGRAPHIC ANALYSIS OF THIN-SECTIONS OF, (2008).
- [22] H. End, E. Albee, *The Complete Guide to Easter Island Inventing ' Easter Island '*, 22 (2008) 66–68.
- [23] S.W. Hixon, C.P. Lipo, B. McMorran, T.L. Hunt, The colossal hats (pukao) of monumental statues on Rapa Nui (Easter Island, Chile): Analyses of pukao variability, transport, and emplacement, *J. Archaeol. Sci.* 100 (2018) 148–157. <https://doi.org/10.1016/j.jas.2018.04.011>.
- [24] A. Gioncada, O. Gonzalez-Ferran, M. Lezzerini, R. Mazzuoli, M. Bisson, S.A. Rapu, The volcanic rocks of Easter Island (Chile) and their use for the Moai sculptures, *Eur. J. Mineral.* 22 (2010) 855–867. <https://doi.org/10.1127/0935-1221/2010/0022-2057>.
- [25] C.P. Lipo, T.L. Hunt, S.R. Haoa, The “walking” megalithic statues (moai) of Easter Island, *J. Archaeol. Sci.* 40 (2013) 2859–2866. <https://doi.org/10.1016/j.jas.2012.09.029>.
- [26] E. Edwards, A. Edwards, *When the Universe was an island: exploring the cultural and spiritual Cosmos of Ancient Rapa Nui*, (2013).
- [27] M.A. Mulrooney, T.N. Ladefoged, C.M. Stevenson, S. Haoa, R. Nui, Empirical Assessment of a Pre-European Societal Collapse on Rapa Nui (Easter Island), *Gotl. Pap. Sel. Pap. from VII Int. Conf. Easter Isl. Pacific Migr. Identity, Cult. Herit.* 11 (2010) 141–154.
- [28] T. Robinson, C.M. Stevenson, The Cult of the Birdman: Religious Change at @_Orongo, Rapa Nui (Easter Island), *J. Pacific Archaeol.* 8 (2017) 88–102.
- [29] G. Brandt, A. Merico, The slow demise of Easter Island: Insights from a modeling investigation, *Front. Ecol. Evol.* 3 (2015). <https://doi.org/10.3389/fevo.2015.00013>.
- [30] J.F. Scott, Reports of the Norwegian Archaeological Expedition to Easter Island and the East Pacific. Vol. II: Miscellaneous Papers, *Hispan. Am. Hist. Rev.* 49 (1969) 522–524. <https://doi.org/10.1215/00182168-49.3.522>.

- [31] J. Diamond, *Collapse*, n.d.
- [32] J.M. Wilmshurst, T.L. Hunt, C.P. Lipo, A.J. Anderson, High-precision radiocarbon dating shows recent and rapid initial human colonization of East Polynesia, *Proc. Natl. Acad. Sci. U. S. A.* 108 (2011) 1815–1820. <https://doi.org/10.1073/pnas.1015876108>.
- [33] C.P. Lipo, T.L. Hunt, R. Horneman, V. Bonhomme, Weapons of war? Rapa Nui mata'a morphometric analyses, *Antiquity*. 90 (2016) 172–187. <https://doi.org/10.15184/aqy.2015.189>.
- [34] J.M. Diamond, *Twilight at Easter*, 2005. <https://doi.org/10.1017/CBO9781107415324.004>.
- [35] P. Rainbird, A message for our future? The Rapa Nui (Easter Island) ecodisaster and Pacific island environments, *World Archaeol.* 33 (2002) 436–451. <https://doi.org/10.1080/00438240120107468>.
- [36] B.J.A. Brander, M.S. Taylor, American Economic Association *The Simple Economics of Easter Island : A Ricardo-Malthus Model of Renewable Resource Use* Author (s): James A . Brander and M . Scott Taylor Source : *The American Economic Review* , Vol . 88 , No . 1 (Mar . , 1998), pp . 11, Source *Am. Econ. Rev.* 88 (2016) 119–138. https://aae.wisc.edu/aae641/Ref/Brander_Taylor_Easter_Island_AER_1998.pdf.
- [37] G.D. Middleton, Nothing Lasts Forever: Environmental Discourses on the Collapse of Past Societies, *J. Archaeol. Res.* 20 (2012) 257–307. <https://doi.org/10.1007/s10814-011-9054-1>.
- [38] V. Rull, Natural and anthropogenic drivers of cultural change on Easter Island: Review and new insights, *Quat. Sci. Rev.* 150 (2016) 31–41. <https://doi.org/10.1016/j.quascirev.2016.08.015>.
- [39] G. McCall, Tradition and Survival on Easter Island, 36 (1994) 153–155.
- [40] T.L. Hunt, C.P. Lipo, Evidence for a shorter chronology on Rapa Nui (Easter Island), *J. Isl. Coast. Archaeol.* 3 (2008) 140–148. <https://doi.org/10.1080/15564890801990797>.
- [41] T.L. Hunt, C.P. Lipo, Revisiting Rapa Nui (Easter Island) “ecocide,” *Pacific Sci.* 63 (2009) 601–616. <https://doi.org/10.2984/049.063.0407>.
- [42] J.M. Diamond, *Collapse : how societies choose to fail or succeed*, Viking, 2005.
- [43] V. Rull, N. Cañellas-boltà, A. Sáez, O. Margalef, R. Bao, Challenging Easter Island ' s collapse : the need for interdisciplinary synergies, 1 (2013) 1–5. <https://doi.org/10.3389/fevo.2013.00003>.
- [44] N. Cañellas-Boltà, V. Rull, A. Sáez, O. Margalef, R. Bao, S. Pla-Rabes, M. Blaauw, B. Valero-Garcés, S. Giralt, Vegetation changes and human settlement of Easter Island during the last millennia: A multiproxy study of the Lake Raraku sediments, *Quat. Sci. Rev.* 72 (2013) 36–48. <https://doi.org/10.1016/j.quascirev.2013.04.004>.
- [45] T.L.H. and C.P. Lipo, *Ecological Catastrophe and Collapse: The Myth of “Ecocide” on Rapa Nui (Easter Island)*, (2011).

CHAPTER TWO: RAPA NUI CLIMATE AND ENVIRONMENT

The present day Rapa Nui vegetation is largely covered by grass and shrubs, with about 5% of recently planted forest [1]. However, it has been generally established that the present-day vegetation is different from the prehistoric Rapa Nui vegetation, which has been estimated to be covered by 80% forest [2,3]. This hypothesis emerges from the earlier palaeoecological studies of lake sediment, which shows an abrupt and removal of palm dominated pollen replaced by grass pollen between 800 and 1200 CE [4]. Recent palaeoecological analysis has rejected the assumption of abrupt removal of palm trees from Rapa Nui, stating that the forest replacement was a gradual process that occurred at a different time and scale.

I discussed the ethnological and archaeological heritage of Rapa Nui in the previous chapter. This chapter will be focused on the Rapa Nui climate and environmental evolution, from a palaeoecological perspective.

2.1 Rapa Nui Climate

Rapa Nui have a subtropical oceanic climate, with an annual temperature that average between 20 and 21 °C, and an average precipitation of 1,200 mm, with approximately 140 rainy days [5]. April to June is more humid with an average rainfall of 120–140 mm/month, the precipitation during this period is due to depression fronts, which results from the migration of the South Pacific Convergence Zone (SPCZ) towards the north, the cyclones storms which is carried by the South Westerlies (SW) and the weakening of South Pacific Anticyclone (SPA). November to January are typically drier months with average rainfall of ~70–90 mm/month, which is mainly facilitated by land-sea breeze [6]. The island have an average annual evapotranspiration between 850 and 950 mm, which is an indication that precipitation-evapotranspiration ratio (PE) is above 1, which means there is no water deficit for the period of a typical year [7]. The precipitation variability from year to year is often high, ranging between 500 and 1800 mm. However, the variability between year-to-year precipitation is highly unpredictable, because there has not been any correlation between annual rainfall on the island and year-to-year periodic climate oscillators such as El Nino southern oscillation (ENSO) [6].

The island have a few source of stable fresh water because surface infiltrates into the highly porous volcanic rocks beneath the surface almost immediately after rainfall [7]. The only source of freshwater are the *Ranos*, a local name for a volcanic crater that holds water [8–10]. There are three *Ranos* on the island. The biggest is Rano Kao, covering about 1,250 m in diameter. It is located at the southwestern part of the island, with an elevation of about 100 m above sea level. the lake has a water column of about 10 m deep, which is covered by a floating aquatic vegetation of up to 3 m deep [11]. The second water body is Rano Raraku, a shallow lake with 2-3 m depth and ~300 m in diameter. The lake is located at the eastern costal lowlands and it sits at ~80 m elevation above sea level, with sedimentary infill of about 12 m deep [12]. Rano Aroi is the third water body, a 150 m in diameter mire, located in the north Terevaka uplands, with an elevation of about 130 m above sea level. Its primary source of fresh water is through precipitation and the water level is controlled by groundwater input. The mire is surrounded by grassland and recently planted forest, the aquatic vegetation is mainly *polygonum acuminatum* and *scirpus californics* [13]. The infill of the mire is mainly peat, with about 16 m thickness in the center [12,14].

2.2 Modern vegetation

The post-contact Rapa Nui vegetation introduces an anthropogenic landscape, where the land management have deeply modified the ecosystem [15,16]. The present-day vegetation is ~90% grassland, *Paspalum scrobiculatum* and *porobolus indicus* are the most distributed grass species in the in the lowlands while *Axonopus paschalis* are more dominant in highlands. The island is having ~5% forest, and most trees are recently planted (*Eucalyptus* from Australian origin), (*Dodonaea viscosa* South American origin), ~5% shrublands, mostly invasive species (*Psidium guajava* from centra America), and Wetlands plants (*Polygonum acuminatum* and *Scirpus californicus*) both from tropic American origin. he ruderal vegetation and crops cover about ~1% of the total vegetation. [17]. Only four species (*Paspalum forsterianum*, *Danthonia paschalis*, *Axonopus paschalis*, *Sophora toromiro*) of more than 200 vascular plants are endemic to the island. For example, the island has 180 species of angiosperm flora, 79% are foreign, 17% are autochthonous, and 4% are of unknown origin. Only 48% of the introduced plants are believed to be naturalized, and the rest are considered invasive [18].

Prehistoric agriculture

The forest of Rapa Nui coexisted with crops after the settlement of Rapanui [19], it is assumed that the Rapanui managed the forest for the purpose of nutritious substance like palm sap for sugar, this assumption is based on the contemporary use of *jubaea chilensis* in Chile [20]. Archaeological evidence suggest that Rapanui did not practice widespread irrigation, instead they planted crops in small garden called *manavai*, which depended on rainfall for water supply [21]. The Rapanui cultivated crops along the coast for the first 500 years of human settlement, while the inland was dominated by forest, however, most of the forest were replaced by the *Manavai* cultivation structure by 1500 CE [22,23]. The *Manavai* wall was built with a rock and it is at least 22 m, this was to prevent surface runoff, wind, and also to reduce evaporation [24,25]. the numbers of *Manavai* structure were about 2,500 as identified through Satellite imagery at first estimation, it covered about 10% surface area on the island, it was later estimated to cover 19% surface area in the island, and 13% in the coastal zone [15,26]. Recent studies suggest that the Rapanui continue the agricultural practice until the arrival of Europeans [27,28]. Palaeoecological study revealed a possible local cultivation on the wetland shores, such as Rano Aroi marsh, Rano Raraku and Rano Kao [29]. Analysis of microfossils of wetland sediments and soils from dryland has helped in the classification of the major plants of Polynesian origin that were planted on the island before contact with Europeans, these plants includes, yam (*Dioscorea*), banana (*Musa sp*), mahute (*Broussonetia papyrifera*), Sweet potato (*Ipomoea babatas*), bottle ground (*Lagenaria siceraria*), ti (*Cordyline fruticose*), and taro (*Colocasia esculenta*) [4].

2.3 Rapa Nui Sedimentary records

Earlier sedimentary records

The baseline palaeoecological study of Rapa Nui comes from the analysis of pollen in lake sediment cores (Rano Aroi, Rano Raraku and Rano Kao) between 1977 and 1983, by a research team led by John Flenley [2,30]. The first published article indicates that Rapa Nui was covered by palm dominated forest for 37,000 years, which later disappeared during the last millennium [30]. Morphological analysis determined that the palm pollen belongs to the Cocosoidae subfamily species, which is related to the wild-spread Chilean wine palm

(*Jubaea chilensis*) and coconut (*Cocos nucifera*) located on the Chilean coasts [13]. The comparison was challenged based on the difference between Chilean coasts' environmental conditions and that of Rapa Nui [31–33]. A study based on endocarp morphology, indicated that palm trees on Rapa Nui belong to an extinct species called *Paschalococos disperta* [18]. However, Resent phytolith analysis disclosed that Rapa Nui pollen is similar to a species named *J.chilensis*. It was later discovered through statistical analysis that there were more than one species of palm trees in the island [17,34]. Research also suggested several shrubs pollen together with palm pollen, which indicates the presence of shrubby undergrowth whose main element would been *triumfetta*, *sophora*, *coprosma*, *macaranga* and several unknown species. The abundance of these components varies but they all have palm dominated forest elements [3,12].



Figure 2.1: different pollen types from Rapa Nui, (Rano Aroi) pollen 1 to 6) while (pollen 7 and 8 (Rano Raraku) (1) Unknown species, (2) Poaceae, (3) Cyperaceae, (4) Compositae, (5) Polygonum, (6) Triumfetta, (7) and (8) *Verbena litoralis* [17].

several years later, John Flenley carried out a detailed reconstruction of the anthropogenic activities, vegetation and landscape changes, using pollen and geochemical proxies in lake sediments [2]. The analysis indicates a clear shift from forest to grassland in the records obtained from Rano Raraku and Rano Kao, however, records from Rano Aroi indicate difference in vegetation and landscape. Flenley’s Rano Raraku record indicates that Rapa Nui

was covered by palm forest from 35,000 to 28,000 ^{14}C yr BP which led to the appearance of shrubs layers, the island vegetation returned to its original forest state by 12,000 ^{14}C yr BP, before the sudden disappearance of palm forest and shrubs which was replaced by grassland [12,35].

Rano Kao records provided a better resolution of the removal of palm forest compared to the previous study, however this record was limited to 1550 ^{14}C yr BP. The record shows gradual decrease of forest from 1300 ^{14}C yr BP and a total forest removal by 950 ^{14}C yr BP, the Rano Kao record was also interpreted as anthropogenic removal of forest from the island as there was presence of charcoal although the core. The Flenely's Rano Aroi sedimentary record was different from that of Rano Raraku and Rano Kao as the record shows fluctuation between palm and shrubs pollen, this indicates a decrease in palm and shrub after 2000 ^{14}C yr BP which corresponds with the increase in charcoal particles in the record, suggesting human induced fire [2,17].

The same research team retrieved another sedimentary core from Rano Kao (KAO2), which was successfully dated. but the date lack precision compared to the sediment core retrieved from Rano Raraku. The charcoal and pollen record in this core suggests two deforestation events, the first happened between 1900 and 1850 cal yr BP, while the second event happened around 600 cal yr BP. The record also indicates a phase of forest regeneration between the two deforestation events [36,37]. But it was difficult to specify their chronology due to age inversion.

Further analysis of microfossils such as phytoliths, starch and pollen, provided a major deforestation occurrence, but a reliable age-depth model was not possible due to age inconsistencies. A palynological study was also carried out on samples retrieved from a floating mat in Rano Kao [38].

Recent Records

Several research have been carried out in recent years between 2005 and 2022. This period can be divided into 2 phases, 2005 to 2010 which marked the phase of few publications and analysis of 20 sediment cores, 9 of the cores were retrieved from Rano Raraku, 7 from Rano Kao and 4 from Rano Aroi. While 2012 to 2020 marked the second phase which mainly consist of publications of data from the analysis of the first phase [39–41].

The Radiocarbon age-depth model of Rano Kao core (KAO05-3A) retrieved in 2005 shows a chronological coherency that contrasted the records of previous Rano Aroi sedimentary study, this dating was based on *scirpus californicus* seeds. However, The pollen record was not as useful in resolving deforestation patterns compared to the records of Raraku and Ario [42,43]. Butler and Flenley resumed analysis on Rano Aroi sedimentary core retrieved in 2001, using the Radiocarbon dating based *scirpus californicus* seeds in other to improve the age-dept model, the record shows fire episode followed by an improved evidence of forest replacement by grassland between 50 and 100 CE. The authors interpreted the deforestation to be a result of anthropogenic activity or natural events such as volcanic fire and climatic changes [44]. The KAO2 record also suggest a partial recovery of forest between 100 and 950 CE, which might by caused by increased precipitation. Before the final deforestation between 1350 and 1800 CE which also corresponds to fire occurrence [45].

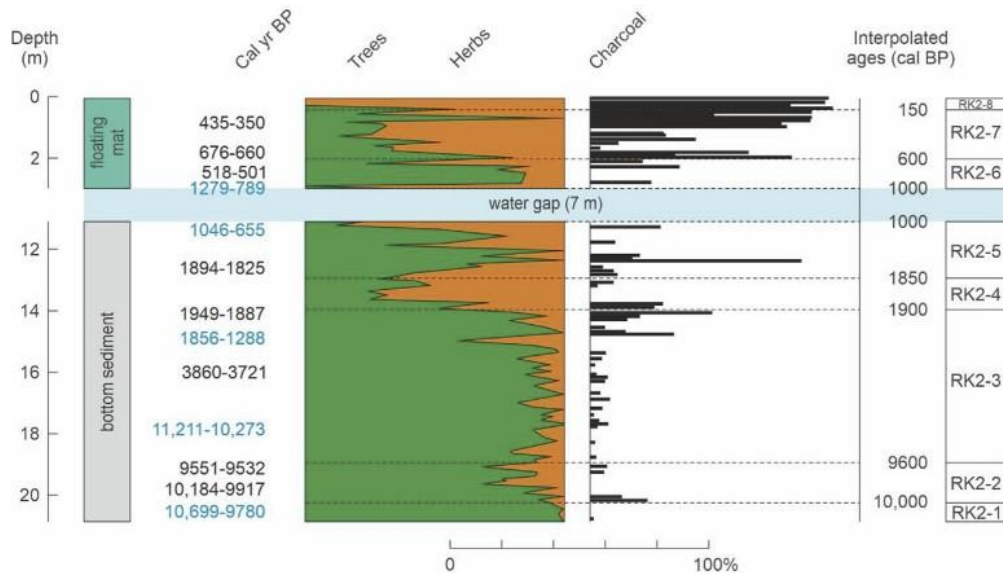


Figure 2.2: Rano Kao pollen (KAO2) pollen diagram with Radiocarbon age based dating based *scirpus californicus* seeds by Butler an Flenley (2010)

Several papers published between 2010 to 2022 focused on the use of pollen analysis and physiochemical proxies to reconstruct the Rapa Nui palaeoecological trend of the last millennia. Pollen, starch and phytolith were analyzed in the 4 sediment cores retrieved from the southwest margin of Rano Kao, the record show trace of gardening around the lake. However, the authors could not achieve reliable chronography because the radiocarbon dating of the 4 sedimentary cores shows age inversion [46]. The same research team studied another sedimentary core called 1, the core shows multiple age inversions for last millennium which was the main focus for the research, there was gap between 12,00 and 2500 cal yr BP,

however, there was consistency in the age depth model between 3500 and 1000 ca yr BP, the record shows high concentration of charcoal fragments, which was interpreted by the authors to be an erosion event which resulted from forest removal by fire which is also associated with agriculture but the entire was difficult to interpret because of the inversions in the age depth model [29]. The same authors also analyzed lake sediment cores which were retrieved from Rano Raraku and Rano Aroi. The Rano Raraku records indicates that the replacement of forest by grassland happens occurred between 1325 and 1437, also corresponding to increased charcoal, and the first appearance of starch. The authors concluded that Rano Raraku catchment and surroundings was also used as multi-cropping site, which also indicates human contribution to the forest removal [46,47].

More authors focused on multiproxy approach to reconstruct the Rapa Nui palaeoecological evolution using sediment cores with age depth models free from age inversions and large sedimentary gaps. This was possible from the three sedimentary cores retrieved from Rano Kao (KAO08-03), Rano Raraku (RAR08) and Rano Aroi (ARO08). The last millennia which was missing from most of the previous researches was present in the RAR08 core [14]. The record shows that the Rapa Nui deforestation was a gradual process with 3 three major decline pulses at 450 BCE, 1200 CE and 1475 CE. The first pulse corresponds with increase in charcoal and an the first appearance of *Verena Liroralis*, which is commonly associated with areas that have frequent human activities such as agriculture [48,49]. The second pulse occurred at ~1200 CE, the authors describe this deforestation phase to be climate and human induced, because it occurred shortly after the little ice age (LIA), and there was also increase in charcoal particles in the sediment core. The record indicates total deforestation in Around Rano Raraku catchment at ~1475 CE, this was accompanied by and the permeant spread of grass and a significant increase in charcoal particles [47].

The Rano Aroi sedimentary core (ARO08-2) record indicates 3 different vegetation phases, the first phase occurred between 750 and 1250 CE, during this phase, the site was dominated by palm trees [50]. The second phase occurred between 1250 and 1520 CE, the phase introduced a semi aquatic vegetation which indicates increased in water table and wet climate, it I believed by the authors that this climate condition might be responsible for the expansion of palm forest that happened during this phase. The final phase occurred between 1520 and 1620 CE, palm forest where abruptly remove and replaced by grassland, which corresponds with an increase in charcoal particles in the sedimentary core, this was interpreted by the authors to be human indued activities.

The Rano Kao sedimentary core (KAO08-03) record suggests a slow deforestation with three pulses at 1070 CE, 1410 CE and 1600 CE. There were regeneration phases between the first two pulses, the second regeneration phase was interrupted by the 1600 CE deforestation, which lead to complete removal of palm forest from Rano Kao catchment. The trend of the Rano Kao deforestation occurred at the rate of -9% of palm pollen per century [51].

2.4 Research objective

It is not uncommon to believe that Rapa Nui deforestation was abrupt and simultaneous across the island. However, recent studies from Rano Raraku, Rano Aroi and Rano Kao have shown that deforestation occurred at different times and rate. But the hypotheses about the Rapa Nui deforestation have brought about the following questions.

- Did deforestation occur as a consequence of climate change?
- Was civilization collapse due to unsustainable anthropogenic land use?
- When did the Rapa Nui deforestation happen?

The development of novel methods and multi-proxy analysis for reconstructing environmental changes is an essential step to understanding past climate and ecological dynamics. In this study, I reconstructed the past human environmental-interaction, changes in redox condition, and weathering process in Rapa Nui through multiproxy analysis (biomarker, trace, and rare earth elements) in lake sediments to determine the cause of Rapa Nui deforestation and the supposed civilization effect. The analytical method is based on Gas chromatography-mass spectrometry (GC-MS) and inductively coupled plasma mass spectrometry (ICP-MS).

Reference

- [1] V. Rull, Contributions of paleoecology to Easter Island's prehistory: A thorough review, *Quat. Sci. Rev.* 252 (2021) 106751. <https://doi.org/10.1016/j.quascirev.2020.106751>.
- [2] J. Flenley, P. Bahn, *The Enigmas of Easter Island*, Oxford University Press, UK, 2003. <https://books.google.com/books?id=PtKS1p4X3oMC>.
- [3] J.R. Flenley, S.M. King, Late Quaternary Pollen records from Easter Island, *Nature*. 307 (1984) 47–50. <https://doi.org/10.1038/307047a0>.
- [4] J.R. Flenley, Further Evidence of Vegetational Change on Easter Island History of Easter Island View project Classifynder View project, 1996. <https://www.researchgate.net/publication/38407638>.
- [5] Corporación Nacional Forestal - Chile, Plan de Manejo Parque Nacional Rapa Nui, (1997) 167. http://www.conaf.cl/wp-content/files_mf/1382466339PNRapaNui.pdf.
- [6] R. Garreaud, P. Aceituno, Interannual Rainfall Variability over the South American Altiplano, *J. Clim. - J Clim.* 14 (2001) 2779–2789. [https://doi.org/10.1175/1520-0442\(2001\)014<2779:IRVOTS>2.0.CO;2](https://doi.org/10.1175/1520-0442(2001)014<2779:IRVOTS>2.0.CO;2).
- [7] C. Herrera, E. Custodio, Conceptual hydrogeological model of volcanic Easter Island (Chile) after chemical and isotopic surveys, *Hydrogeol. J.* 16 (2008) 1329–1348. <https://doi.org/10.1007/s10040-008-0316-z>.
- [8] C. Herrera, E. Custodio, Conceptual hydrogeological model of volcanic Easter Island (Chile) after chemical and isotopic surveys, *Hydrogeol. J.* 16 (2008) 1329–1348. <https://doi.org/10.1007/s10040-008-0316-z>.
- [9] V. Rull, Human discovery and settlement of the remote easter island (Se pacific), *Quaternary*. 2 (2019). <https://doi.org/10.3390/quat2020015>.
- [10] R.J. DiNapoli, C.P. Lipo, T. Brosnan, T.L. Hunt, S. Hixon, A.E. Morrison, M. Becker, Rapa Nui (Easter Island) monument (ahu) locations explained by freshwater sources, *PLoS One*. 14 (2019) 4–6. <https://doi.org/10.1371/journal.pone.0210409>.
- [11] J.R. Flenley, P. Bahn, Conflicting views of Easter Island, *Rapa Nui J.* 21 (2007) 11–13. <http://islandheritage.org/wordpress/wp->

content/uploads/2010/06/RNJ_21_1_Flenley_Bahn.pdf.

- [12] V. Rull, N. Cañellas-Boltà, O. Margalef, S. Pla-Rabes, A. Sáez, S. Giralt, Three millennia of climatic, ecological, and cultural change on Easter Island: An integrative overview, *Front. Ecol. Evol.* 4 (2016) 1–4. <https://doi.org/10.3389/fevo.2016.00029>.
- [13] G. Zizka, Flowering Plants of Easter Island, *Palmarum Hortus Fr.* 3 (1991) 1–108.
- [14] V. Rull, The deforestation of Easter Island, (2019) 1–51. <https://doi.org/10.1111/brv.12556>.
- [15] J.M. Wilmshurst, T.L. Hunt, C.P. Lipo, A.J. Anderson, High-precision radiocarbon dating shows recent and rapid initial human colonization of East Polynesia, *Proc. Natl. Acad. Sci. U. S. A.* 108 (2011) 1815–1820. <https://doi.org/10.1073/pnas.1015876108>.
- [16] T. Hunt, C. Lipo, Late colonization of Easter Island, *Science* (80-.). 311 (2006) 1603–1606. <https://doi.org/10.1126/science.1121879>.
- [17] V. Rull, The deforestation of Easter Island, *Biol. Rev.* 95 (2020) 124–141. <https://doi.org/10.1111/brv.12556>.
- [18] G. Zizka, Flowering Plants EasterIslands, 1991.
- [19] J.M. Diamond, *Collapse : how societies choose to fail or succeed*, Viking, 2005.
- [20] A. Mieth, THE KEY ROLE OF JUBAEA PALM TREES IN THE HISTORY OF EASTER ISLAND - A PROVOCATIVE INTERPRETATIO, (2003).
- [21] C.O. Puleston, T.N. Ladefoged, S. Haoa, O.A. Chadwick, P.M. Vitousek, C.M. Stevenson, Rain, sun, soil, and sweat: A consideration of population limits on Rapa Nui (Easter Island) before European contact, *Front. Ecol. Evol.* 5 (2017) 1–14. <https://doi.org/10.3389/fevo.2017.00069>.
- [22] A. Mieth, H. Bork, Degradation of resources and successful land-use management on prehistoric Rapa Nui: Two sides of the same coin, *Easter Isl. Collapse or Transform.* (2015) 9–10.
- [23] V. Rull, E. Montoya, I. Seco, N. Cañellas-Boltà, S. Giralt, O. Margalef, S. Pla-Rabes, W. D’Andrea, R. Bradley, A. Sáez, CLAFS, a Holistic climatic-ecological-anthropogenic hypothesis on Easter Island’s deforestation and cultural change: Proposals and testing prospects, *Front. Ecol. Evol.* 6 (2018).

- <https://doi.org/10.3389/fevo.2018.00032>.
- [24] C.M. Stevenson, J. Wozniak, S. Haoa, Prehistoric agricultural production on Easter Island (Rapa Nui), Chile, *Antiquity*. 73 (1999) 801–812.
<https://doi.org/10.1017/S0003598X00065546>.
- [25] J. Greskowiak, *Geophysical Research Letters*, *Geophys. Prospect.* (2014) 6413–6419.
<https://doi.org/10.1002/2014GL061184>.Received.
- [26] T.N. Ladefoged, A. Flaws, C.M. Stevenson, The distribution of rock gardens on Rapa Nui (Easter Island) as determined from satellite imagery, *J. Archaeol. Sci.* 40 (2013) 1203–1212. <https://doi.org/10.1016/j.jas.2012.09.006>.
- [27] M.A. Mulrooney, An island-wide assessment of the chronology of settlement and land use on Rapa Nui (Easter Island) based on radiocarbon data, *J. Archaeol. Sci.* 40 (2013) 4377–4399. <https://doi.org/10.1016/j.jas.2013.06.020>.
- [28] C.M. Stevenson, C.O. Puleston, P.M. Vitousek, O.A. Chadwick, S. Haoa, T.N. Ladefoged, Variation in Rapa Nui (Easter Island) land use indicates production and population peaks prior to European contact, *Proc. Natl. Acad. Sci. U. S. A.* 112 (2015) 1025–1030. <https://doi.org/10.1073/pnas.1420712112>.
- [29] M. Horrocks, W.T. Baisden, M.A. Harper, M. Marra, J. Flenley, D. Feek, S. Haoa-Cardinali, E.D. Keller, L.G. Nualart, T.E. Gorman, A plant microfossil record of Late Quaternary environments and human activity from Rano Aroi and surroundings, Easter Island, *J. Paleolimnol.* 54 (2015) 279–303. <https://doi.org/10.1007/s10933-015-9852-4>.
- [30] J.R. Flenley, S.M. King, Late Quaternary pollen records from Easter Island, *Nature*. 307 (1984) 47–50. <https://doi.org/10.1038/307047a0>.
- [31] T.L. and C.P.L. Hunt, Late Colonization of Easter Island, 343 (2006) 881–886.
- [32] T.L. Hunt, C.P. Lipo, Revisiting Rapa Nui (Easter Island) “ecocide,” *Pacific Sci.* 63 (2009) 601–616. <https://doi.org/10.2984/049.063.0407>.
- [33] J. Dransfield, J.R. Flenley, S.M. King, D.D. Harkness, S. Rapu, A recently extinct palm from Easter Island, *Nature*. 312 (1984) 750–752.
<https://doi.org/10.1038/312750a0>.
- [34] C. Delhon, C. Orliac, The vanish palm trees of Easter Island : New radiocarbon and

- phytolith data The Vanished Palm Trees of Easter Island : New Radiocarbon and Phytolith Data, (2015).
- [35] V. Rull, Contributions of paleoecology to Easter Island’s prehistory: A thorough review, *Quat. Sci. Rev.* 252 (2021). <https://doi.org/10.1016/j.quascirev.2020.106751>.
- [36] N. Cañellas-Boltà, V. Rull, A. Sáez, O. Margalef, S. Giralt, J.J. Pueyo, H.H. Birks, H.J.B. Birks, S. Pla-Rabes, Macrofossils in Raraku Lake (Easter Island) integrated with sedimentary and geochemical records: Towards a palaeoecological synthesis for the last 34,000 years, *Quat. Sci. Rev.* 34 (2012) 113–126. <https://doi.org/10.1016/j.quascirev.2011.12.013>.
- [37] O. Margalef, N. Cañellas-Boltà, S. Pla-Rabes, S. Giralt, J.J. Pueyo, H. Joosten, V. Rull, T. Buchaca, A. Hernández, B.L. Valero-Garcés, A. Moreno, A. Sáez, A 70,000 year multiproxy record of climatic and environmental change from Rano Aroi peatland (Easter Island), *Glob. Planet. Change.* 108 (2013) 72–84. <https://doi.org/10.1016/j.gloplacha.2013.05.016>.
- [38] I. Seco, V. Rull, E. Montoya, N. Cañellas-bolt, S. Giralt, O. Margalef, S. Pla-rabes, W.J.D. Andrea, R.S. Bradley, S. Alberto, A Continuous Palynological Record of Forest Clearing at Rano Kao (Easter Island , SE Pacific) During the Last Millennium : Preliminary Report, (n.d.) 1–7.
- [39] O. Margalef, A. Martínez Cortizas, M. Kylander, S. Pla-Rabes, N. Cañellas-Boltà, J.J. Pueyo, A. Sáez, B.L. Valero-Garcés, S. Giralt, Environmental processes in Rano Aroi (Easter Island) peat geochemistry forced by climate variability during the last 70kyr, *Palaeogeogr. Palaeoclimatol. Palaeoecol.* 414 (2014) 438–450. <https://doi.org/10.1016/j.palaeo.2014.09.025>.
- [40] N. Cañellas-Boltà, V. Rull, A. Sáez, O. Margalef, S. Pla-Rabes, B. Valero-Garcés, S. Giralt, Vegetation dynamics at Raraku Lake catchment (Easter Island) during the past 34,000years, *Palaeogeogr. Palaeoclimatol. Palaeoecol.* 446 (2016) 55–69. <https://doi.org/10.1016/j.palaeo.2016.01.019>.
- [41] V. Rull, E. Montoya, I. Seco, N. Cañellas-Boltà, S. Giralt, O. Margalef, S. Pla-Rabes, W. D’Andrea, R. Bradley, A. Sáez, CLAFS, a Holistic climatic-ecological-anthropogenic hypothesis on Easter Island’s deforestation and cultural change: Proposals and testing prospects, *Front. Ecol. Evol.* 6 (2018) 1–12.

<https://doi.org/10.3389/fevo.2018.00032>.

- [42] R.W. Battarbee, J.-A. Grytnes, R. Thompson, P.G. Appleby, J. Catalan, A. Korhola, H.J.B. Birks, E. Heegaard, A. Lami, Comparing palaeolimnological and instrumental evidence of climate change for remote mountain lakes over the last 200 years, 2002.
- [43] O. González Ferrán, GEOLOGÍA DEL COMPLEJO VOLCÁNICO ISLA DE PASCUA-RAPA NUI, CHILE. V REGION - VALPARAISO, วารสารวิชาการมหาวิทยาลัยอีสเทิร์นเอเชีย. 4 (2007) 88–100.
- [44] K.R. Butler, J.R. Flenley, The Rano Kau 2 Pollen Diagram: Palaeoecology Revealed, Rapa Nui J. 24 (2010) 5–10.
- [45] A. Cole, J. Flenley, Modelling human population change on Easter Island far-from-equilibrium, 184 (2008) 150–165. <https://doi.org/10.1016/j.quaint.2007.09.019>.
- [46] M. Horrocks, W.T. Baisden, J. Flenley, D. Feek, L.G. Nualart, S. Haoa-Cardinali, T.E. Gorman, Fossil plant remains at Rano Raraku, Easter Island’s statue quarry: Evidence for past elevated lake level and ancient Polynesian agriculture, J. Paleolimnol. 48 (2012) 767–783. <https://doi.org/10.1007/s10933-012-9643-0>.
- [47] V. Rull, Contributions of paleoecology to Easter Island ’ s prehistory : A thorough review, Quat. Sci. Rev. 252 (2021) 106751. <https://doi.org/10.1016/j.quascirev.2020.106751>.
- [48] V. Rull, N. Cañellas-Boltà, A. Sáez, S. Giralt, S. Pla, O. Margalef, Paleoecology of Easter Island: Evidence and uncertainties, Earth-Science Rev. 99 (2010) 50–60. <https://doi.org/10.1016/j.earscirev.2010.02.003>.
- [49] N. Cañellas-Boltà, V. Rull, A. Sáez, O. Margalef, R. Bao, S. Pla-Rabes, M. Blaauw, B. Valero-Garcés, S. Giralt, Vegetation changes and human settlement of Easter Island during the last millennia: A multiproxy study of the Lake Raraku sediments, Quat. Sci. Rev. 72 (2013) 36–48. <https://doi.org/10.1016/j.quascirev.2013.04.004>.
- [50] V. Rull, N. Cañellas-Boltà, O. Margalef, A. Sáez, S. Pla-Rabes, S. Giralt, Late Holocene vegetation dynamics and deforestation in Rano Aroi: Implications for Easter Island’s ecological and cultural history, Quat. Sci. Rev. 126 (2015) 219–226. <https://doi.org/10.1016/j.quascirev.2015.09.008>.
- [51] B. Van Geel, J. Buurman, O. Brinkkemper, J. Schelvis, G. Van Reenen, T. Hakbijl,

Environmental reconstruction of a Roman Period settlement site in Uitgeest (The Netherlands), with special reference to coprophilous fungi, 30 (2003) 873–883.
[https://doi.org/10.1016/S0305-4403\(02\)00265-0](https://doi.org/10.1016/S0305-4403(02)00265-0).

CHAPTER THREE: PALEOENVIRONMENTAL AND PALEOCLIMATE PROXIES

3.1 Paleoclimatology

Paleoclimatology is the study and interpretation of past biological, physical, and chemical dynamics of a given environment. The study is to assess the evolution of the Earth's climate and environmental system in the absence of instrumental records. Instrumental records provide insufficient assessment of the Earth's climatic variation because it covers less than 10^{-7} of the Earth's climate history [1]. However, occurrence in environmental provides climate archives with proxies, which can be used to access a more extended climate and environmental variability; the study of such proxy data in climate archives makes up the foundation of paleoclimatology [2]. Therefore, the study of past climate and environmental variation must begin with understanding the types of climate archives, the available proxies within a given archive and the analytical methods [3]. It is important to take into consideration the possible difficulties associated with each analytical method.

3.2 Climate archives

Climate archives are biologic and geologic materials that have accumulated over time with evidence of past climate and environmental variations [4]. Archives contain proxies which can be investigated through different analytical methods to provide a detailed and consistent record of past climatic variation. Examples of climate archives are Ice core, lake and ocean sediments, tree rings, cave deposits (speleothems), and coral reefs. The amount of climatic information retrieved from a given archive mainly depends on two factors: (1) the disturbance rate of the climate record during and after deposition and (2) the accumulation rate of the record [5]. However, there is a wide range of temporal resolution and time span between different archives. High resolution Archives are comparatively short-termed when compared with poorly resolved archive [6,7]. Lake sediment was used for this research because it falls within the target of the

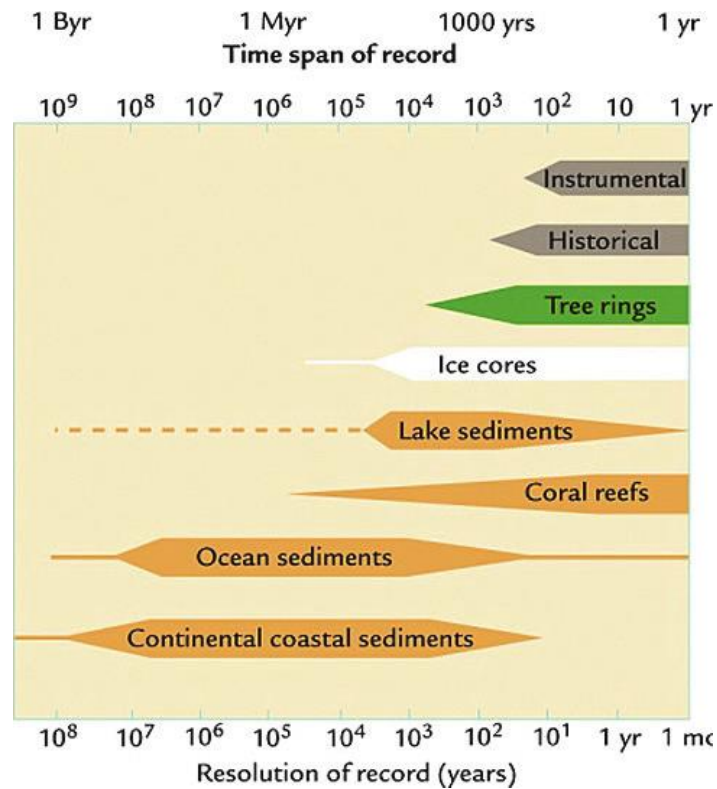


Figure 3.1: Temporal resolution and time span of marine and continental climate archives (in a geologic time plotted in log scale by the power of 10) [6]

3.3 Lake sediment as a climate archive

Lakes are one of the most sensitive landscape features suitable for paleoclimate study due to its ability to react to intrinsic and extrinsic changes in the environment through sedimentation [8]. They can originate from tectonic crust deformation, depression from formal glacial, volcanism, bedrocks shaped from erosion, as well as depositional activities by rivers. Lakes can be found in different environmental conditions, depending on how it was formed, location and the age, and the sedimentation process of the lake [9]. Sediments are often deposited in lakes through atmospheric deposition and surface runoff. Rainfall produces runoff which erodes surrounding debris such as exposed rocks in the continent, tree leaves and other environmental materials. The eroded debris are sometimes transported and deposited as sediments into lakes, this deposition may continue for thousands of years and accumulates into multiple layers of undisturbed sediment secessions, layers of undisturbed sediments guarantees records of local to region environmental changes [10,11]. Sediments deposited in lakes consist of allochthonous and autochthonous deposits. The first refers to biological remains and non-biological materials like biogenic, chemical and terrigenous

deposits, as well as volcanic particles, pollutants and fossils transported into lakes through the atmosphere and surface runoff. The second refers to biological remains which originates from the lake itself [12–14]. Lake sediment represents one of the most reliable archives for paleoenvironmental data due to the wide range of climate information that can be extracted from the archive through the analysis of multiple proxies (biomarkers, charcoal, pollen and geochemistry of the sediments) [15].

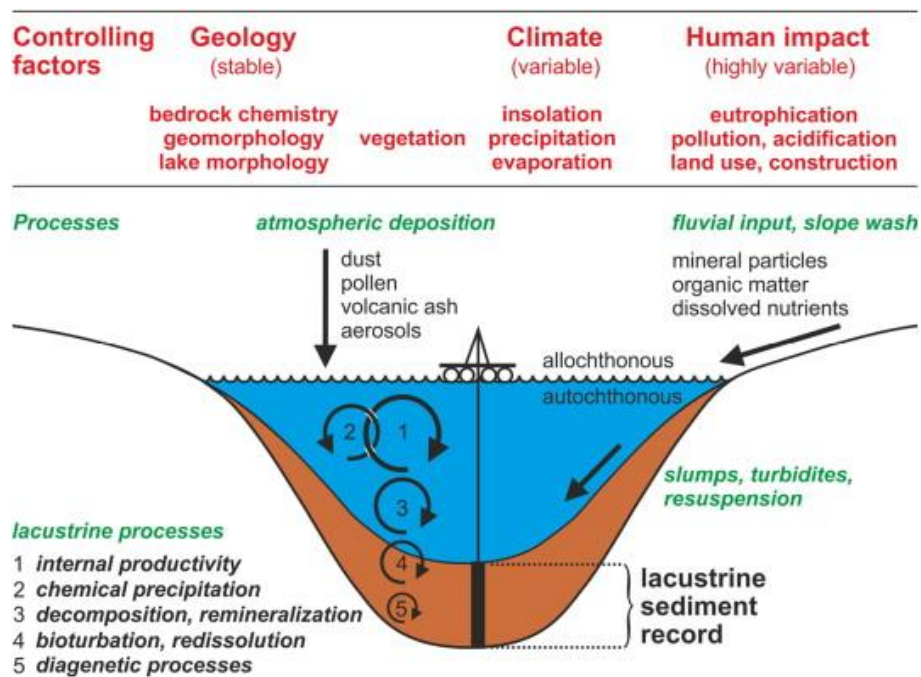


Figure 3.2: Formation of lake sediments: controlling factors and processes (figure: Zolitschka 2015 [12]).

3.4 Proxies

Proxies are biological, physical, and chemical materials conserved within a given climate archive, they can be extracted, analyzed, and correlated with climate and environmental parameters to access past climate condition [16]. Proxies preserve climate and environmental information differently because they are generated from diverse environmental sources. Therefore, each proxy gives different climate information. However, The combined and thorough use of multiple proxies in lake sediment can provide a more robust understanding of past climate and environmental variations, including long-term climate changes, fire occurrence, deforestation as well as human contribution to these changes [15,17]. This research focused on multiple lake sediment proxies; charcoal, polycyclic aromatic

hydrocarbon, monosaccharide anhydride, *n*-alkanes, fecal sterols, trace, and rare earth elements. These proxies are primarily used as markers for past fire occurrence, vegetation distribution, human presence in the environment, and water availability. Below is a detailed description of the proxies.

Charcoal

Sedimentary charcoal is produced through incomplete combustion of biomass materials at a temperature between 280°C and 500°C. Particle size and production rate highly depend on fire characteristics such as fuel source, fire frequency, and combustion efficiency [18–20]. The transportation and deposition process are determined by the charcoal particle size, i.e., particle size >1000 µm diameter are deposited close to the fire source and are often transported to lake basins through surface runoff, such particle size represents local fire occurrence, while particle size between 125 µm and 200 µm in diameter are typically deposited about <7 km from source fire, representing extra-local fire occurrence. Regional fire are often detected by particles size <100 µm as it can travel up to 100 m in the atmosphere before deposition [21]. Sedimentary charcoal data is comprised of primary and secondary charcoal. Primary charcoal are deposited in lakes during or shortly after a fire event while secondary charcoal introduced into a lake during non-fire events or non-fire years [18]. The analysis of Sedimentary charcoal quantifies the accumulation of charcoal particles in sediments during fire events as direct evidence of burning, and it is a reliable method for reconstructing long/short-term variation in fire occurrence. However, charcoal production are biased towards woody fuel [22]. Therefore, reconstructing or estimating fire intensity and size through charcoal analysis is done in the most general terms [23].

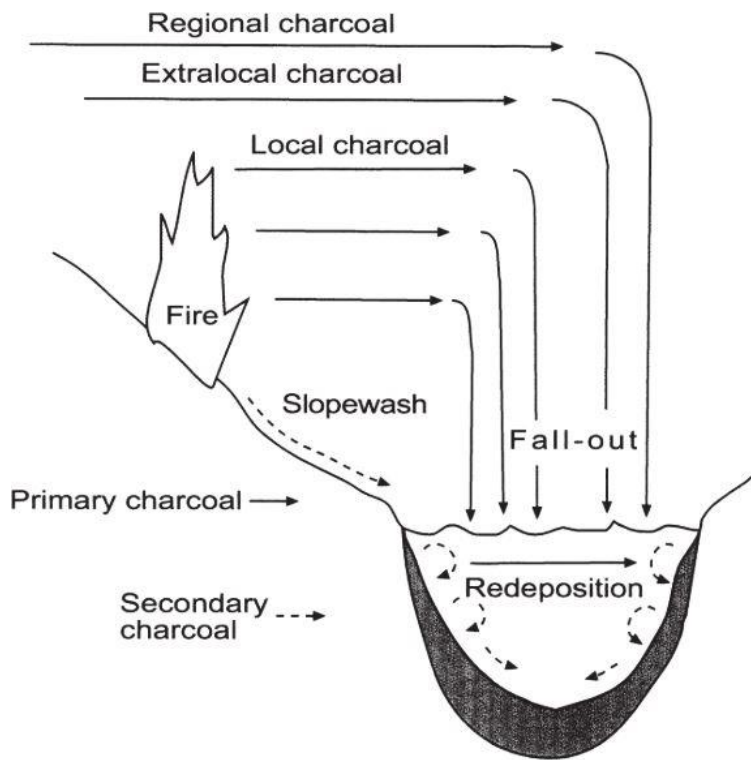


Figure 3.2. Diagram demonstrating the sources of primary and secondary charcoal (Figure: Whitlock and Larsen (2001) [20]).

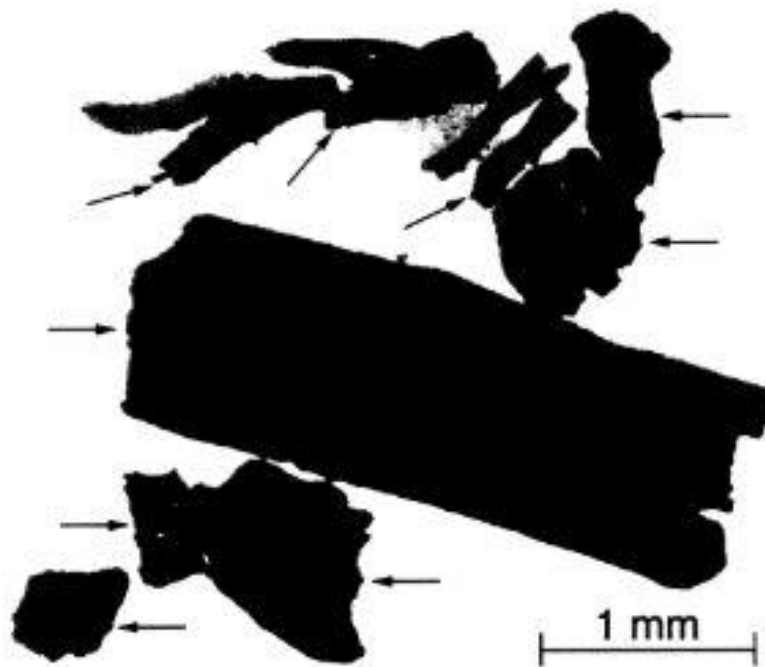
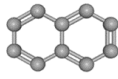
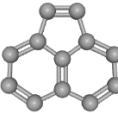
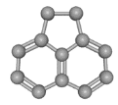
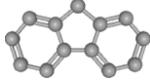
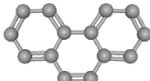
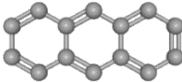
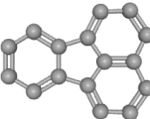
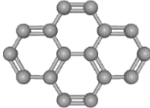
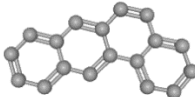
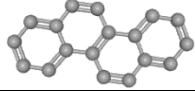


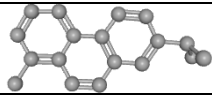
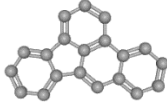
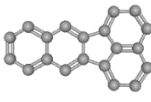
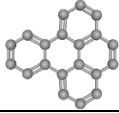
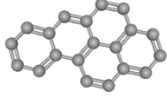
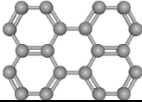
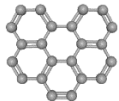
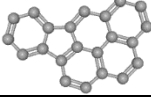
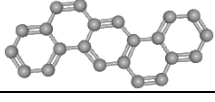
Figure 3.3. Macroscopic charcoal particles (arrow) left after washing sediment through a 250µm screen (figure: Whitlock and Larsen (2001)) [24]

Polycyclic aromatic hydrocarbon

Polycyclic aromatic hydrocarbon (PAHs) are ubiquitous organic compounds with two or more fused aromatic rings, generally found in the atmosphere, sediments, as well as terrestrial and marine areas. They go through different environmental transformations such as photochemical degradation, volatilization and biodegradation [25]. PAHs are produced during the combustion of organic material at a temperature between 200 °C and 700 °C [26–28], and they are introduced into the environment through natural and anthropogenic process. Natural source includes volcanic eruption, petroleum thermal maturation, forest fire and organic matter in sedimentary rock [25]. Anthropogenic source is mainly through the combustion of fossil fuels such as forest fire, industrial and commercial heating system, cigarette, industrial boiler, ships, power plant and aircraft [29]. PAHs in the environment also get of attention due to their carcinogen and teratogenic effects on organism. However, the chemical composition of PAHs in sediment archive are useful in paleoclimates study, as they can provide information on past fire occurrence [30]. The molecular weight of PAHs is directly related the numbers aromatic. Light weight PAHs have the lowest number of aromatic rings, and these attributes can be used to infare the temperature and intensity of past fire events [31]. Light molecular weight (2 and 3 rings) PAHs are formed at a temperature between 300 °C and 500 °C, medium molecular weight (4 rings) are formed at temperature between 500 °C and 600 °C, while heavy molecular weight (5 and 6 rings) are formed at temperature above 600 °C [32,33]. PAHs are often transported through the atmosphere and can travel for thousands of km; however, lightweight PAHs can travel farther than heavyweight PAHs as the molecular weight plays a huge role in the transportation phase. Lighter weight PAHs can be used to determine local to regional fire occurrence, while heavyweight PAHs are often closer to the fire source as they usually do not travel far. [27,34,35]. A total number of 19 PAHs from light to heavy molecular weight were considered in this research.

Table 3:1 List of the 19 PAHs considered in this research (source: <https://pubchem.ncbi.nlm.nih.gov/>)

Light molecular weight PAHs			
Compound Name	Structure	Molecular Formula	Molecular Weight
Naphthalene		C ₁₀ H ₈	128
Acenaphthylene		C ₁₂ H ₈	152
Acenaphthene		C ₁₂ H ₁₀	154
Fluorene		C ₁₃ H ₁₀	166
Mid molecular weight PAHs			
Phenanthrene		C ₁₄ H ₁₀	178
Anthracene		C ₁₄ H ₁₀	178
Fluoranthene		C ₁₆ H ₁₀	202
Pyrene		C ₁₆ H ₁₀	202
Benzo(a)Anthracene		C ₁₈ H ₁₂	228
Chrysene		C ₁₈ H ₁₂	228

Retene		$C_{18}H_{18}$	234
Heavy molecular weight PAHs (5-6 rings PAHs)			
Benzo(b)Fluoranthene		$C_{20}H_{12}$	252
Benzo(k)Fluoranthene		$C_{20}H_{12}$	252
Benzo(e)Pyrene		$C_{20}H_{12}$	252
Benzo(a)Pyrene		$C_{20}H_{12}$	252
Perylene		$C_{20}H_{12}$	252
Benzo(ghi)Perylene		$C_{22}H_{12}$	276
Indeno(1,2,3-c,d)Pyrene		$C_{22}H_{12}$	276
Dibenzo(A,H)Anthracene		$C_{22}H_{14}$	278

Monosaccharide anhydrides

Plants store energy from the sun through photosynthesis in the form of cell wall polymers or lignocellulose that can be accessed through burning or bioconversion process [36]. The main components of lignocellulose are cellulose, hemicellulose, and lignin. The most abundant is cellulose, constituting between 35 and 50% of the total dry weight of lignocellulose, hemicellulose is the second most abundant structure, consisting between 20–35%, lignin is the least abundant of the three components, constituting between 15 and 35% [37]. Cellulose is a linked chain of glucose molecules, bonded by $\beta(1\rightarrow4)$ glycosidic, while hemicellulose consists of 5 to 6 monosaccharide carbon units (arabinose, galactose, glucose, mannose, xylose) that form a complex bond by binding celluloses fibers to create microfibrils which then cross-link with lignin, this complex bound creates a strong structure which makes hemicellulose more resistance to biodegradation than cellulose [1,38]. Lignin is a complex three-dimensional polymer belonging to the phenylpropanoid units, and it uses a different chemical bond to cross-link molecules, it also has the strongest chemical bond among the lignocellulose components as well as most resistance to microbial degradation [39].

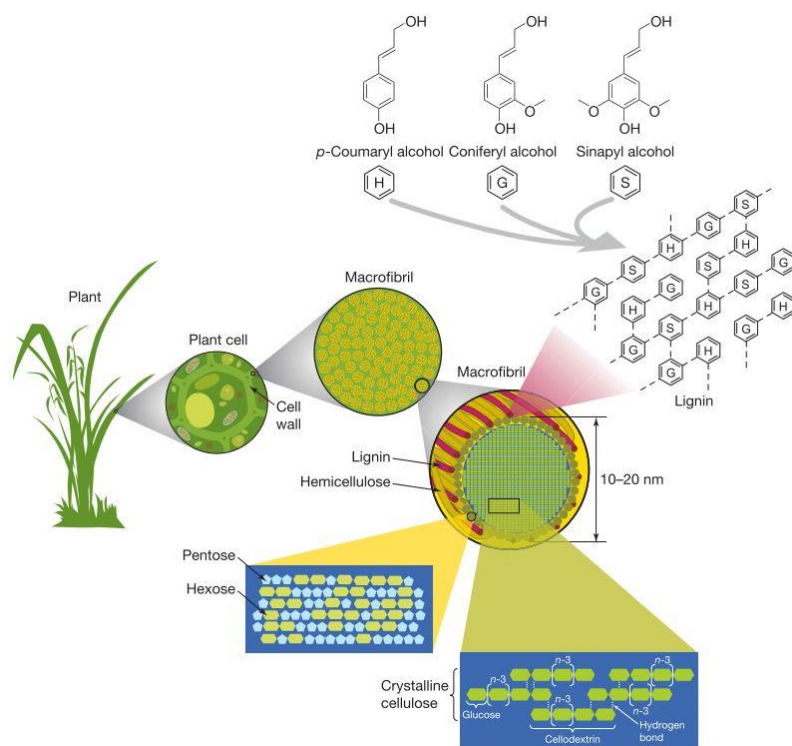


Figure 3.4 Cellulose, hemicellulose, and lignin structures (figure: Rubin 2008) [36].

The release of cell wall polymers through the burning of plant/wood at temperature $>300^{\circ}\text{C}$ creates fire proxies called monosaccharide anhydrides such as 1,6-anhydro-E-D-glucopyranose (levoglucosan), 1,6-anhydro-E-D-mannopyranose (mannosan), and 1,6-anhydro-E-D-galactopyranose (galactosan), these three anhydrous sugars are isomers, and their production rate depends on the temperature and component of the plant that is being burnt [36,38,40].

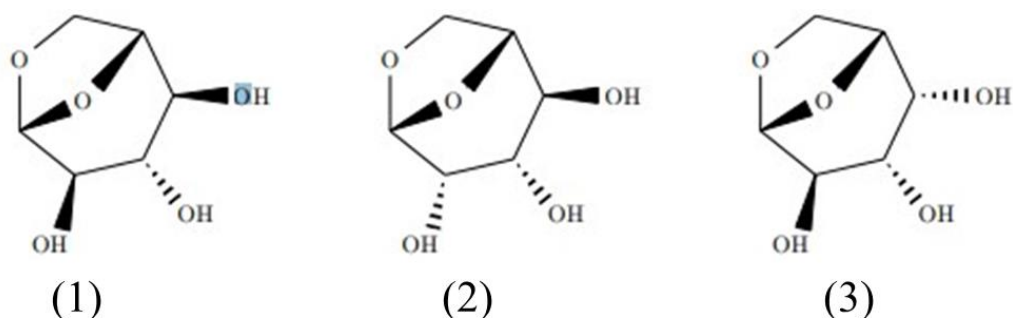


Figure 3.5. Structures of monosaccharide anhydride; Levoglucosan (1), mannosan (2), and galactosan (3).

Levoglucosan is exclusively produced during the combustion of cellulose components at temperatures between 300°C and 350°C , while its isomers Mannosan and galactosan are released during the combustion of hemicellulose [41–43]. Levoglucosan is the most reliable proxy amongst monosaccharide anhydride; it consists of more than 90% of the total monosaccharide anhydride. It is the most abundant in smoke particles, its emission ranges from $40\text{--}2000\text{ mg kg}^{-1}$ for in burning wood. It is stable in the atmosphere and can travel up to thousands of km from the fire source [38,44–48].

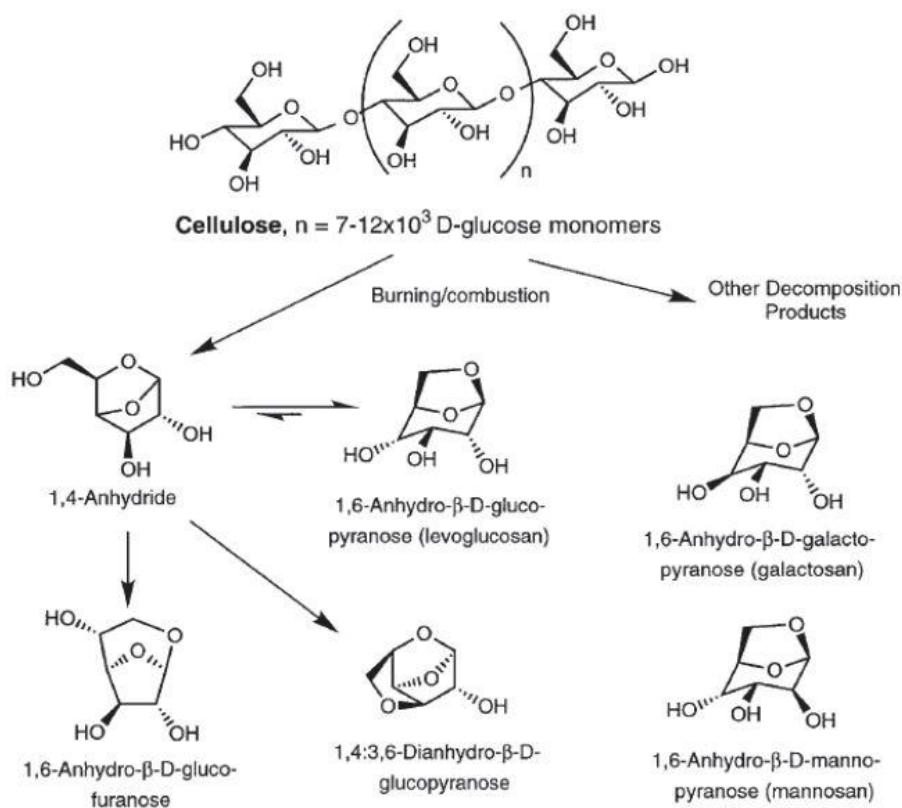


Figure 3.6. Formation of levoglucosan through decomposition of cellulose (figure: Simoneit (1999)) [48].

n-Alkanes

Plants use the wax coats on their leaves and organs to produce a range of predominately odd-over-even *n*-alkanes, usually with one or two dominant chain lengths. *n*-alkanes have high resistance to biochemical degradation and can survive in lake sediment for millions of years [49,50]. They are relatively important in reconstructing paleoenvironmental vegetation because the its pattern and distribution vary from plant to plant; hence the presence/absence, and relative quantities of *n*-alkane in a plant provide useful information on vegetation distribution through the application of compound-specific carbon and hydrogen ratios [51]. Terrestrial plants primarily produce long-chain *n*-alkanes (LHC) while shorter chain *n*-alkanes are derived from aquatic plants; for example, C_{27} and C_{29} are derived from woody plants, while C_{31} is derived from grasses. Mid-chain *n*-alkanes (C_{20} – C_{25}) are produced by aquatic macrophytes. Fungi, bacterial, and algae produce short *n*-alkanes (C_{14} – C_{22} [52,53]. Several indices have been employed for the characterization of *n*-alkane distribution, in addition to the abundance of individual *n*-alkanes.

average chain length: (ACL) Average chain length could be related to vegetation types and latitude. Higher ACL values are suggestive of warmer climates, while lower value indicates colder climate condition [51,54].

$$ACL = [25(nC_{25}) + 27(nC_{27}) + 29(nC_{29}) + 31(nC_{31}) + 33(nC_{33})] / (nC_{25} + nC_{27} + nC_{29} + nC_{31} + nC_{33})$$

Terrigenous/aquatic ratio (TAR) This ratio differentiates between terrestrial and aquatic sources of *n*-alkanes by evaluating the aquatic input with the terrestrial input. The reduced value of TAR indicates aquatic source while the high value indicates terrestrial origin [55].

$$TAR = (C_{27} + C_{29} + C_{31}) / (C_{15} + C_{17} + C_{19})$$

Carbon preference index (CPI) in lake sediment differentiate between vegetable and petroleum origin of *n*-alkanes, CPI >1 indicates a predominance of odd over even chain length. It reveals terrestrial plant source, while <1 indicates an aquatic plant or while petrogenic origin, grass CPI typically ranges from 3.49 and 12.76, tree leaves have CPI from 6.43 to 17.25 [50,51,54,56]

$$CPI = [\sum_{\text{odd}} (C_{21} - C_{33}) + \sum_{\text{odd}} (C_{23} - C_{35})] / (2\sum_{\text{even}} C_{22} - C_{34})$$

P_{aq} is an index used for the identification of submerged plants and emergent aquatic plants, through the difference in the mid and long chain length.

$$P_{aq} = (C_{27} + C_{29} + C_{31}) / (C_{15} + C_{17} + C_{19})$$

Long hydrocarbon chai (LHC) Though LHC, like every other index, is not species-specific, it is useful to understand alkanes sources in sediments and vegetation shifts in the environment [103]. Long-chain *n*-alkanes (LCH > C₂₃) are used for deducing past vegetation types: by dividing odd long-chain *n*-alkanes by the total amount of *n*-alkanes. High concentration is an indication of higher plants, like woody plants and grass.

$$\text{LHC} = (nC_{27} + nC_{29} + nC_{31} + nC_{31}) / (\sum\text{CH})$$

Fecal sterols

Disentangling the outcomes of natural climate change versus human enhanced environmental change has been one of the main challenges in paleoenvironmental studies [57,58]. But a novel biomarker method has been developed to reconstruct the presence of humans and grazing animals within a lake catchment [46,59]. The use of these biomarkers, particularly stanols, gives a beneficial method that help to determine past human presence and infare their activity in the environment [60]. Stanols are formed through microbial reduction of Δ^5 -sterols in the gut of mammals which is then released into the environment through feces [59,61]. The diet of a mammal determines the stanols found in their feces, therefor, the sterol fingerprint produced by animal feces can distinguish between the human and animal sources of fecal pollution and paleoenvironmental reconstructions. For example, the dominant sterol in human feces is coprostanol, which is relatively stable for a long time but it can be converted to epi-coprostanol by bacterial degradation in the environment [62]. Human and a few domestic animals such as pigs have coprostanol as their primary product from microbial hydrogenation of cholesterol. While omnivorous mammals such as cow and sheep have lower concentrations of coprostanol, but higher campestanol and stigmastanol [62–64]. Using this difference, an increased presence of humans is therefore indicated by the increase concentration of fecal sterols (5β -coprostanol and 5β -epicoprostanol) in the environment [59,65]. Higher concentration of campestanol and stigmastanol in the environment can be interpreted as animal husbandry pratice

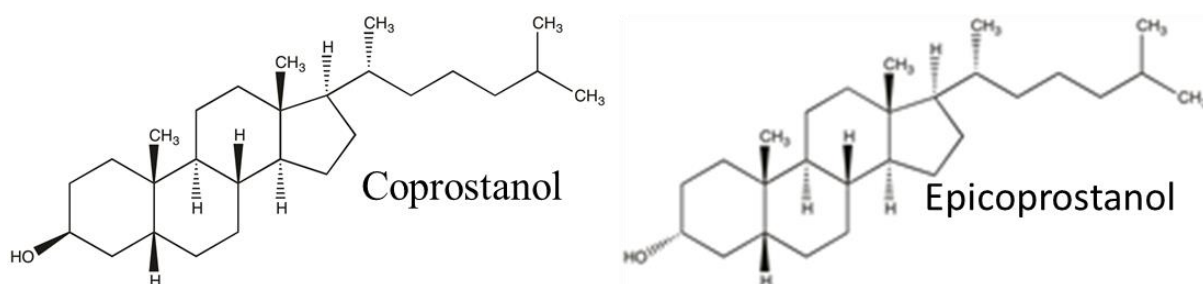


Figure 3.7. structure of coprostanol and epicoprostanol

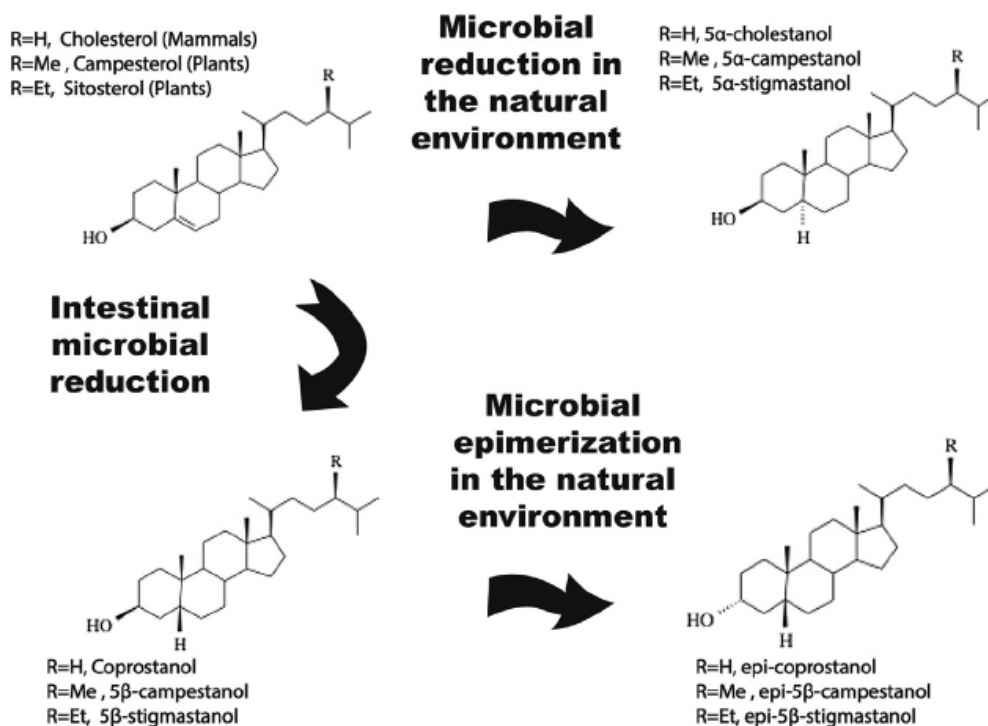


Figure 3.8. Microbial reduction of fecal in the intestinal and environment (figure: Sistiaga 2014) [66]

Geochemical composition

The geochemical composition in sedimentary archive can provide information on past climate variation, through reconstruction of water level, redox condition, as well as physical and chemical weathering in the sediment. An increase in the lithogenic elements such as Aluminum and Titanium in an active lake is generally characterized by episodes of enhanced exogenous sedimentation, these elements have high resistance to chemical weathering due to their low mobility, and they are often transported through the atmosphere as dust particles before deposition [67–71]. poorly weathered mineral deposit in sediments often lead to high potassium concentration when compared aluminum or titanium concentration. However, physical weathering processes leads to increased concentration of potassium because, parent rocks such as potassium are less diminished in mobile elements compared to titanium or aluminum. Hence potassium/titanium (k/Ti) ratio or potassium/aluminum (K/Al) ratio can be used to determine physical weathering in lake sediment [72].

The redox condition of a lake is controlled by the changes in the water table, which then regulates the lakes mineralization and humification. The mineralization of organic matter accelerates lake/peats degradation, which signifies a dryer condition with lower water tables

[73,74]. A higher concentration of Fe under oxic conditions in lakes is due to mineralization; therefore, redox-sensitive elements such as Fe and Mn can be used to infer Redox conditions in lakes. Fe is enriched under oxic conditions and indicates periods of droughts that affect the saturation of the lake [75]. Fe and Mn can also infer the transport and deposition episodes because they are associated with coarser particles entering the lake [73,76].

Reference

- [1] J.P.H. Van Wyk, Biowaste as a resource for bioproduct development, *Environ. Earth Sci.* 19 (2011) 875–883. <https://doi.org/10.1007/978-3-540-95991-5-82>.
- [2] D.A. Sear, M.S. Allen, J.D. Hassall, A.E. Maloney, P.G. Langdon, A.E. Morrison, A.C.G. Henderson, H. Mackay, I.W. Croudace, C. Clarke, J.P. Sachs, G. Macdonald, R.C. Chiverrell, M.J. Leng, L.M. Cisneros-Dozal, T. Fonville, Human settlement of East Polynesia earlier, incremental, and coincident with prolonged South Pacific drought, *Proc. Natl. Acad. Sci. U. S. A.* 117 (2020) 8813–8819. <https://doi.org/10.1073/pnas.1920975117>.
- [3] S.A. Elias, R.S. Bradley, *Paleoclimatology: Reconstructing Climates of the Quaternary*, 1999. <https://doi.org/10.2307/1552264>.
- [4] T. Mazurczyk, N. Piekielek, E. Tansey, B. Goldman, American archives and climate change: Risks and adaptation, *Clim. Risk Manag.* 20 (2018) 111–125. <https://doi.org/10.1016/j.crm.2018.03.005>.
- [5] W.F. Ruddiman, *Earth's Climate- Past and Future*, (2002).
- [6] R.S. Bradley, *Paleoclimatic Reconstruction*, 3rd ed., Elsevier Inc., 2015. <https://doi.org/10.1016/B978-0-12-386913-5.00001-6>.
- [7] E. Piovano, N. Scientific, S. Stutz, *Limnogeology in Southern South America : An overview LIMNOGEOLOGY IN SOUTHERN SOUTH AMERICA :*, (2014).
- [8] W. Ruddiman, W.H. Freeman, *Climate Archives , Data , and Models*, (2008).
- [9] D.G. Frey, *What is paleolimnology ?*, Kluwer Academic Publishers, 1988.
- [10] Y.A.O. Xiaojun, L.I.U. Shiyin, H.A.N. Lei, S.U.N. Meiping, Z. Linlin, Definition and classification system of glacial lake for inventory and hazards study, 28 (2018) 193–205.
- [11] G. Hutchinson, E, *A treatise on limnology*, (1957) 472–474.
- [12] B. Zolitschka, P. Francus, A.E.K. Ojala, A. Schimmelmann, Varves in lake sediments - a review, *Quat. Sci. Rev.* 117 (2015) 1–41. <https://doi.org/10.1016/j.quascirev.2015.03.019>.
- [13] D.A. Cenderelli, E.E. Wohl, Peak discharge estimates of glacial-lake outburst floods

- and A normal B climatic floods in the Mount Everest region , Nepal, (2001).
- [14] Zewdie Wondatir, Paleolakes, *Angew. Chemie Int. Ed.* 6(11), 951–952. (2012).
<https://doi.org/10.1007/978-1-4020-4410-6>.
- [15] W.M. Last, J.P. Smol, *Tracking Environmental Change Using Lake Sediments. Volume 2: Physical and Geochemical Methods*, 2002. https://doi.org/10.1007/0-306-47670-3_5.
- [16] B. Kaphle, K. Narayan Paudyal, B.R. Khanal, Lake Sediment proxies and their response to Indian Summer Monsoon: A Review from the Himalayas, *Bull. Nepal Geol. Soc.* 36 (2019).
- [17] C. Omuombo, D. Williamson, D. Olago, Biogeochemical proxy evidence of gradual and muted geolimnological response of Lake Nkunga, Mt. Kenya to climate changes and human influence during the past millennium, *Sci. African.* 8 (2020) e00416.
<https://doi.org/10.1016/j.sciaf.2020.e00416>.
- [18] J. Charles Umbanhowar, Recent Fire History of the Northern Great Plains, 135 (1996) 115–121.
- [19] Y. Ruan, M. Mohtadi, L.M. Dupont, D. Hebbeln, S. van der Kaars, E.C. Hopmans, S. Schouten, E.J. Hyer, E. Schefuß, Interaction of Fire, Vegetation, and Climate in Tropical Ecosystems: A Multiproxy Study Over the Past 22,000 Years, *Global Biogeochem. Cycles.* 34 (2020). <https://doi.org/10.1029/2020GB006677>.
- [20] C. Whitlock, C. Larsen, Charcoal as a Fire Proxy, (2002) 75–97.
https://doi.org/10.1007/0-306-47668-1_5.
- [21] J.M. Szeicz, Book Review: Sediment records of biomass burning and global change, 1998. <https://doi.org/10.1177/095968369800800317>.
- [22] A.T. Karp, A.I. Holman, P. Hopper, K. Grice, K.H. Freeman, Refined interpretations of polycyclic aromatic hydrocarbons for paleo-applications, *Geochim. Cosmochim. Acta.* 289 (2020) 93–113. <https://doi.org/10.1016/j.gca.2020.08.024>.
- [23] W.M.L. John P. Smol, H. John B. Birks, *Tracking Environmental Change Using Lake Sediments. Volume 3: Terrestrial, Algal, and Siliceous Indicators*, 2002.
- [24] C. Whitlock, *Tracking Environmental Change Using Lake Sediments*, (2001).

<https://doi.org/10.1007/0-306-47668-1-5>.

- [25] S.K. Id, M. Yamamoto, H. Shaari, R. Hayashi, The significance of pyrogenic polycyclic aromatic hydrocarbons in Borneo peat core for the reconstruction of fire history, (2021) 1–15. <https://doi.org/10.1371/journal.pone.0256853>.
- [26] A. Callegaro, D. Battistel, N.M. Kehrwald, F. Matsubara Pereira, T. Kirchgeorg, M. Del Carmen Villoslada Hidalgo, B.W. Bird, C. Barbante, Fire, vegetation, and Holocene climate in a southeastern Tibetan lake: A multi-biomarker reconstruction from Paru Co, *Clim. Past.* 14 (2018) 1543–1563. <https://doi.org/10.5194/cp-14-1543-2018>.
- [27] A.L.C. Lima, J.W. Farrington, C.M. Reddy, Combustion-derived polycyclic aromatic hydrocarbons in the environment - A review, *Environ. Forensics.* 6 (2005) 109–131. <https://doi.org/10.1080/15275920590952739>.
- [28] H.I. Abdel-Shafy, M.S.M. Mansour, A review on polycyclic aromatic hydrocarbons: Source, environmental impact, effect on human health and remediation, *Egypt. J. Pet.* 25 (2015) 107–123. <https://doi.org/10.1016/j.ejpe.2015.03.011>.
- [29] M.A. Olivella, T.G. Ribalta, A.R. De Febrer, J.M. Mollet, F.X.C.D.H. T, Distribution of polycyclic aromatic hydrocarbons in riverine waters after Mediterranean forest fires, 355 (2006) 156–166. <https://doi.org/10.1016/j.scitotenv.2005.02.033>.
- [30] C.L. Friedman, N.E. Selin, Long-range atmospheric transport of polycyclic aromatic hydrocarbons: A global 3-D model analysis including evaluation of arctic sources, *Environ. Sci. Technol.* 46 (2012) 9501–9510. <https://doi.org/10.1021/es301904d>.
- [31] T.E. Mcgrath, W.G. Chan, R. Hajaligol, Low temperature mechanism for the formation of polycyclic aromatic hydrocarbons from the pyrolysis of cellulose, 66 (2003) 51–70.
- [32] A.R. Bakhtiari, M.P. Zakaria, M.I. Yaziz, M.N.H. Lajis, X. Bi, M.R.M. Shafiee, M. Sakari, Distribution of PAHS and n-alkanes in Klang River Surface Sediments, Malaysia, *Pertanika J. Sci. Technol.* 18 (2010) 167–179.
- [33] B.A. Musa Bandowe, P. Srinivasan, M. Seelge, F. Sirocko, W. Wilcke, A 2600-year record of past polycyclic aromatic hydrocarbons (PAHs) deposition at Holzmaar (Eifel, Germany), *Palaeogeogr. Palaeoclimatol. Palaeoecol.* 401 (2014) 111–121.

- <https://doi.org/10.1016/j.palaeo.2014.02.021>.
- [34] M. Hajaligol, B. Waymack, D. Kellogg, Low temperature formation of aromatic hydrocarbon from pyrolysis of cellulosic materials, 80 (2001).
- [35] E.H. Denis, J.L. Toney, R. Tarozo, R. Scott Anderson, L.D. Roach, Y. Huang, Polycyclic aromatic hydrocarbons (PAHs) in lake sediments record historic fire events: Validation using HPLC-fluorescence detection, *Org. Geochem.* 45 (2012) 7–17. <https://doi.org/10.1016/j.orggeochem.2012.01.005>.
- [36] E.M. Rubin, Genomics of cellulosic biofuels, 454 (2008) 841–845. <https://doi.org/10.1038/nature07190>.
- [37] H. Yang, R. Yan, H. Chen, C. Zheng, D.H. Lee, D.T. Liang, In-depth investigation of biomass pyrolysis based on three major components: Hemicellulose, cellulose and lignin, *Energy and Fuels.* 20 (2006) 388–393. <https://doi.org/10.1021/ef0580117>.
- [38] L.J. Kuo, P. Louchouart, B.E. Herbert, Influence of combustion conditions on yields of solvent-extractable anhydrosugars and lignin phenols in chars: Implications for characterizations of biomass combustion residues, *Chemosphere.* 85 (2011) 797–805. <https://doi.org/10.1016/j.chemosphere.2011.06.074>.
- [39] J.C. Del Río, G. Marques, J. Rencoret, Á.T. Martínez, A. Gutiérrez, Occurrence of naturally acetylated lignin units, *J. Agric. Food Chem.* 55 (2007) 5461–5468. <https://doi.org/10.1021/jf0705264>.
- [40] P. McKendry, Energy production from biomass (part 1): Overview of biomass, *Bioresour. Technol.* 83 (2002) 37–46. [https://doi.org/10.1016/S0960-8524\(01\)00118-3](https://doi.org/10.1016/S0960-8524(01)00118-3).
- [41] M. Conedera, W. Tinner, C. Neff, M. Meurer, A.F. Dickens, P. Krebs, Reconstructing past fire regimes: methods, applications, and relevance to fire management and conservation, *Quat. Sci. Rev.* 28 (2009) 555–576. <https://doi.org/10.1016/j.quascirev.2008.11.005>.
- [42] D. Chen, A. Gao, K. Cen, J. Zhang, X. Cao, Z. Ma, Investigation of biomass torrefaction based on three major components: Hemicellulose, cellulose, and lignin, *Energy Convers. Manag.* 169 (2018) 228–237. <https://doi.org/10.1016/j.enconman.2018.05.063>.

- [43] N. Kehrwald, R. Zangrando, A. Gambaro, C. Barbante, Fire and climate: Biomass burning recorded in ice and lake cores, *EPJ Web Conf.* 9 (2010) 105–114. <https://doi.org/10.1051/epjconf/201009008>.
- [44] T. Kirchgeorg, S. Schüpbach, N. Kehrwald, D.B. McWethy, C. Barbante, Method for the determination of specific molecular markers of biomass burning in lake sediments, *Org. Geochem.* 71 (2014) 1–6. <https://doi.org/10.1016/j.orggeochem.2014.02.014>.
- [45] G. Leavesley, *Integrated Modeling and Decision Support for Water - and Environmental - Resources Management*, (2016).
- [46] E. Argiriadis, D. Battistel, D.B. McWethy, M. Vecchiato, T. Kirchgeorg, N.M. Kehrwald, C. Whitlock, J.M. Wilmschurst, C. Barbante, Lake sediment fecal and biomass burning biomarkers provide direct evidence for prehistoric human-lit fires in New Zealand, *Sci. Rep.* 8 (2018) 12113. <https://doi.org/10.1038/s41598-018-30606-3>.
- [47] M. Conedera, W. Tinner, C. Neff, M. Meurer, A.F. Dickens, P. Krebs, Reconstructing past fire regimes: methods, applications, and relevance to fire management and conservation, *Quat. Sci. Rev.* 28 (2009) 555–576. <https://doi.org/10.1016/j.quascirev.2008.11.005>.
- [48] B.R.T. Simoneit, J.J. Schauer, C.G. Nolte, D.R. Oros, V.O. Elias, M.P. Fraser, W.F. Rogge, G.R. Cass, Levoglucosan, a tracer for cellulose in biomass burning and atmospheric particles, *Atmos. Environ.* 33 (1999) 173–182. [https://doi.org/10.1016/S1352-2310\(98\)00145-9](https://doi.org/10.1016/S1352-2310(98)00145-9).
- [49] K.E. Peters, C.C. Walters, J.M. Moldowan, *The Biomarker Guide*, Cambridge University Press, 2004. <https://doi.org/10.1017/CBO9781107326040>.
- [50] R.T. Bush, F.A. McInerney, Leaf wax n-alkane distributions in and across modern plants: Implications for paleoecology and chemotaxonomy, *Geochim. Cosmochim. Acta.* 117 (2013) 161–179. <https://doi.org/10.1016/j.gca.2013.04.016>.
- [51] X. Wang, X. Huang, D. Sachse, W. Ding, J. Xue, Molecular paleoclimate reconstructions over the last 9 ka from a peat sequence in south China, *PLoS One.* 11 (2016). <https://doi.org/10.1371/journal.pone.0160934>.
- [52] a. O. Badejo, B.-H. Choi, H.-G. Cho, H.-I. Yi, K.-H. Shin, A paleoenvironmental reconstruction of the last 15 000 cal yr BP via Yellow Sea sediments using biomarkers

- and isotopic composition of organic matter, *Clim. Past Discuss.* 10 (2014) 1527–1565. <https://doi.org/10.5194/cpd-10-1527-2014>.
- [53] J. Han, M. Calvin, Hydrocarbon distribution of algae and bacteria, and microbiological activity in sediments., *Proc. Natl. Acad. Sci. U. S. A.* 64 (1969) 436–443. <https://doi.org/10.1073/pnas.64.2.436>.
- [54] D.R. Oros, B.R.T. Simoneit, Identification and emission factors of molecular tracers in organic aerosols from biomass burning Part 2. Deciduous trees, *Appl. Geochemistry.* 16 (2001) 1545–1565. [https://doi.org/10.1016/S0883-2927\(01\)00022-1](https://doi.org/10.1016/S0883-2927(01)00022-1).
- [55] R.C. Clark,, M. Blumer, DISTRIBUTION OF n-PARAFFINS IN MARINE ORGANISMS AND SEDIMENT, *Limnol. Oceanogr.* 12 (1967) 79–87. <https://doi.org/10.4319/lo.1967.12.1.0079>.
- [56] Y. Duan, J. He, Distribution and isotopic composition of n-alkanes from grass, reed and tree leaves along a latitudinal gradient in China, *Geochem. J.* 45 (2011) 199–207. <https://doi.org/10.2343/geochemj.1.0115>.
- [57] I.D. Bull, Matthew J. Lockheart, Mohamed M. Elhmmali, David J. Roberts, Richard P. Evershed, , Evershed RP (2002) The Origin of Faeces by Means of Biomarker Detection. *Environ Int - Google Scholar, Environ. Int.* 27 (2002) 647–654. https://scholar.google.de/scholar?hl=en&q=%2C+Evershed+RP+%282002%29+The+Origin+of+Faeces+by+Means+of+Biomarker+Detection.+Environ+Int&btnG=&as_sdt=1%2C5&as_sdtp=.
- [58] A. Callegaro, F. Matsubara Pereira, D. Battistel, N. Kehrwald, B. Bird, T. Kirchgeorg, C. Barbante, Fire, vegetation and Holocene climate in the south-eastern Tibetan Plateau: a multi-biomarker reconstruction from Paru Co, N/D (2018) 1–33. <https://doi.org/10.5194/cp-2018-19>.
- [59] R.M. D’Anjou, R.S. Bradley, N.L. Balascio, D.B. Finkelstein, Climate impacts on human settlement and agricultural activities in northern Norway revealed through sediment biogeochemistry., *Proc. Natl. Acad. Sci. U. S. A.* 109 (2012) 20332–20337. <https://doi.org/10.1073/pnas.1212730109>.
- [60] A. Ball, Using Faecal Sterols From Humans and Animals To Distinguish Faecal Pollution in Receiving Waters, 30 (1996) 2893–2900.

- [61] H. Birks, *Introduction to Quaternary Palaeoecology*, (2011) 1–10.
- [62] D. Battistel, R. Piazza, E. Argiriadis, E. Marchiori, M. Radaelli, C. Barbante, GC-MS method for determining faecal sterols as biomarkers of human and pastoral animal presence in freshwater sediments, *Anal. Bioanal. Chem.* 407 (2015) 8505–8514. <https://doi.org/10.1007/s00216-015-8998-2>.
- [63] I.D. Bull, I. a. Simpson, P.F. van Bergen, R.P. Evershed, Muck'n'molecules: organic geochemical methods for detecting ancient manuring, *Antiquity.* 3 (1999) 86–96. <https://doi.org/10.1017/S0003598X0008786X>.
- [64] V.C. Obuseng, F. Nareetsile, Bile Acids As Specific Faecal Pollution Indicators in Water and Sediments, *Eur. Sci. J.* 9 (2013) 273–286.
- [65] J. Holtvoeth, H. Vogel, B. Wagner, G.A. Wolff, Lipid biomarkers in Holocene and glacial sediments from ancient Lake Ohrid (Macedonia, Albania), *Biogeosciences.* 7 (2010) 3473–3489. <https://doi.org/10.5194/bg-7-3473-2010>.
- [66] A. Sistiaga, C. Mallol, B. Galván, R.E. Summons, The Neanderthal meal: A new perspective using faecal biomarkers, *PLoS One.* 9 (2014) 6–11. <https://doi.org/10.1371/journal.pone.0101045>.
- [67] J. Muller, M. Kylander, R.A.J. Wüst, D. Weiss, A. Martinez-Cortizas, A.N. LeGrande, T. Jennerjahn, H. Behling, W.T. Anderson, G. Jacobson, Possible evidence for wet Heinrich phases in tropical NE Australia: the Lynch's Crater deposit, *Quat. Sci. Rev.* 27 (2008) 468–475. <https://doi.org/10.1016/j.quascirev.2007.11.006>.
- [68] T. Ise, A.L. Dunn, S.C. Wofsy, P.R. Moorcroft, High sensitivity of peat decomposition to climate change through water-table feedback, *Nat. Geosci.* 1 (2008) 763–766. <https://doi.org/10.1038/ngeo331>.
- [69] G. Le Roux, E. Laverret, W. Shotyk, Fate of calcite, apatite and feldspars in an ombrotrophic peat bog, Black Forest, Germany, *J. Geol. Soc. London.* 163 (2006) 641–646. <https://doi.org/10.1144/0016-764920-035>.
- [70] H. Biester, Y.M. Hermanns, A. Martinez Cortizas, The influence of organic matter decay on the distribution of major and trace elements in ombrotrophic mires - a case study from the Harz Mountains, *Geochim. Cosmochim. Acta.* 84 (2012) 126–136. <https://doi.org/10.1016/j.gca.2012.01.003>.

- [71] W. Shotyk, Peat bog archives of atmospheric metal deposition: Geochemical evaluation of peat profiles, natural variations in metal concentrations, and metal enrichment factors, *Environ. Rev.* 4 (1996) 149–183. <https://doi.org/10.1139/a96-010>.
- [72] F. Arnaud, J. Poulenard, C. Giguët-Covex, B. Wilhelm, S. Révillon, J.P. Jenny, M. Revel, D. Enters, M. Bajard, L. Fouinat, E. Doyen, A. Simonneau, C. Pignol, E. Chapron, B. Vannièrè, P. Sabatier, Erosion under climate and human pressures: An alpine lake sediment perspective, *Quat. Sci. Rev.* 152 (2016) 1–18. <https://doi.org/10.1016/j.quascirev.2016.09.018>.
- [73] W. Chesworth, A.M. Cortizas, E. García-Rodeja, Chapter 8 The redox-pH approach to the geochemistry of the Earth's land surface, with application to peatlands, *Dev. Earth Surf. Process.* 9 (2006) 175–195.
- [74] J. Beer, K. Lee, M. Whitticar, C. Blodau, Geochemical controls on anaerobic organic matter decomposition in a northern peatland, *Limnol. Oceanogr.* 53 (2008) 1393–1407. <https://doi.org/10.4319/lo.2008.53.4.1393>.
- [75] O. Margalef, A. Martínez Cortizas, M. Kylander, S. Pla-Rabes, N. Cañellas-Boltà, J.J. Pueyo, A. Sáez, B.L. Valero-Garcés, S. Giralt, Environmental processes in Rano Aroi (Easter Island) peat geochemistry forced by climate variability during the last 70kyr, *Palaeogeogr. Palaeoclimatol. Palaeoecol.* 414 (2014) 438–450. <https://doi.org/10.1016/j.palaeo.2014.09.025>.
- [76] K. Schitteck, S.T. Kock, A. Lücke, J. Hense, C. Ohlendorf, J.J. Kulemeyer, L.C. Lupo, F. Schäbitz, A high-altitude peatland record of environmental changes in the NW Argentine Andes (24 ° S) over the last 2100 years, *Clim. Past.* 12 (2016) 1165–1180. <https://doi.org/10.5194/cp-12-1165-2016>.

CHAPTER FOUR: MATERIALS AND METHODS

Lake sediments are natural archives which give opportunity for the reconstruction of past climate and environmental changes as discussed in previous chapters. However, the degree to which past climate information can be retrieved from lake sediments depends on the sediment preservation capacity, such as sedimentation rate and disturbance during and after deposition [1]. Therefore, unstratified or unconsolidated lake sediment may not be suitable for reconstructing past climate conditions.

In this study, Sediment core were retrieved from the three Rapa Nui lakes (Rano Aroi, Rano Raraku and Rano Kao), for the purpose of past climate and environmental reconstruction. However, the particles of the sediment core retrieved from Rano Kao were non cemented together, the sediment was unstratified and unconsolidated which is not suitable for paleoclimate reconstruction. Consequently, only the sediment cores from Rano Raraku and Rano Aroi were considered for this research.

Below is a description of the sediment coring methods and the analytical methods used in this research.

4.1 Sediment core and water samples

Rano Aroi sediment and water sampling

Two parallel sediment cores of about 290 cm long were retrieved from Rano Aroi wetland (LTS-AROI17-1A) and (LTS-AROI17-1B), with a Livingstone corer that has a serrated edge, to enable the coring of sediments that are mixed with peat and wetland. Both cores were retrieved in three sections while standing on the surface of the wetland because no platform was required. The sediment core has a lighter band between 15 and 32 cm, which may likely result from mineral sedimentation.

I focused on the top 130 cm covering the last ~ 2000 cal years BP. Because previous studies have estimated human settlement on Rapa Nui to be between 800 CE to 1200 CE [2, 3]. Rano Aroi sediment core was sub-sampled at 1-cm vertical resolution for analysis [4]. About ~0.5 L of water was also collected from Rano Aroi to analyze trace elements (Te) and rare earth elements (REE). 0.45 μm polycarbonate system equipped with a manual vacuum pump was

used to filter the water samples in *in situ* through 0.45 μm cellulose nitrate membranes. The filtered water was in 50 mL HDPE bottles separate from membrane with suspended particulate matter (SPM).

Rano Raraku sediment and water sampling

Sediment core (LTS-RKU17-1A-1P-1) of about 100 cm long was retrieved from Rano Raraku with a Livingstone surface corer at 95 cm below the water surface. The sediment core has a mixture of older with younger sediment, likely caused by reservoir effect between 20 cm and 60 cm, which resulted in dating inconsistency.

Three surface water samples of ~ 0.5 L, and a total of six 4-cm thick topsoil samples of ~ 5 g was retrieved from Rano Raraku; samples were named corresponding to depth. Water samples were named (P1) 90, (P2) 51, and (P3) 38cm, while topsoil samples were named (P4), (P5), (P6) (P7), respectively. Samples were kept in a cool place at 4 $^{\circ}\text{C}$ before being transported to Ca`Foscari University of Venice (Italy) for analysis.



Figure 4.1. Present day images of the lake Rano Raraku (a), and Rano Aroi (b)

Table 4.1 Samples and sampling locations at Rano Raraku

	Lat.	Long.	Samples	Depth	Volume/weight
P1	-27.12220	-109.29031	• Water	0 cm	500 ml
			• Suspended particulate matter (SPM)		
			• Deep water	90 cm	500 ml
			• Suspended particulate matter (SPM)		
• Water-sediment interface (WSI)	0-2 cm	5 g			
• Bed sediment (BS)	3-5 cm	5 g			
P2	-27.12207	-109.28992	• Water	0 cm	500 ml
			• Suspended particulate matter (SPM)		
			• Deep water	50 cm	500 ml
• Suspended particulate matter (SPM)					
P3	-27.12221	-109.28951	• Water	0 cm	500 ml
			• Suspended particulate matter (SPM)		
			• Deep water	38 cm	500 ml
• Suspended particulate matter (SPM)					
P4	-27.12220	-109.29067	• Topsoil	-	5 g
P5	-27.12163	-109.29060	• Topsoil	-	5 g
P6	-27.12039	-109.28820	• Topsoil	-	5 g
P7	-27.12460	-109.28939	• Topsoil	-	5 g

4.2 Instrumental equipment and Sample preparation

Most of the analysis in this research was done at the Environmental Analytical Chemistry laboratories of Ca' Foscari University of Venice (Italy), while part of the analysis was conducted at the Paleoecology Lab of the Montana State University (Bozeman, MT, USA).

Different analytical methods were used to investigate different proxies or groups of proxies in this research. Biomarkers (levoglucosan, PAH, and fecal sterols) were analyzed using Gas chromatography-mass spectrometry (GC-MS) / ion chromatography-mass spectrometry (IC-MS), charcoal was analyzed through microscopic charcoal count, while multi-element analysis was analyzed using Inductively coupled plasma mass spectrometry (ICP-MS). The analytical methods are based on several literatures [5–11]. Each method is briefly explained below in details

4.3 Biomarker analytical process

Sample preparation

Sediment cores were sub-sampled at 1-cm vertical resolution and each sample were freeze-dried with *Edwards Modulyo freeze dryer*, the dried samples were ball milled with *Retsch Mixer Mill MM 400*. Samples were weighted to get the right amount for extraction.

Extraction

liquid-phase extraction was done using *Dionex Thermo Fisher ASE 350* (Accelerated Solvent Extractor), equipped with 20 mL stainless steel extraction cells. Each cell was prepared by placing a glass fiber filter at the bottom of the cell, followed by some diatomaceous earth, then 20 g of milled sediment sample. Internal standards were introduced (internal standard solution for monosaccharide anhydride, PAHs, and sterols) before adding sodium sulfate (Na_2SO_4) (to eliminate any form of moisture/water from the cell), the cells were filled with to the brim with diatomaceous earth and sealed. 10 sample cells and 2 blank cells (loaded with

diatomaceous earth and Na₂SO₄, spiked with internal standard) were extracted in every sequence. The samples were extracted using 9:1 mixture of dichloromethane and methanol (DCM-MeOH (v / v)) 3 extraction cycles were carried out at 100 °C and 1500 psi static: 5 followed by three statics lasting 5 minutes each min.

Volume reduction

Extract volume reduction was carried out using the Turbovap® (Caliper Life Science), extracts collected for the analysis for *n*-alkane, PAH, and fecal sterols were placed in a Turbovap at 23 °C under a gentle stream of nitrogen and evaporated to 0.5 mL.

Sample cleanup and concentration

The cleanup was based on solid-phase extraction method (SPE) with silica tubes topped, conditioned with a 40 mL mixture of *n*-hexane: dichloromethane = 1:1 until the stationary phase appeared to be homogeneous and translucent, then samples were loaded onto the SPE tubes. Samples were further separated into two fractions during the cleanup process, fraction 1 (F1) and fraction 2 (F2). F1 was used to analyze *n*-alkanes and PAHs, while F2 was used to analyze fecal sterols. F1 was eluted with 15 mL of HEX: DCM = 1:1 (containing PAHs and *n*-alkanes). The F2 was eluted with 40 mL of DCM (containing fecal sterols), the third fraction was eluted with 30 mL of MeOH to analyze monosaccharide anhydride. F1 was placed in the TurboVap II® and concentrated up to a volume of 250 µL, then transferred into a gas chromatography vial for analysis. F2 was set in the TurboVap II® at the same temperature and concentrated to 100-200 µL, after which it was to a 2 mL vial with a crew cap for derivatization. The third fraction (containing levoglucosan, mannosan, and galactosan) was reduced to complete dryness at 39 °C in TurboVap II; it was then recovered with 500 µL of ultrapure water and filtered by 0.22 µm filter syringes. Samples were transferred into plastic screw-capped vials and stored in the freezer until ready for analysis.

Derivatization

The F2 samples were derivatized before the analysis of fecal sterol, samples were placed in a 2mL vail and concentrated on completing dryness, the samples were recovered with 100 µL of DCM and 100 µL of 1% N, O-Bis(trimethylsilyl)trifluoroacetamide (BSTFA) TMCS solution, and heated at 70 °C in an hour in a thermoblock, then placed in a room temperature

for 24 hours to increase volatility and make the compound easily detectable in GC-MS during analysis.

Gas chromatography-mass spectrometry

Fractions 1 and 2 were analyzed by Agilent 7890 Gas chromatography system coupled to an Agilent 5975 MSD quadrupole mass spectrometer (GC-MS); this instrument uses gas chromatography (GC) for the separation of analytes and mass spectrometry (MS) for quantification. The solution is vaporized in the GC inlet immediately after the sample is injected. It is then moved to the chromatographic column (Agilent HP5-MS capillary column by the carrier gas (helium), (5%-phenyl)-methylpolysiloxane, 60 m, 0.25 mm inner diameter, 0.25 μm film thickness), the oven temperature increases. It separates compounds corresponding to their boiling point. After separation, compounds are transferred into the ion source and analyzed through a single quadrupole.

Ion chromatography-mass spectrometry

Monosaccharide anhydrides were analyzed by an ion chromatographic system (Dionex, ICS 5000, Thermo Fisher Scientific) coupled to a single quadrupole mass spectrometer (MSQ Plus, Thermo Fisher Scientific); this instrument is used to analyze ionic compounds that are soluble in water. A CarboPacTM PA10 column (ethylvinylbenzene 55% divinylbenzene, 2 x 250 mm, Thermo Fisher Scientific) with a guard column AminoTrapTM (polymer resin-based, 2 x 50mm, Thermo Fisher Scientific) to block amino acids that could interfere with the analysis. The reproducibility in the preparation of the solution is guaranteed by the mobile phase, which is a solution of NaOH prepared by an eluent generator. The operating flow is 250 $\mu\text{L min}^{-1}$. The sample is injected at a volume of 50 μL . It elutes from 0 to 30 minutes at a concentration of 20 mM in the mobile phase; between 30 and 45 minutes, a NaOH solution is used 100 mM (washing step); it returns to the initial concentration of 20 mM to rebalance the column between 45 and 55 minutes before entering the detector the mobile phase is removed by a suppressor (ASRS 500, 2 mm, Thermo Fisher Scientific). A solution of MeOH / ammonia (7 %) at 0.025 mL min^{-1} to increase the volatility of the aqueous solvent and thus improve the ionization yield of the analytes. The ion source is an electrospray (ESI) and

works as an interface between the high working pressure (2000 psi) of the chromatographic system and the vacuum of the mass spectrometer.

Quantification

Response factor was injected into GC-MS three times for every 14 samples (1 batch) that were injected, the limit of detection (LOD) and limit of quantification (LOQ) of every batch of analyses sample was quantified by the total average of the 3-response factor, which was injected same day as the samples and the mean of the blanks. The method uncertainty was estimated about 15/20% of the amount obtained for each class of biomarker analyzed. Each chromatograph was integrated using retention times of the associated response factor for comparison.

m/z 71 was used to quantify the n-alkanes in the range C₁₂-C₃₅.

Three different internal standards were used for the quantification of PAHs. ¹³C-Acenaphthylene was used in the quantification of light molecular weight PAHs (3rings), mid-weight PAHs

They were quantified ¹³C-Phenanthrene, while ¹³C-Benzo(a)Pyrene was used for the quantification of heavyweight PAHs.

The target ion for monosaccharide anhydride is quantification was m/z 161, and qualifiers were m/z 110 and 113.

Table 4.2 Mass to charge ratios and response fact of the biomarkers considered in this study

<i>n</i> - alkane	<i>m/z</i>
C ₁₀ -C ₃₅	71

PAH	<i>m/z</i>	Response factor
Light molecular weights PAHs		
Naphthalene	128	
Acenaphthylene	152	

Acenaphthene	154	¹³ C Acenaphthylene 158 <i>m/z</i>
Fluorene	166	
Mid molecular weight PAHs		
Phenanthrene	178	¹³ C Anthracene 184 <i>m/z</i>
Anthracene	178	
Fluoranthene	202	
Pyrene	202	
Benzo(a)Anthracene	228	
Chrysen	228	
Retene	234	
Heavy molecular weight PAHs (5-6 rings PAHs)		
Benzo(b)Fluoranthene	252	¹³ C Benzo(a)Pyrene 256 <i>m/z</i>
Benzo(k)Fluoranthene	252	
Benzo(e)Pyrene	252	
Benzo(a)Pyrene	252	
Perylene	252	
Benzo(ghi)Perylene	276	
Indeno(1,2,3-c,d)Pyrene	276	
Dibenzo(A, H)Anthracene	278	

Monosaccharide Anhydride	<i>m/z</i>	Response factor
Levoglucosan	161	

Mannosan	110	¹³ C ₆ Levoglucosan 167 <i>m/z</i>
Galactosan	113	

Fecal Sterol	<i>m/z</i>	
Coprostanol (CoP)	215	
epiCoprostanol (e-CoP)	215	

4.4 Charcoal analytical process

The sedimentary charcoal count was carried out using charcoal microscopic analysis at Montana State University (Bozeman, MT, USA). Sediment was subsampled into 1 cm intervals, two cc was taken from each sample and deflocculated in 50 ml of 10% Na (PO₃)₃ (sodium hexametaphosphate) solution, mixed with 50 ml of disinfecting bleach for 24 hours, deflocculated sediment was wet sieved with distilled water through 125 μm screen, the charcoal particles were identified, tallied and counted with dissecting microscope ~50 magnification. Charcoal was identified and characterized based on three main factors, particle texture, color, and size. (1) particles which have cellular structure and can be brittle when spiked under a microscope, signifying burnt biomass, (2) Large particles generally indicates local fire occurrences, such particle size does not travel far from the source fire (3) the most important factor for charcoal count classification is the color, only completely black particles are counted, brown particles that may represent an incomplete burn are not counted.

4.5 multi-elemental analysis

43 Trace element (TE) and rare earth element (REE) including Na, U, Ge, Al, Si, P, Ca, Sc, Ti, V, Cr, Mn, Fe, K, Co, Ni, Cu, Mg, Ga, As, Se, Y, Mo, Cd, B, Ba, Pb, Th and Sr (TE); La, Eu, Pr, Nd, Sm, Gd, Dy, Ho, Ce, Er, Tb, Tm, Yb and Lu (REE) was analyzed in Rano Aroi core, TEs and REEs in sediment and suspended particulate matter (SPM) was analyzed through acid digestion (mixture of HNO₃, HCl and HF (6:2:1 mL, super purity grade acids,

Romil)) in a microwave oven, at a temperature up to 200 °C in a pressurized Teflon vessels with a controlled program explicitly enhanced for complete mineralization. Samples were then diluted in ultra-pure water to meet the calibration range before it was introduced into inductively coupled plasma-mass spectrometry (ICP-MS) using an iCAP RQ (Thermo Scientific) instrument equipped with an ASX-560 autosampler (Teledyne Cetac Technologies). PFA cyclonic spray chamber at 2.7 °C, sapphire injector, quartz torch, Ni cones and 1550 W of plasma radio frequency power, kinetic energy discrimination – high matrix mode using He as the collision gas (4.3 mL min⁻¹) was used to perform the acquisition.

External calibration with multi-elemental standards was used to quantify all elements, and a combination of the certified multi-elemental solutions IMS-101, IMS-102, and IMS-104 (10 µg g⁻¹, Ultra Scientific) was used to prepare the standards in ultrapure grade HNO₃ 2% v/v, to cover 0.02-200 ng g⁻¹ (TE) or 0.002-20 ng g⁻¹ (REE) range.

Inductively coupled plasma with sector field mass spectrometer (ICP-SFMS model Element-XR, Thermo Scientific) was used for the quantification of TEs and REEs in ultrapure water, while HNO₃ (Romil) was used to satisfy water sample before the analysis, and the method accuracy was access through certified reference material (TMRAIN95).

Total Organic Carbon in sediments (OC %) was analyzed using a Flash 2000 Thermo Scientific Elemental Analyzer. 200 µg of the dry sample was treated with HCl (1:1) and then sealed in tin capsules, after which samples were placed in a 950 °C CHNO quartz reactor.

4.6 Rano Raraku water sample preparation and analysis

0.45 µm cellulose nitrate membranes (Whatman) was used to filter water samples *in situ* with a polycarbonate system equipped with a manual vacuum pump. Plastic Petri dishes were used to store Membranes containing suspended particulate matter (SPM), while the filtered water was kept in 50 mL HDPE bottles.

Liquid samples were injected into ion chromatography system (883 Basic IC plus, Metrohm) equipped with a Metrosep Cation 1-2 (particle size 7 µm; eluent: HNO₃ 3 mM) and a Metrosep Anion supp/4 (particle size 5 µm; eluent: HCO₃⁻/CO₃²⁻ 1.7/1.8 mM) for Ion's

analysis (Cl^- , SO_4^{2-} , NO_3^- , NH_4^+ , Na^+ , K^+ , Ca^{2+} and Mg^{2+}) after samples were filtered through 0.45 μm syringe filters.

Reference

1. Ellegaard, M., Clokie, M.R.J., Cypionka, T., Frisch, D., Godhe, A., Kremp, A., Letarov, A., McGenity, T.J., Ribeiro, S., John Anderson, N.: Dead or alive: sediment DNA archives as tools for tracking aquatic evolution and adaptation. *Commun. Biol.* 3, 1–11 (2020). <https://doi.org/10.1038/s42003-020-0899-z>
2. Flenley, J.R., King, S.M.: Late Quaternary Pollen records from Easter Island. *Nature.* 307, 47–50 (1984). <https://doi.org/10.1038/307047a0>
3. Hunt, T.L., Lipo, C.P., Science, S., Series, N., Mar, N., Hunt, T.L., Rpo, C.: Late Colonization of Easter Island Published by : American Association for the Advancement of Science Stable URL : <http://www.jstor.com/stable/3845669> Linked references are available on JSTOR for this article : Late Colonization of Easter Island. 311, 1603–1606 (2006)
4. Argiriadis, E., Martino, M., Segnana, M., Poto, L., Vecchiato, M., Battistel, D., Gambaro, A., Barbante, C.: Multi-proxy biomarker determination in peat: Optimized extraction and cleanup method for paleoenvironmental application. *Microchem. J.* 156, 104821 (2020). <https://doi.org/10.1016/j.microc.2020.104821>
5. Battistel, D., Piazza, R., Argiriadis, E., Marchiori, E., Radaelli, M., Barbante, C.: GC-MS method for determining faecal sterols as biomarkers of human and pastoral animal presence in freshwater sediments. *Anal. Bioanal. Chem.* 407, 8505–8514 (2015). <https://doi.org/10.1007/s00216-015-8998-2>
6. Battistel, D., Argiriadis, E., Kehrwald, N., Spigariol, M., Russell, J.M., Barbante, C.: Fire and human record at Lake Victoria, East Africa, during the Early Iron Age: Did humans or climate cause massive ecosystem changes? *Holocene.* 27, 997–1007 (2017). <https://doi.org/10.1177/0959683616678466>
7. Schroeter, N., Lauterbach, S., Stebich, M., Kalanke, J., Mingram, J., Yildiz, C., Schouten, S., Gleixner, G.: Biomolecular Evidence of Early Human Occupation of a

- High-Altitude Site in Western Central Asia During the Holocene. *Front. Earth Sci.* 8, 1–13 (2020). <https://doi.org/10.3389/feart.2020.00020>
8. Li, Y., Yang, S., Xiao, J., Jiang, W., Yang, X.: Hydrogen isotope ratios of leaf wax n-alkanes in loess and floodplain deposits in northern China since the Last Glacial Maximum and their paleoclimatic significance. *Palaeogeogr. Palaeoclimatol. Palaeoecol.* 509, 91–97 (2018). <https://doi.org/10.1016/j.palaeo.2017.08.009>
 9. Gregoris, E., Argiriadis, E., Vecchiato, M., Zambon, S., De Pieri, S., Donato, A., Contini, D., Piazza, R., Barbante, C., Gambaro, A.: Gas-particle distributions, sources and health effects of polycyclic aromatic hydrocarbons (PAHs), polychlorinated biphenyls (PCBs) and polychlorinated naphthalenes (PCNs) in Venice aerosols. *Sci. Total Environ.* 476–477, 393–405 (2014). <https://doi.org/10.1016/j.scitotenv.2014.01.036>
 10. Vecchiato, M., Bonato, T., Bertin, A., Argiriadis, E., Barbante, C., Piazza, R.: Plant Residues as Direct and Indirect Sources of Hydrocarbons in Soils: Current Issues and Legal Implications. (2017). <https://doi.org/10.1021/acs.estlett.7b00464>
 11. Whitlock, C., Larsen, C.: Charcoal as a Fire Proxy. 75–97 (2002). https://doi.org/10.1007/0-306-47668-1_5

CHAPTER FIVE: RANO RARAKU

5.1 Rano Raraku age model

Eight sample points of the Rano Raraku core were dated in Beta Analytic lab (Miami, FL, USA), an accelerator mass spectrometer (AMS) ^{14}C was used to analyze the sample (Table 2). This dating method relies on the decay rate of ^{14}C ; by using the AMS to measure the amount of ^{14}C in the samples, the result is then calibrated using the difference in the concentration of ^{14}C present in the environment. the chronography of the Rano Raraku core could not be determined due to reservoir effect in the sediment core between 20 cm and 60 cm [1].

Table 5.1 Rano Raraku age model data

Lab ID	Depth (cm)	Weight (mg)
LTS_RKU_8-9	8.5	1.4
LTS_RKU_30-32	31.5	1.7
LTS_RKU_38-42	40	16.1
LTS_RKU_47-49	48	6.6
LTS_RKU_61-62	61.5	19.2
LTS_RKU_68-70	69	12.2
LTS_RKU_78-80	79.5	4.5
LTS_RKU_85-86	85.5	~ 1

Mixture of old and young
Sediment in Rano Raraku core

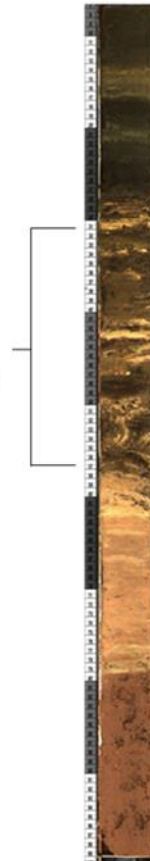


Figure 5.1 Images of the Rano Raraku sediment core showing a mixture between old and young sediment (reservoir effect) between 0.2 m and 0.6 m

5.2 Results

The Rano Raraku result presented in this study focused on identifying the primary mechanism that characterized the lake. The tables below present the trace (TE) and rare earth elements (REE), isotopic composition, ions, and diagnostic element ratios for the matrices analyzed.

Major elements and ions

Table 5.1 reports the concentrations of the major elements filtered in water samples. Chloride and sodium (970 ± 30 and 610 ± 10 mg L⁻¹) were the most abundant in the dissolve fraction, followed by magnesium and sulfate (53 and 30 mg L⁻¹, respectively); Na/Cl ratio is 0.63 on average, which is slightly higher when Na: Cl ratio in seawater (0.56), revealing a significant contribution marine source, Major ions in Rano Raraku (Cl⁻, SO₄²⁻, Na⁺, K⁺, Ca²⁺, and Mg²⁺)

correlate to ($r^2 = 0.970$; with a slope of 18 ± 1 ; p -value < 0.001) revealing marine fingerprint between Rano Raraku and typical seawater [2]. SO_4 : Cl value stands at 0.03, substantially lower than seawater (0.14); this may be due to less precipitation of soluble sulfate salts. The lower concentration of nitrate ($< 0.5 \text{ mg L}^{-1}$) and ammonium ($\sim 5 \text{ mg L}^{-1}$) can be attributed to lack of nitrification reactions, where an increase in dissolved forms of manganese compared to iron ($\text{Mn/Fe} = 1.3$; $\text{SD} = 0.5$) was observed.

The concentration of terrigenous elements is particularly high in Suspended particulate matter (SPM), especially elements that likely precipitate or adsorb organic material or mineral particles. Ca, Mg, Fe, Al and Mn are strongly partitioned in SPM. Conversely, the more soluble Na ions are preferentially distributed in the aqueous phase. Although Fe and Mn have a higher concentration in SPM, their concentration becomes lesser than iron when compared to the dissolved fraction ($\text{Mn/Fe} = 0.07$; $\text{SD} = 0.02$). However, we were unable to analyze the major anions content in the SPM because of a limited amount of filter samples.

The variability of elements in topsoil samples is higher compared to water and filters. The most abundant elements are Si, Fe, and Al, with concentrations of 310-410, 135-180, and 100-150 mg g^{-1} , respectively. The equation proposed by Reinmann and De Caritat (2000) [3] was used for the calculation of enrichment factors (EFs), and Al was used to normalize the element concentration used as a conservative element. EFs were calculated referring to Upper crust composition, through the [4], which resulted in a slightly concentration increase in iron and manganese (2.25 and 2.04 respectively), contributing to providing the soil's reddish color. The Rano Raraku soil has a higher concentration of Fe and Mn; the Mn/Fe ratio was 0.018 ($\text{SD} = 0.004$), comparable to the upper crust ratio ($\text{Mn/Fe} \approx 0.020$; p -value=0.28). However, Mn/Fe is notably lower than water and SPM (p -value < 0.005). The sodium concentration is low at (40-280 $\mu\text{g g}^{-1}$) compared to the composition of the upper crust ($\text{EF} \sim 10^{-3}$). Sodium depletion and variability can be ascribed to leaching and/ lake level oscillation.

Table 5.2. Major ions, trace and rare earth elements, isotopic composition, and diagnostic element ratios in water samples from Rano Raraku

Element	Water (n=6*)	SPM (n=6)	Soil (n=6)		EF (soil)
Cl^- (mg L^{-1})	970 ± 20	n.a.	-	-	-
SO_4^{2-} (mg L^{-1})	30 ± 10	n.a.	-	-	-
Na (mg L^{-1})	610 ± 10	15 ± 5	$\mu\text{g g}^{-1}$	100 ± 100	$(3 \pm 2) 10^{-3}$
K (mg L^{-1})	22.3 ± 0.4	16 ± 6	mg g^{-1}	5 ± 2	0.13 ± 0.05

Ca (mg L ⁻¹)	14.6 ± 0.3	60 ± 30	“	1.0 ± 0.8	0.03 ± 0.02
Mg (mg L ⁻¹)	53.0 ± 0.7	140 ± 60	“	7 ± 4	0.3 ± 0.2
NH ₄ ⁺ (mg L ⁻¹)	5 ± 2	n.a.		n.a.	-
Fe (µg L ⁻¹)	2.1 ± 0.7	900 ± 600	“	150 ± 20	2.2 ± 0.3
Al (µg L ⁻¹)	64 ± 10	800 ± 600	“	140 ± 20	
Mn (µg L ⁻¹)	2.5 ± 0.5	60 ± 20	“	2.7 ± 0.7	2.0 ± 0.5
Si	-	n.a.	“	360 ± 30	0.5 ± 0.1
Ti	-	n.a.	“	9 ± 2	1.4 ± 0.2
Mn/Fe	1.3 (0.5)	0.07 (0.02)		0.018 (0.004)	0.020

Trace Elements

The trace elements (Ba, Sr, Cd, Pb, V, Cr, Co, Ni, Cu) analyzed in all the environmental matrices are shown in Table 5.2. Sr has a higher concentration than Ba (Sr: Ba ≈ 25); this might be affected by a marine input; however, Ba ratio is close to 1 in the SPM, while soil has a higher concentration in Ba (Ba: Sr ≈ 8.6). The dissolved forms of Cd, Cr, V, Pb, Co, and Ni have a range of concentration between 60 and 135 µg L⁻¹, while Cu concentration in SPM stays below 1 µg L⁻¹, Cr and V have a higher concentration compared to the other elements, while Cd content is below 20 ng L⁻¹. There is no evidence of concordable enrichments among the trace elements analysed in soils. Instead, there is a significant depletion in most aspects such as Pb, V, and Ni (EF < 0.1).

Table 5.3. Trace elements in filtered water, suspended matter, and soils from Rano Raraku.

Element	Water (n=6*)	Suspended Matter (n=6)		Soil (n=6)	EF (soil)
Ba (µg L ⁻¹)	25 ± 5	2 ± 1	µg g ⁻¹	210 ± 40	0.20 ± 0.05
Sr (µg L ⁻¹)	600 ± 100	1.7 ± 0.8	“	30 ± 10	0.05 ± 0.01
Cd (µg L ⁻¹)	33 ± 8	0.013 ± 0.004	ng g ⁻¹	73 ± 8	0.47 ± 0.01
Pb (µg L ⁻¹)	130 ± 30	0.11 ± 0.08	µg g ⁻¹	1.6 ± 0.1	0.05 ± 0.01
V (µg L ⁻¹)	120 ± 30	1.9 ± 0.4	“	4 ± 2	0.03 ± 0.01
Cr (µg L ⁻¹)	60 ± 10	6.4 ± 0.8	“	60 ± 20	0.4 ± 0.1
Co (µg L ⁻¹)	75 ± 4	0.2 ± 0.1	“	50 ± 20	1.6 ± 0.5
Ni (µg L ⁻¹)	120 ± 50	0.3 ± 0.1	“	5 ± 1	0.07 ± 0.02

Cu ($\mu\text{g L}^{-1}$)	0.7 ± 0.2	0.8 ± 0.2	“	40 ± 10	0.8 ± 0.3
-----------------------------	---------------	---------------	---	-------------	---------------

Rare Earth Elements

the results of the analyzed rare earth elements (REE) in SPE, soil sample, and water sample are presented in **Table 11**, concentrations of REE in filtered water and SPM ranges between 0.2 and 3.5 ng L^{-1} and from 1 to 92 ng L^{-1} , respectively. In contrast, the concentration in soil samples ranges from 0.2 to 38 $\mu\text{g g}^{-1}$. The EFs values are between 0.1 and 0.5, more noticeable low rare earth elements (LREE), Ce excluded, rather than high rare earth elements (HREE). Rano Raraku soil is slightly depleted in REEs; however, this depletion is not significant ($0.1 < \text{EF}_{\text{REE}} < 10$). s

The diagnostic ratio between LREE (La, Pr, and Nd) and HREE (Er, Tm, Yb, and Lu) was calculated based on the following equation for all the samples:

$$\left(\frac{\text{LREE}}{\text{HREE}}\right)_i = \frac{4 \cdot \left(\frac{[\text{La}]_i}{[\text{La}]_c} + \frac{[\text{Pr}]_i}{[\text{Pr}]_c} + \frac{[\text{Nd}]_i}{[\text{Nd}]_c}\right)}{3 \cdot \left(\frac{[\text{Er}]_i}{[\text{Er}]_c} + \frac{[\text{Tm}]_i}{[\text{Tm}]_c} + \frac{[\text{Yb}]_i}{[\text{Yb}]_c} + \frac{[\text{Lu}]_i}{[\text{Lu}]_c}\right)}$$

The subscript i indicates the concentration in samples (water, SPM, or soil), and the subscript c refers to the upper crust concentration [4]. The Rano Raraku water has LREE/HREE ratio that is significantly lower than the concentration in SPM (p -value < 0.002), while the concentration in SPM is lower than that of soil.

Cerium anomaly was defined as (Ce/Ce^*) and calculated using the following equation, using the Elderfield et al., 1982 method [5].

$$\frac{\text{Ce}}{\text{Ce}^*} = \frac{3 \cdot \left(\frac{[\text{Ce}]_i}{[\text{Ce}]_c}\right)}{2 \cdot \left(\frac{[\text{La}]_i}{[\text{La}]_c} + \frac{[\text{Nd}]_i}{[\text{Nd}]_c}\right)}$$

The values of Ce anomalies were higher in soil (between 1.27 and 5.87), the average value of 2.87 (SD=1.68) compared to the values in water and SPM 0.43 (SD=0.05) and 0.75 (SD=0.03), respectively. However, REE concentration is depleted compared to the upper crust composition (ranges between 0.10 and 0.45); cerium has a higher concentration than REEs, indicating that Ce/Ce^* may be affected by the selected fractionation process.

Table 5.4. Rare Earth Elements in filtered water suspended matter and soils from Rano Raraku.

Element	Water (n=5)	Suspended Matter (n=6)	Soil (n=6)	EF
La (ng L ⁻¹)	2.3 ± 0.7	40 ± 30	μg g ⁻¹ 5 ± 3	0.10 ± 0.06
Ce (ng L ⁻¹)	3 ± 1	90 ± 70	“ 38 ± 7	0.35 ± 0.05
Pr (ng L ⁻¹)	0.7 ± 0.2	13 ± 9	“ 1.9 ± 0.9	0.16 ± 0.09
Nd (ng L ⁻¹)	3.1 ± 0.8	42 ± 31	“ 6 ± 3	0.14 ± 0.08
Sm (ng L ⁻¹)	2.8 ± 0.7	9 ± 7	“ 1.6 ± 0.7	0.2 ± 0.1
Eu (ng L ⁻¹)	0.8 ± 0.1	4 ± 3	“ 0.7 ± 0.3	0.4 ± 0.2
Gd (ng L ⁻¹)	1.2 ± 0.3	10 ± 7	“ 2.0 ± 0.9	0.3 ± 0.1
Tb (ng L ⁻¹)	0.25 ± 0.03	2 ± 1	“ 0.4 ± 0.2	0.4 ± 0.2
Dy (ng L ⁻¹)	1.7 ± 0.3	9 ± 7	“ 2 ± 1	0.4 ± 0.2
Ho (ng L ⁻¹)	0.49 ± 0.07	3 ± 2	“ 0.6 ± 0.3	0.4 ± 0.2
Er (ng L ⁻¹)	1.6 ± 0.2	6 ± 4	“ 1.4 ± 0.7	0.4 ± 0.2
Tm (ng L ⁻¹)	0.28 ± 0.04	1.3 ± 0.6	“ 0.2 ± 0.1	0.4 ± 0.2
Yb (ng L ⁻¹)	1.9 ± 0.2	4 ± 3	“ 1.2 ± 0.5	0.4 ± 0.2
Lu (ng L ⁻¹)	0.42 ± 0.04	1.2 ± 0.6	“ 0.2 ± 0.1	0.4 ± 0.2
LREE/HREE	0.10 (0.01)*	0.47 (0.08)	0.33 (0.09)	
Cerium Anomaly	0.43 (0.07)	0.75 (0.04)	2.9 (1.7)	

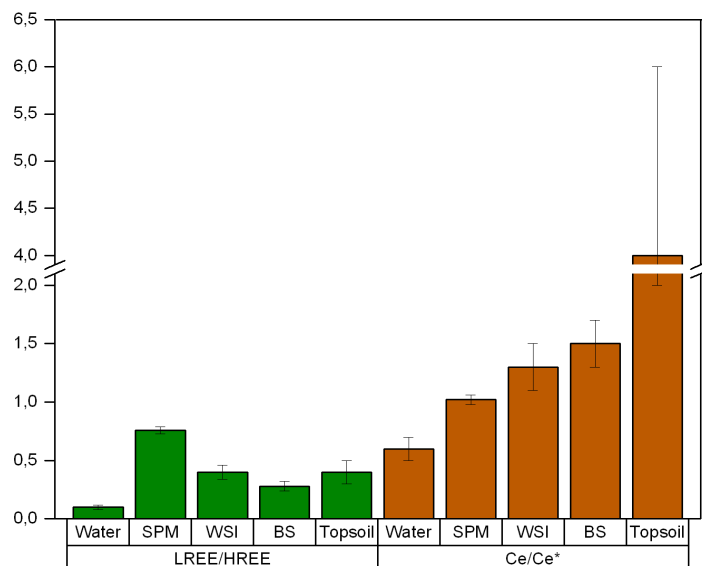


Figure 5.2. Ce/Ce* and LREE/HREE mean ratios with standard deviation in the considered matrices

Water isotopic composition

Determination of $\delta^2\text{H}$ and $\delta^{18}\text{O}$ in six water samples were 24.60 ± 1.35 ‰ and 4.01 ± 0.06 ‰; respectively, this positive value is an indication of an affected lake by predominant evaporation processes. A simple model that neglects the resistance in mixing in the liquid phase [6] can be used to model a close water system with no inflow/outflow, and evaporation is the only factor the drives isotopic composition. Using the Craig-Gordon model, the observed slope of the evaporation line (LEL) is:

$$S_{LEL} = \frac{\left[\frac{h(\delta_A - \delta_P) + (1 + \delta_P) \left(\varepsilon_K + \frac{\varepsilon^+}{\alpha^+} \right)}{h - \varepsilon_K - \frac{\varepsilon^+}{\alpha^+}} \right]_{\delta^2\text{H}}}{\left[\frac{h(\delta_A - \delta_P) + (1 + \delta_P) \left(\varepsilon_K + \frac{\varepsilon^+}{\alpha^+} \right)}{h - \varepsilon_K - \frac{\varepsilon^+}{\alpha^+}} \right]_{\delta^{18}\text{O}}}$$

δ_A is the isotopic compositions of atmospheric moisture,

δ_P the isotopic composition of the precipitation,

h is the relative humidity,

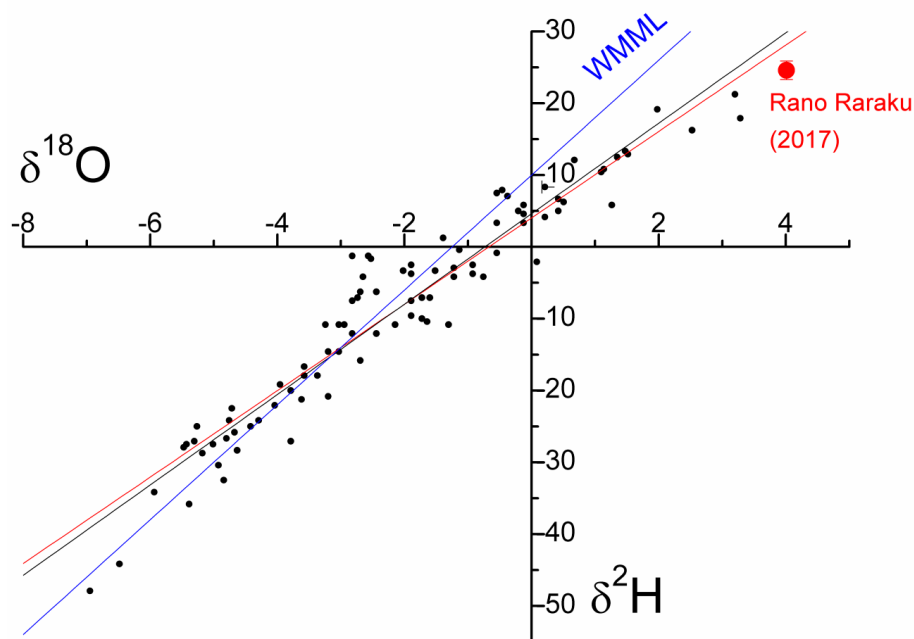
α^+ is the liquid-vapor equilibrium isotopic fractionation,

ε^+ is the equilibrium isotopic separation between liquid and vapor,

ε_K is the equivalent kinetic isotopic separation based on tunnel experiments.

Mean values of -8.58 and -2.10 ‰ for $\delta^2\text{H}$ and $\delta^{18}\text{O}$, respectively, based on δ_P values on the isotopic composition of rainfalls reported in Herrera and Custodio (fig 5.3) [7], precipitation equilibrium assumption $\delta_A = \frac{(\delta_P - \varepsilon^+)}{\alpha^+}$ was used to determine the value of δ_A , Horita and

Wesolowski equation was used in the estimation of α^+ value, where α^+ is a exclusively a function of the temperature which was assumed to be 20°C in this study [8], the assumption was because Rapa Nui temperatures range between 18°C in July/September and 23°C in January/Mar [7], $\varepsilon^+ = \alpha^+ - 1$ was used for the calculation of value of ε^+ , were $\varepsilon_K = n \cdot C_K^0 \cdot \theta \cdot (1 - h)$ was used for the determination ε_K values, open bodies for $n = 0.5$, C_K^0 is 25.0‰ and 28.6 ‰ for ^2H and ^{18}O , respectively, respectively, and θ was assumed ≈ 1 for small water bodies. Relative humidity was set to $h=0.79$, the value of LEL was slight 6.02, slower than the mean meteoric water line ($\delta^2\text{H}=8 \cdot \delta^{18}\text{O}+10$ ‰ fig), which forced the straight line through the mean value, $\delta^2\text{H}=6.02 \cdot \delta^{18}\text{O} + 4.04$ was obtained.ss



5.3 Isotopic composition of rainfalls in Rapa Nui (black dots; from Herrera and Custodio 2008) and Rano Raraku water in 2007 (red dot). Mean meteoric water line (blue), rainfalls best fit (black line), and straight-line derived from evaporation model (red line).

The Marine Origin of Rano Raraku Water

The Rano Raraku water can be ~20 times diluted seawater because the major elements and ions in the aqueous phase reveal that the lake gets a substantial input from marine origin; this is, however, supported by the lack of stream inflow from another water body, which means the primary source of input is from meteoric water, saline rainfall should be expected typically along the coast in an island located in the middle of the Pacific Ocean like Rapa Nui. Concentration in precipitations of Chloride and sodium that were collected at Hanga Roa In 2002-2003 ranges between 3-14 mg L⁻¹ [7]; a similar value was obtained in this study between 6 and 12 mg L⁻¹ of Cl⁻ in meteoric waters at a distance of about 1 km from the sea, with the use of Erikson (1952) proposed equation. The Na: Cl ratio in Rano Raraku waters (0.63) was slightly higher than seawater (0.56), but similar to meteoric waters at Hanga Roa that was 0.74 ± 0.12 (p -value = 0.016) [1], however terrestrial input does not contribute to the excess value of Na obtained from Rano Raraku waters, therefore, meteoric water is the main source of Rano Raraku Cl and Na. this is the cause of Na shortage in the soil around Rano Raraku basin. However, SO₄ in rainfalls is considerably higher in seawater than Rano Raraku [7], although SO₄ was not analyzed in superficial sediments and SPM in this study due to

lack of samples. Sr and Ba distributions can be used to explain the SO₄ depletion. The concentration of Ba in Rano Raraku waters (180 nmol L⁻¹). Carbonate-rich saline lakes such as lake Airkhan and lake Tsagaan, have similar Ba concentration as Rano Raraku (Ba concentration, Airkhan 61.8 1 nmol L⁻¹, Tsagaan 44.4 nmol L⁻¹, Rano Raraku, 180 nmol L⁻¹) [9]. Sr values were like Airkhan 5.29 L⁻¹, Tsagaan 10.1 μmol L⁻¹ Rano Raraku, 7.1 μmol L⁻¹. It should be noted that Airkhan and lake Tsagaan are both saline water with Cl concentrations ranges between 2.5 and 4 g L⁻¹ and SO₄ between 90 and 120 mg L⁻¹. The SO₄: Cl ratios were close to 0.03, indicating a low concentration of sulfate compared to seawater. The Sr in Rano Raraku dissolves in fraction while it is relatively depleted in SPM and the sedimentary core. However, the Sr and Ba may be of terrestrial origin rather than saline precipitation. The difference in the solubility constant (K_{sp}) of BaSO₄ and SrSO₄ (K_{sp}^{BaSO₄} = 1.1 10⁻¹⁰ and K_{sp}^{SrSO₄} = 3.2 10⁻⁷) can be used to explain the Ba and Sr fractionation.

Lake level oscillations

Previous studies reported that Rano Raraku water levels were almost constant with a maximum depth of 2-4 meters in 2010; in 1998, the water level reached 6-7 m in-depth. It has occasionally gotten to 12 m during the last decade. Nevertheless, the maximum depth of the lake was less than 1 m during the time of retrieving samples for this study in September 2017 and was almost completely dry a few months later (fig 5.4)

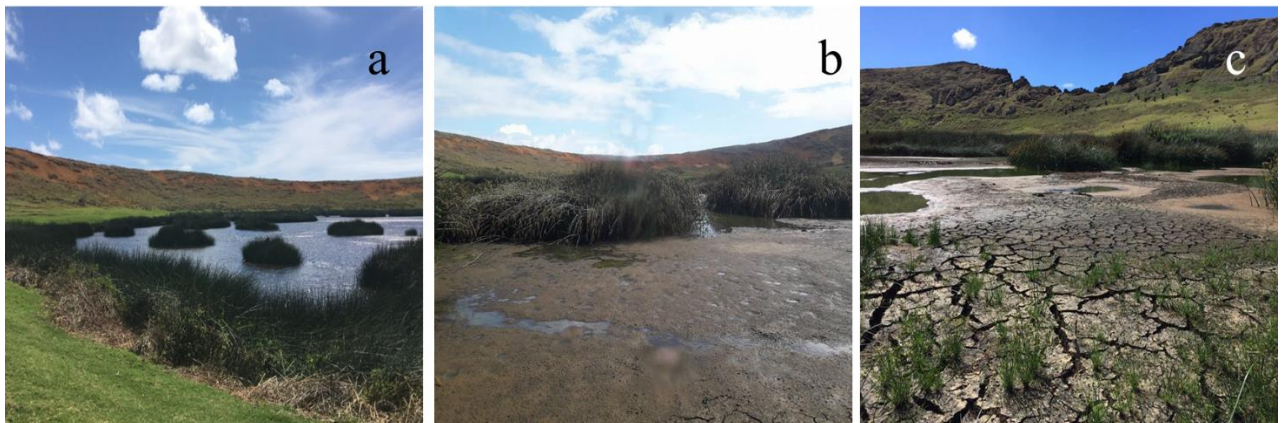


Figure 5.4 Rano Raraku water level, from 1 m to almost completely dry in few months. (a) 7 September 2017, (b) 25 January 2018, (c) 3 March 2018 (Photo by Dario Battistel)

Chloride mass balance

Chloride balance was estimated to evaluate the precipitation-evaporation balance during the last decades; it was assumed that saline rainfalls are the primary source of Cl in the lake, while the salinity of the water is further increased through evaporation in 2017, the concentration of chloride was 970 mg L^{-1} . Considering a mean lake depth of 0.6 m and assuming a lake surface of 0.0706 km^2 , 41 tons was calculated to be the amount of chloride. A different area of Rapa Nui get different amounts of rainfall; Vaitea has more rainfall compared to the rest places in the island [7], a monthly precipitation from the Mataveru airport gauge in Hanga Roa between 1954-2018 (fig 4.5) represents the only multi-decadal record available for Easter Island [10]. The annual precipitation in Mataveru is like the rainfall in Rano Raraku; therefore, Rano Raraku means yearly precipitation can be estimated around $1200 (\pm 100) \text{ mm y}^{-1}$, with an estimated chloride concentration of about 8 mg L^{-1} , it was also estimated that meteoric water is the only source of chloride in the basin, which average averaged 680 kg y^{-1} (in the 2017 lake level conditions) based on assumption. The number of chlorides provided by precipitation since 1954 that resulted in about 40 tons, was calculated using the precipitation record. The computed value is like the 41 tons of chloride estimated in Rano Raraku in 2017.

Reference

- [1] E. Argiriadis, M. Bortolini, N.M. Kehrwald, M. Roman, C. Turetta, S. Hanif, E.O. Erhenhi, J.M. Ramirez Aliaga, D.B. McWethy, A.E. Myrbo, A. Pauchard, C. Barbante, D. Battistel, Rapa Nui (Easter Island) Rano Raraku crater lake basin: Geochemical characterization and implications for the Ahu-Moai Period, *PLoS One*. 16 (2021) 1–23. <https://doi.org/10.1371/journal.pone.0254793>.
- [2] F.J. Millero, The Physical Chemistry of Seawater, *Annu. Rev. Earth Planet. Sci.* 2 (1974) 101–150. <https://doi.org/10.1146/annurev.ea.02.050174.000533>.
- [3] C. Reimann, P. de Caritat, Intrinsic flaws of element enrichment factors (EFs) in environmental geochemistry, *Environ. Sci. & Technol.* 34 (2000) 5084–5091.
- [4] R.L. Rudnick, S. Gao, 4.1 - Composition of the Continental Crust, in: H.D. Holland, K.K. Turekian (Eds.), *Treatise Geochemistry (Second Ed., Second Edi*, Elsevier, Oxford, 2014: pp. 1–51. <https://doi.org/https://doi.org/10.1016/B978-0-08-095975-7.00301-6>.
- [5] H. Elderfield, M.J. Greaves, The rare earth elements in seawater, *Nature*. 296 (1982) 214–219. <https://doi.org/10.1038/296214a0>.
- [6] B.J. Tipple, M.A. Berke, B. Hambach, J.S. Roden, J.R. Ehleringer, Predicting leaf wax n-alkane $^2\text{H}/^1\text{H}$ ratios: Controlled water source and humidity experiments with hydroponically grown trees confirm predictions of Craig-Gordon model, *Plant, Cell Environ.* 38 (2015) 1035–1047. <https://doi.org/10.1111/pce.12457>.
- [7] C. Herrera, E. Custodio, Conceptual hydrogeological model of volcanic Easter Island (Chile) after chemical and isotopic surveys, *Hydrogeol. J.* 16 (2008) 1329–1348. <https://doi.org/10.1007/s10040-008-0316-z>.
- [8] J. Horita, D.J. Wesolowski, Liquid-vapor fractionation of oxygen and hydrogen isotopes of water from the freezing to the critical temperature, *Geochim. Cosmochim. Acta.* 58 (1994) 3425–3437. [https://doi.org/https://doi.org/10.1016/0016-7037\(94\)90096-5](https://doi.org/https://doi.org/10.1016/0016-7037(94)90096-5).
- [9] A. Mochizuki, T. Murata, K. Hosoda, A. Dulmaa, C. Ayushsuren, D. Ganchimeg, V. V. Drucker, V.A. Fialkov, T. Depci, T. Üner, F. Oğhan, M. Sugiyama, Distribution of trace elements and the influence of major-ion water chemistry in saline lakes, *Limnol. Oceanogr.* 63 (2018) 1253–1263. <https://doi.org/10.1002/lno.10770>.
- [10] C.O. Puleston, T.N. Ladefoged, S. Haoa, O.A. Chadwick, P.M. Vitousek, C.M. Stevenson, Rain, sun, soil, and sweat: A consideration of population limits on Rapa Nui (Easter Island) before European contact, *Front. Ecol. Evol.* 5 (2017) 1–14. <https://doi.org/10.3389/fevo.2017.00069>.

CHAPTER SIX: RANO AROI

Rano Aroi can be characterized as a mire or peatland, located at the upper slopes of Mauna Terevaka, close to the most elevated area of Rapa Nui (area with higher precipitation) [1], the infill is primarily peat and has a minimum of 16 m thickness at the center, which appears to be an extrapolated age of about 70,000 years. [2,3]. An artificial outlet that was constructed in the 1960s has partially drained the mire [4]. The flowing water of Rano Aroi have similar chemical composition to that of groundwater (slightly acidic, pH = 5.5-6.5). And the isotopic data of the water ($\delta^{18}\text{O}$, δD) suggest that the water have a short residence time. Therefore, the water level is regulated by variations of seasonal rainfall, supported by input from groundwater that has been in contact with mineral soil [5,6].

6.2 Rano Aroi age model

Eleven sample points of plant macrofossil were sampled and dated at National Oceanic Sciences Accelerator mass spectrometry facility (NOSAMS) corresponding to the AMS standard protocols. The mobile organic phases and removal of inorganic carbon was carried out using acid-based pretreatment, this is because lithological analysis classified the samples as peat. Eleven accelerator mass spectrometry ^{14}C ages were derived from the plant macrofossils samples. SHCal13 calibration curve was used to convert the ^{14}C ages, and Bayesian accumulation histories for deposits (BACON) software for modeling in R (R Core Team, 2019) was used to include all the radiocarbon ages in the age-depth model (fig 6.1) [7]. Reservoir effects were presumed to be insignificant because of the lake's efficient CO_2 exchange with the atmosphere [8]. Several proxies were analyzed as discussed in the earlier chapters, including Monosaccharide anhydride (represented by levoglucosan in this study as it was the dominant compound in its group), polycyclic aromatic hydrocarbon (PAH), fecal sterols, charcoal, and geochemical composition. Most part of the results has been published in the Quaternary Science journal.

Table 6.1 Rano Aroi sediment core conventional Radiocarbon Age in CRA (years before present).

Lab ID	Depth (cm)	CRA years (error)	Calibrated Age years median (range)
161633	40	105 (15)	65 (26-238)
161634	50	265 (15)	292 (283-303)
161635	60	390 (20)	393 (329-485)
161636	70	385 (15)	381 (329-466)
161637	80	455 (15)	494 (487-503)
161638	90	665 (15)	606 (559-614)
161639	110	995 (15)	854 (809-911)
161640	150	3340 (20)	3522 (3481-3563)

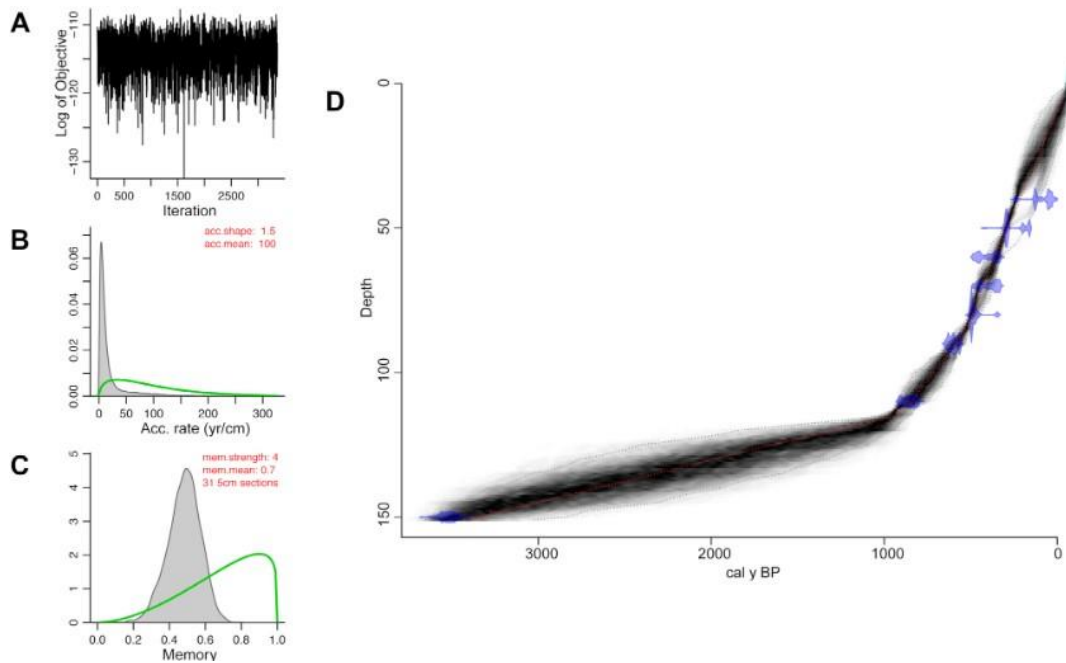


Figure 6.1. Rano Aroi age-depth chronology based on ^{14}C ages (A) MCMC iterations showing distribution of stationary; (B) green curve and grey histogram for the accumulation rate; (C) green curve and grey histogram for memory distribution; (D) Calibrated ^{14}C dates (transparent blue) and the depth-age model (darker greys indicate more likely calendar ages, grey stippled lines indicates 95% confidence intervals) (figure: Roman 2021)

[8].

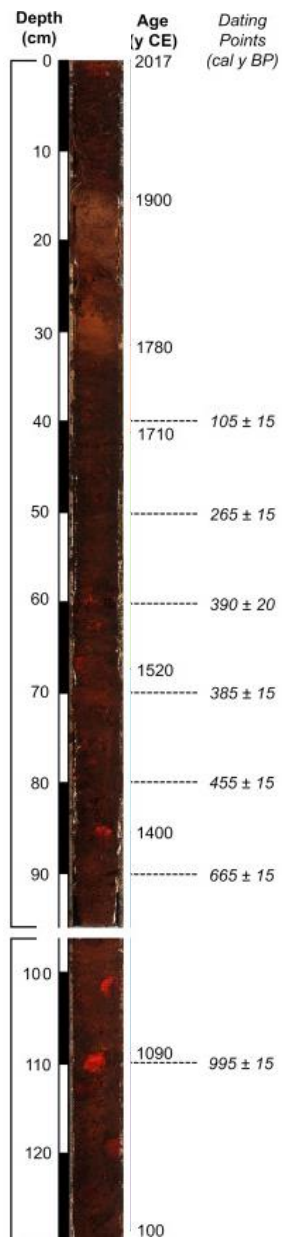


Figure 6.2 Rano Aroi sediment core (LTS-AROI17-1A and parts LTS-AROI17-1B (bottom)) with Depth (right) and calibrated radiocarbon ages (right)

6.3 Biomarkers and Charcoal

Coprostanol (Cop)

Coprostanol (Cop) flux ($\text{cm}^{-2} \text{yr}^{-1}$) in Rano Aroi sedimentary core was detected between 1463 CE and 1780 CE, trend of the Cop flux has three peaks interval, indicating human presence around Rano Aroi for about 300 years with three episodes of human presence. The first Cop flux indicates human presence from 1463 CE to 1540 CE, with peak at 1500 CE ($6505 \text{ cm}^{-2} \text{yr}^{-1}$). the record shows a slight decrease value which was followed by a higher flux between from 1536 CE to 1661 CE, with its peak at 1536 ($15042 \text{ cm}^{-2} \text{yr}^{-1}$), almost three times as high compared to the first peak, the second Cop flux indicates increased human population around Rano Aroi. The third signal appears between 1661 CE and 1761 CE with peak at 1700 CE ($11070 \text{ cm}^{-2} \text{yr}^{-1}$), this flux shows decrease in human population around the mire compared to the second wave, but the flux is still twice as high as the first wave.

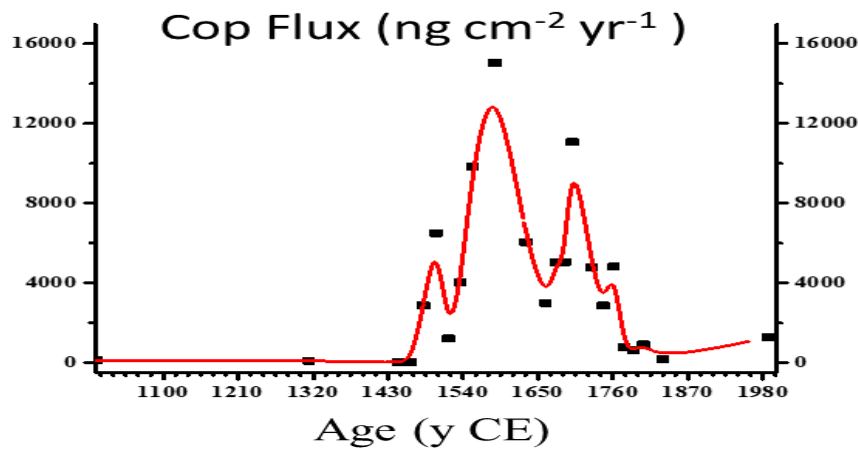


Figure 6.3 Coprostanol flux indices from Rano Aroi Sedimentary core, indicating fire occurrence with moving average (lowess smoothing 5 points)

Levoglucosan (LVG)

levoglucosan concentration ranges from 0.14 to 1968 ng cm⁻² yr⁻¹, the LVG general trend shows an increase between 1457 CE and 1661 CE with the peak 1463 CE (1968 ng g⁻¹), after which the concentration reduces and then varies between 667 and 578 ng cm⁻² yr⁻¹ until 1833 CE, levoglucosan show a higher concentration compared to charcoal and PAHs, the levoglucosan appearance in this study coincides with the second increase Cop flux. In general, the levoglucosan signal indicates a period of direct burning of biomass materials which may be ascribed to human presence around Rano Aroi.

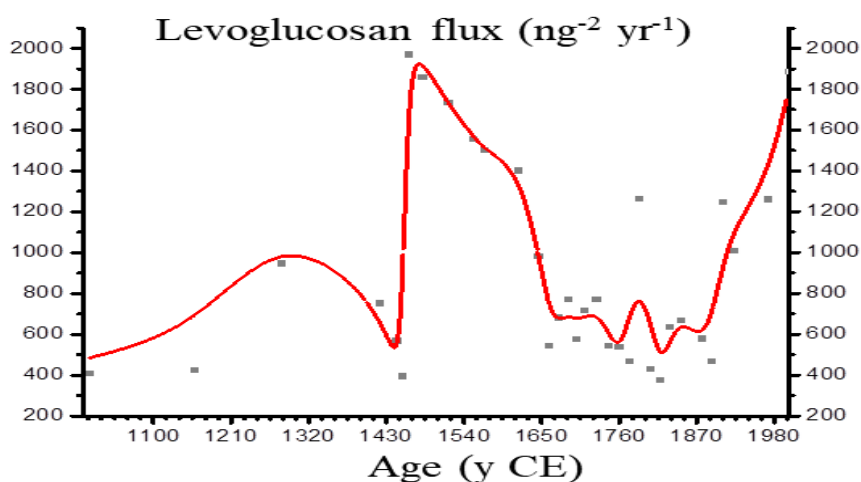


Figure 6.4. Levoglucosan fluxes (ng cm⁻² yr⁻¹) indices from Rano Aroi Sedimentary core with moving average (lowess smoothing 5 points)

Polycyclic aromatic hydrocarbons (PAH)

I analyzed 19 PAHs in 100 sediment samples from Rano Aroi sedimentary core, roughly the first 100 cm depth, corresponding to the last 1000 years. however, about 15% of the total sediment sample had values below the detection limit for all PAHs while more than 30% of the samples had values below the detection limit for some PAHs, these include Acy, Ace, Ant, BaA, BaP, BkF, Chry, BeP, Per and B(ghi)P, this may be as a result of instrumental sensitivity level of GC-MS or by in situ microbial degradation, diagenesis processes and/or decay in the atmosphere as a result of photoreaction. therefore, I added the total PAHs flux (PAHs^{tot}) to determine fire occurrence instead of using PAHs ratios and/or grouping of PAHs

in terms of weight and numbers of aromatic rings. The PAHs^{tot} concentration ranges between 0.30 and 117 ng cm⁻² yr⁻¹, the compound containing 4 and 5 aromatic rings contributed ~60% to the PAHs^{tot}, with Pyrene and Retene being the most abundant compounds. PAH flux was detected at 1450 CE, and drastically increase until a peak at 1536 CE then gradually decreases and stands at a concentration of 20 cm⁻² yr⁻¹ at 1700 CE. the PAHs record was not suitable for paleo-fire reconstruction due to missing points and irregularities.

charcoal

Charcoal was detected around the lake from 1490 CE, with a peak at ~1500 CE. The particles range between 0 and 12 particles cm⁻² yr⁻². I examined changes in charcoal accumulation rates and charcoal particles >125 mm in diameter to infer local fire. The typical value of the charcoal was < 0.5 particles cm⁻² yr⁻¹. The charcoal flux around the mire decreases gradually over the years after the first peak.

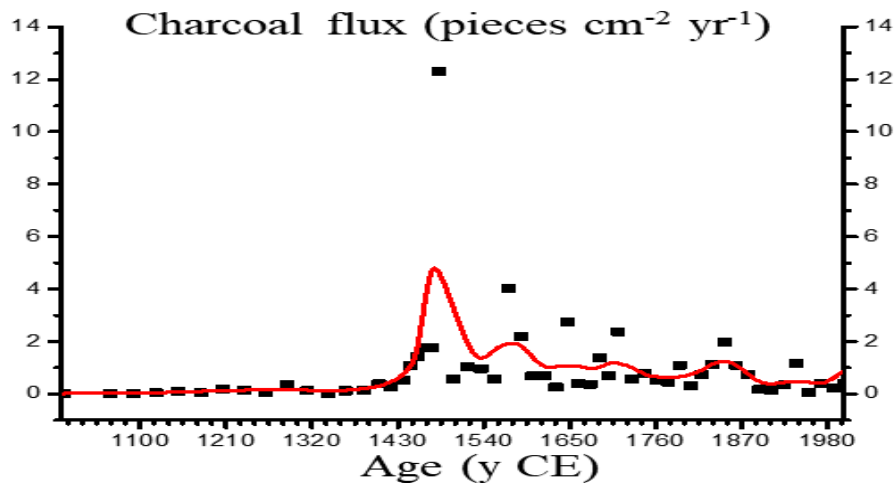


Figure 6.5. charcoal fluxes (cm⁻² yr⁻¹) indices from Rano Aroi Sedimentary core with moving average (lowess smoothing 5 points)

n-Alkanes

The climate condition of an environment can be inferred or described through the knowledge of the vegetation type in the environment. In this study, I used the indices and relative abundances of individual compounds in *n*-alkane to distinguish vegetation types around Rano Aroi. Most of the *n*-alkane indices show a similar trend, indicating higher terrestrial input and vegetation change between 1430 and 1650 CE. The terrestrial aquatic ratio (TAR) value in Rano Aroi sediment core ranges between 0 and 8 cm⁻² yr⁻¹, the index shows an oscillation between aquatic and terrestrial input. However, aquatic input dominates the vegetation around Rano Aroi. The TAR trend corresponds with that of Carbon Preference Index (CPI), which show a robust aquatic input from 1430 to 1650 CE. The CPI value ranges between 0.5 and 20 cm⁻² yr⁻¹. The record clearly shows clear vegetation transition from terrestrial to aquatic origin between 1440 to 1620 CE. The Long Hydrocarbon chain (LHC) index shows a continuous reduction of woody plants from 1480 CE to 1600 CE. This LHC record indicates the period of deforestation around Rano Aroi mire as it is an indicator of woody plants. The general trend of all *n*-alkanes indices indicates the removal of terrestrial vegetation between ~1400 and ~1750. However, LHC record shows that the removal of woody plants happened within the space of 100 years. Which suggests that grass was also burnt or removed after the deforestation of woody plants. It is important to note that *n*-alkane is an indicator for reconstructing vegetation types and plant origin, as it is unable to infare plant species.

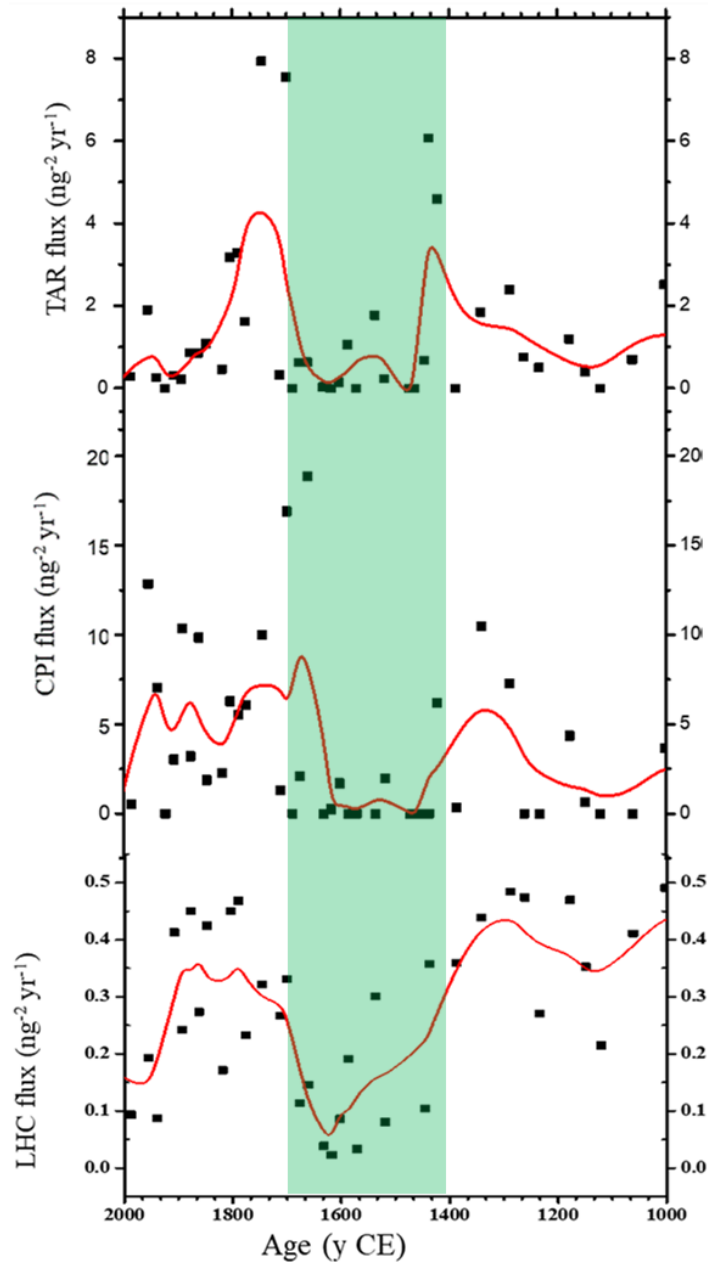


Figure 6.6 *n*-alkane indices from Rano Aroi Sedimentary core indicating change in vegetation with moving average (lowest smoothing 5 points)

6.4 Geochemical composition Results

Trace and major elemental

According to the SW test, the elements in the Rano Aroi core are normally distributed and positively skewed apart from Ca and Sr. Most elemental levels were variable all-through the core. However, Principal component analysis (PCA) and Cluster analysis indicate a clearly identifiable Phases in the sediment core, the dendrogram from the cluster analysis, and a PCA biplots show a cluster of samples in seven groups that coincide with the seven chronologies of the sediment core. 85% of the variance in the sediment core is explained by the PCA.

- PC1 explain ~45% of the total variation, characterized by a positive loading of the OC%. and a negative loading of lithogenic elements such as Al, Sc, V, Ti;
- PC2 explain ~ 20% of the total variance, characterized by negative loadings of K, Cu and Na and positive loadings of Mn, Co, and Fe.
- PC3 explains ~13.5% of the total variance as negative loadings of Sr and Ca
- PC4 only explained ~6% of the variation, characterized by negative loadings of Y and positive loadings of Mg, and the accumulation rate of the total rare earth elements. PC4 was, however, considered because it explains the cluster analysis.

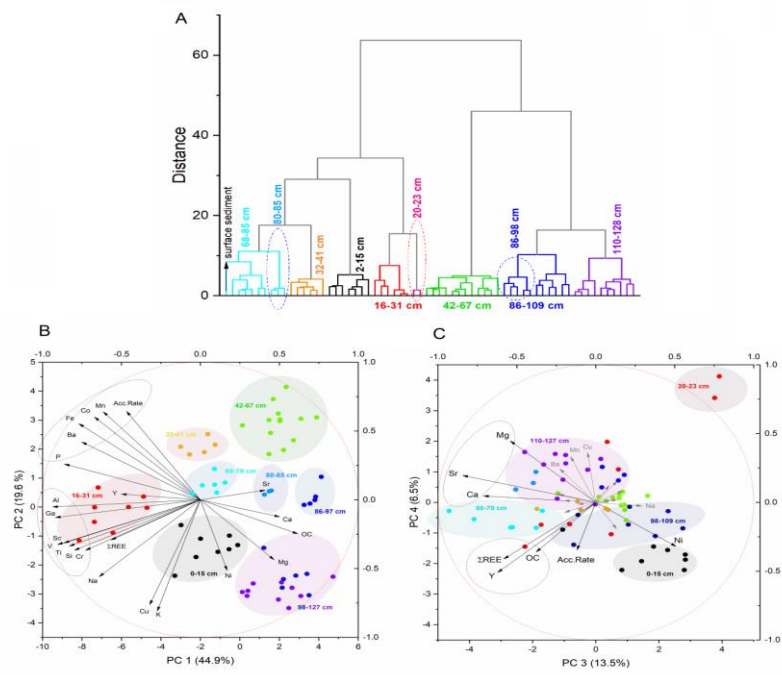


Figure 6.7 (A) Dendrogram obtained by hierarchical cluster analysis using the Euclidean distance and Ward's method.
Principal component bi-plot: PC1 vs PC2 (B) and PC3 vs PC4 (C) [8]

6.2 Trace and major elements determined in the Aroi sedimentary record (mean, maximum and minimum values), water, and suspended particulate matter (SPM) collected in proximity of the outlet (mean \pm standard deviation). W statistics and p-values refer to the Shapiro-Wilk (SW) normality test. H₀: the null hypothesis of normal distribution is accepted vs. H₁: the null hypothesis is rejected. Missing values mark concentrations lower than their respective detection limits.

Element	Sediment			W	p-value	SW hyp	Water		SPM	
	mean	min	max							
Al (g kg ⁻¹)	2.2	0.3	17	0.512	< 0.001	H ₁	152 \pm 15	$\mu\text{g L}^{-1}$	590 \pm 60	$\mu\text{g L}^{-1}$
Ba (mg kg ⁻¹)	4.4	0.9	50	0.412	< 0.001	H ₁	2.3 \pm 0.2	$\mu\text{g L}^{-1}$	0.5 \pm 0.1	$\mu\text{g L}^{-1}$
Ca (mg kg ⁻¹)	240	5	600	0.981	0.430	H ₀	2.0 \pm 0.2	mg L ⁻¹	52 \pm 5	$\mu\text{g L}^{-1}$
Co (mg kg ⁻¹)	2.0	0.5	16	0.459	< 0.001	H ₁	730 \pm 70	ng L ⁻¹	0.5 \pm 0.1	$\mu\text{g L}^{-1}$
Cr (mg kg ⁻¹)	4.3	0.7	40	0.440	< 0.001	H ₁	350 \pm 35	ng L ⁻¹	26 \pm 2	$\mu\text{g L}^{-1}$
Cu (mg kg ⁻¹)	6.8	1.0	36	0.740	< 0.001	H ₁	2.2 \pm 0.2	$\mu\text{g L}^{-1}$	11 \pm 2	$\mu\text{g L}^{-1}$
Fe (g kg ⁻¹)	6.4	0.6	50	0.624	< 0.001	H ₁	700 \pm 65	$\mu\text{g L}^{-1}$	1.9 \pm 0.2	mg L ⁻¹
Ga (mg kg ⁻¹)	2.6	0.1	34	0.357	< 0.001	H ₁			0.6 \pm 0.1	$\mu\text{g L}^{-1}$
K (mg kg ⁻¹)	70	30	320	0.627	< 0.001	H ₁	0.76 \pm 0.08	mg L ⁻¹	103 \pm 10	$\mu\text{g L}^{-1}$
Mg (g kg ⁻¹)	0.74	0.26	1.6	0.932	0.001	H ₁	2.0 \pm 0.2	mg L ⁻¹	70 \pm 7	$\mu\text{g L}^{-1}$
Mn (mg kg ⁻¹)	54	8	380	0.568	< 0.001	H ₁	31 \pm 3	$\mu\text{g L}^{-1}$	4.8 \pm 0.5	$\mu\text{g L}^{-1}$
Na (mg kg ⁻¹)	150	47	500	0.750	< 0.001	H ₁	35 \pm 4	mg L ⁻¹	9.5 \pm 1.0	$\mu\text{g L}^{-1}$
Ni (mg kg ⁻¹)	170	18	1300	0.621	< 0.001	H ₁	750 \pm 80	ng L ⁻¹	1.1 \pm 0.1	$\mu\text{g L}^{-1}$
P (mg kg ⁻¹)	350	100	2000	0.538	< 0.001	H ₁				
Sc (mg kg ⁻¹)	0.7	0.1	6	0.530	< 0.001	H ₁				
Si (g kg ⁻¹)	6.8	0.4	77	0.401	< 0.001	H ₁				
Sr ($\mu\text{g kg}^{-1}$)	28	3	54	0.978	0.310	H ₀	27 \pm 3	$\mu\text{g L}^{-1}$	1.1 \pm 0.1	$\mu\text{g L}^{-1}$
Ti (g kg ⁻¹)	1.9	0.03	30	0.360	< 0.001	H ₁				
V (mg kg ⁻¹)	25	1	300	0.376	< 0.001	H ₁	700 \pm 70	ng L ⁻¹	6.2 \pm 0.5	$\mu\text{g L}^{-1}$
Y ($\mu\text{g kg}^{-1}$)	350	40	1200	0.832	< 0.001	H ₁				
OC %	50.1	29.8	68.6	0.754	< 0.001	H ₁				
$\Sigma\text{REE (mg kg}^{-1}\text{)}$	2.4	0.4	12	0.614	< 0.001	H ₁	330 \pm 40	ng L ⁻¹	97 \pm 10	ng L ⁻¹

The grouping of samples into different sections based on the elemental composition matches the individual temporal variations in the entire Rano Aroi record, as summarized Table 5.2. The positive loading of OC% and the negative loading of AI and Ti in PC1, primarily track the contribution of lithogenic elements that were more substantial during phase 4 and part of phase 3. The dominance of PC1 coincides with lighter sediment band in the sediment core (fig 4.2 b) and may be explained as an increase in the input originating from dust transported from hydric erosion and by the wind. The gradual decrease of PC2 over the last 300 y marks a change in the dominance of positive loadings) in phase 5 to high mobility elements (negative loadings) in phase 7. The PC3 is mainly distinguished by negative loadings of the alkaline earth elements (Ca and Sr) and decline in correspondence to phase 3 and in the earliest part of phase 4. Finally. The negative loadings of Y, OC%, and Σ REEs are the major contributors in phase 4; with a less terrestrial input, PC4 significantly increases throughout this interval, which may indicate the geochemical processes within the Aroi wetland instead of contributions of exogenous material.

Table 6.3 Summary of the trends obtained from the principal component analysis in from the geochemical composition and corresponding chronological phases, — not significant, ▲ slightly positive ▼, slightly negative.

	Phase	Depth (cm)	Age (years CE)	PC1	PC2	PC3	PC4
●	I	110-128	1 st century – 1090	▲	▼	—	▲
●	II-a	98-109	1090-1200	▲	▼	▲	—
●	II-b	86-98 c	1200-1400	▲	—	—	▲
●	III-a	80-85	1400-1440	▲	—	▼	—
●	III-b	68-79	1440-1520	—	—	▼	—
●	IV	42-67	1520-1710	▲	▲	—	—
●	V	32-41	1710-1790	—	▲	—	—
●	VI-a	16-31	1710-1780 E	▼	—	—	—
●	VI-b	20-23 c	1840-1865	▼	—	▲	▲
●	VII	2-15 c	1865-Present	—	▼	▲	▼

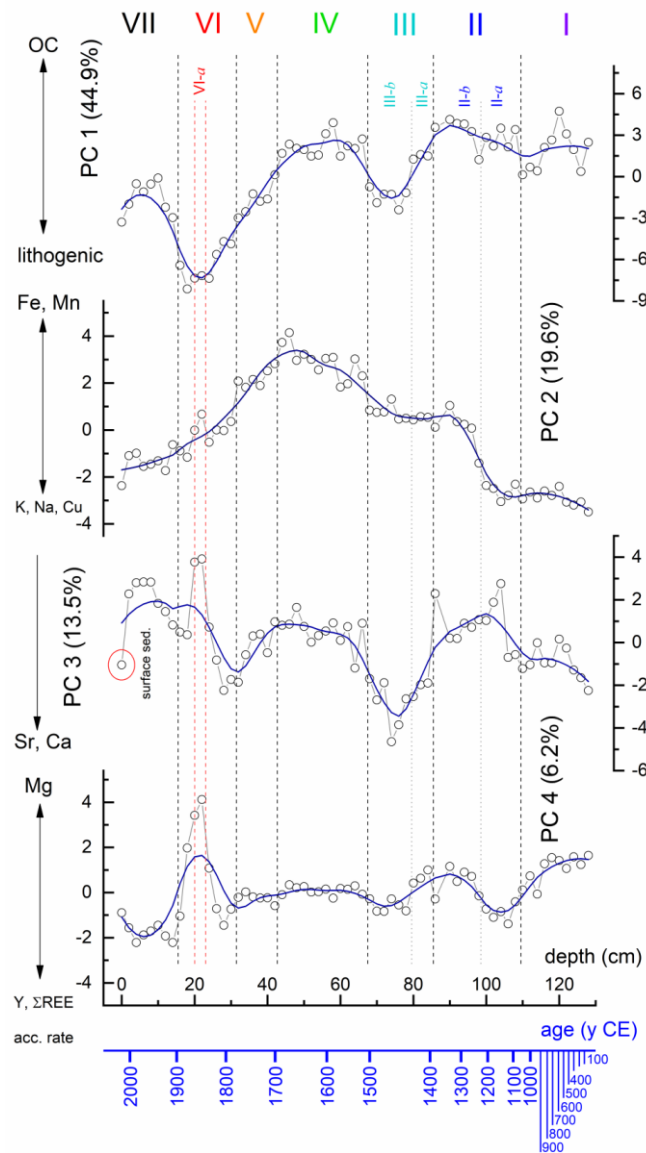


Figure 6.8. Temporal evolution of the PCA in the Rano Aroi record, reported in Table 6.3 (Roman et al. 2021) [8]

Rare earth elements

The concentration of REE significantly varies with enrichment factors throughout the sediment core ranging from 0.10 to ~ 7 (Table S1, for definitions, see Shotyk, 1996) [9], suggesting elemental partition in the Aroi wetland. Eu, Er, and Yb were below their detection limits in every sample from phase 2 and in three samples of phase 5, while Ho, Tb, Lu, and Tm concentrations were below the detection limits in about 50% of the samples. The REEs mean concentrations follow the Oddo-Harkins rule. REEs demonstrate enrichment in light REEs (LREEs) when it is normalized by chondrites; this pattern is consistent with the

observed pattern in basaltic rocks from the three volcanoes of Easter Island [10]. Fractionation between REEs (HREEs, i.e., from Gd to Yb) and LREEs (Pr, La, Nd, Sm) was evaluated through the ratios $(Gd/Yb)_N$, $(La/Yb)_N$ and $(La/Sm)_N$, normalized to UCC. Yb, Gd and La, since many HREEs are below their respective detection limits. The use of different reference standards (WSA, PAAS, or NASC) does not considerably affect the ratios calculated (Table S2). $(Gd/Yb)_N$ values between 1 and 2.5 are provided in all the Rano Aroi core samples, while $(La/Sm)_N$ varies between 0.30 and 1.80 (fig 3.4). Samples from the deepest section of the core have higher $(La/Sm)_N$ values than the surrounding rocks [10].

$(La/Sm)_N$ ratios are 3.01 and 0.16, and $(Gd/Yb)_N$ ratios are 0.80 and 1.16, respectively, in the SPM and water samples collected from the Rano Aroi outlet, resulting in a more marked fractionation of $(La/Sm)_N$ compared to $(Gd/Yb)_N$. LREEs usually are less soluble than medium REEs such as HREEs and MREEs. The fractionation between water and SMP is also confirmed by the ratio $(La/Yb)_N$ (0.33 and 2.03, respectively). The potential effect of environmental redox conditions and/or dynamics involving the formation of organic complexes and/or leaching processes on REE fractionation can be evaluated considering the enrichment/depletion of redox-sensitive elements, such as Ce. In this study, we use the following definition of the Ce anomaly [11] defined by

$$\delta Ce = \frac{3 \cdot Ce_N}{2 \cdot La_N + Nd_N}$$

δCe ranges between 0.6 and 2.1 in Rano Aroi peat samples, phase 6, have higher values than the other REEs. Ce anomalies range between 1.1 and 0.96 in SPM and water, respectively, signifying a constrained partitioning between such phases.

Table 6.4 REE concentrations and ratios normalized by UCC in the Aroi sedimentary record, water, and suspended particulate matter (SPM) collected in proximity of the outlet (mean, maximum and minimum values). W statistics and p-values refer to the Shapiro-Wilk (SW) normality test. H₀: the null hypothesis of normal distribution is accepted vs. H₁: the null hypothesis is rejected, n.d. not determined.

REE	Sediment							Unit	Water	SPM
	Unit	mean	min	max	W	p-value	SW			
La	μg kg ⁻¹	440	62	1535	0.864	< 0.001	H ₁	ng L ⁻¹	40.4	22.1
Ce	“	993	183	6800	0.663	< 0.001	H ₁	“	110.3	41.7
Pr	“	93	18	375	0.763	< 0.001	H ₁	“	15.8	5.6
Nd	“	420	70	1700	0.764	< 0.001	H ₁	“	58.8	10.8
Sm	“	96	13	420	0.731	< 0.001	H ₁	“	37.9	1.1
Eu	“	29	4	120	0.744	< 0.001	H ₁	“	5.8	1.8
Gd	“	98	6	370	0.759	< 0.001	H ₁	“	18.2	1.1
Tb	“	13	5	56	n.d.	n.d.	n.d.	“	2.9	1.8
Dy	“	90	6	340	0.760	< 0.001	H ₁	“	18.2	2.3
Ho	“	14	0.3	60	n.d.	n.d.	n.d.	“	3.6	2.0
Er	“	44	7	175	0.779	< 0.001	H ₁	“	10.2	2.0
Tm	“	-	-	-	n.d.	n.d.	n.d.	“	10.5	1.5
Yb	“	39	6	162	0.775	< 0.001	H ₁	“	9.1	0.8
Lu	“	6	5	19	n.d.	n.d.	n.d.	“	1.5	1.6
δCe		0.94	0.66	2.10	0.650	< 0.001	H ₁		0.95	1.13
(La/Yb) _N		0.87	0.33	3.62	0.723	< 0.001	H ₁		0.33	2.03
(Gd/Yb) _N		1.50	1.02	2.50	0.939	0.005	H ₁		1.16	0.80
(La/Sm) _N		0.73	0.32	1.81	0.836	< 0.001	H ₁		0.16	3.01

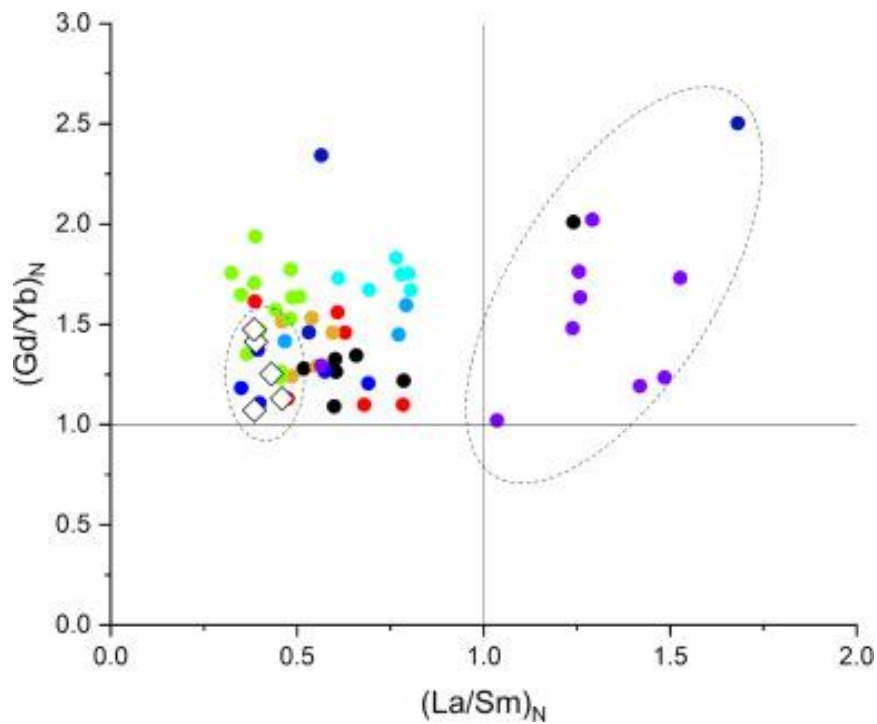


Figure 6.9 (Gd/Yb)_N plotted vs. (La/Sm)_N. Peat samples at different depths are colored dots corresponding to the scale used for indicating groups in figure. 6.8 and 6.9. The composition of the surrounding rocks (Margalef et al., 2014) is reported as empty diamonds [8].

Elemental ratios

Al or T (as molar ratios) was used to normalize key elements including Fe, Ca, K and P in order to investigate the in-peatland dynamics (Fig 6.5). The K/Al had a sparse ratio during phase I, then increased between 1400 and 1520 CE and between 1710 and 1900 CE. The main peak of Ca/Ti ratio stands at 1250 and 1440 CE and between 1520 and 1710 CE. The P/Al ratio peaks at 1090-1400 CE and to 1520-1710 CE, and minima at 1400-1520 CE and 1800-1900 CE, The Fe/Al vary between 1.2 and 3.0, similar to that of the surrounding rocks (Margalef et al., 2014) [10]. An increase in Fe/Al is recorded between 1520 and 1790 CE, and a reduced peak is examined at 1200-1400 CE and 1900 CE-present.

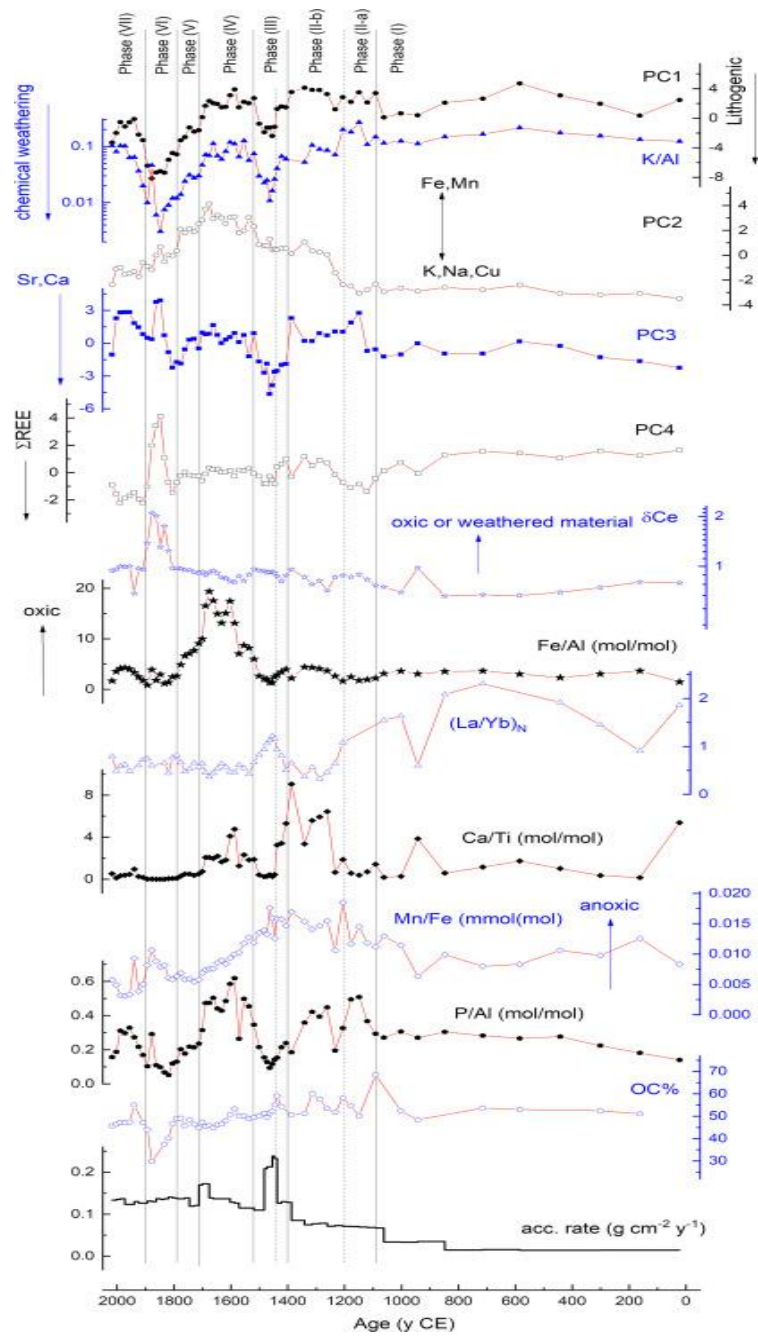


Figure 6.10 Rano Aroi record of the environmental and climatic proxies discussed in this paper: principal components trends (PC1-PC4), weathering dynamics (K/Al); transport and deposition (La/Yb)_N, Ca/Ti; redox conditions (δCe, Mn/Fe and Fe/Al); P/Al, OC% and accumulation rate [8]

6.5 Geochemical composition Record

The geochemical composition of Rano Aroi peat record is discussed in seven main sections as mainly identified by the cluster analysis and PCA covering the geochemistry evolution over the last 2000 years

Phase 1 (1st century - 1090 CE)

The characteristic of this phase is mainly explained by geochemical composition. This phase has a reduced rate of accumulation ($0.01 - 0.03 \text{ g cm}^{-2} \text{ y}^{-1}$), providing a centennial-scale resolution. The PC1 values and the high K/Al ratio indicate that this phase has a low accumulation rate of lithogenic elements (i.e., Ti, Al, Sc, Ga, V, Cr) as a result of negligible hydric erosion, corresponding to scarce chemical weathering. The result agrees with data from Margalef in 2014 [10], there is few of most of the mineral grains in the upper section of the sediment core have (10 - 20 mm) [10]; it is believe that aeolian transport from distant areas of the island may be the main drive of lithogenic input to the wetland during this phase. The PC1 also corresponds with a noticeable increase in LREEs, as shown by high $(\text{La/Yb})_N$ ($\sim 2.0-2.5$) and $(\text{La/Sm})_N$ ($\sim 1.0-1.8$). Weathered source due to the lower solubility of LREEs and/or lower sediment deposition rate is consistent LREE enrichment compared to HREEs [12]. This phase has a low concentration of ion and Mn, and Fe/Al is only weakly enriched compared to the surrounding rocks. This combination is an indication that the lake was exposed to mild anoxic conditions only, and it is further supported by the relatively low δCe and high Mn/Fe values. The condition of Rano Aroi during phase 1 agrees to the baseline study of the mire, according to Margalef, which is described by long-term stability of the water table close to the surface [13]. These Indications point to a relatively dry to mesic environment.

The vegetation during this period is suggested to be from the terrestrial origin as indicated by the *n*-alkane index (LHC and ACL); this data is consistent with the findings by Rull [3], who reported that the vegetation at Rano Aroi, comprised of palm woodland with underlying shrubs. The regional climate in the Eastern part of the island was warm and dry during this period [14], which may be caused to the position of the equatorial convergence zone[15]. Previous study suggested occurrence of drought between ~ 600 and ~ 1000 CE based on the desiccation units in the Rano Raraku sediment archive [16] and anomalies in $\delta^{13}\text{C}$, $\delta^{15}\text{N}$, and

TN in Rano Aroi as seen in (fig. 6.5) [3]. With the support of palynologic evidence, this period is a landscape opening, suggesting shift to grassland-dominated vegetation from a palm-dominated forest. This shift was considered as a sign of the Medieval Climate Anomaly (MCA) that is mostly witnessed in northern hemisphere archives and frequently between 700 and 1300 CE in archives across the globe [17,18]. The MCA In the central tropical Pacific has been associated with a northward movement of the equatorial convergence zone, the dominance of El Nino, weakening of the South Pacific Convergence, and the stronger zonal sea surface temperature gradients relative to the previous period [14]. These combining factors would reduce the moisture carried by the westerlies directed towards Rapa Nui [10]. An apparent anomaly in this study data from Rano Aroi relating to the onset of MCA was not observed within our temporal resolution limits [19]. As a stable warm-dry period. It is concluded that the MCA anomaly was weak at most in the mire, not sufficient to impact the composition of the lake given the compatibility to the hypothesis of a limited influence of ENSO on Rapa Nui's climate and the resilience of the Rano Aroi area [20].

Phase 2 (1090 -1400 CE)

Phase 2 is a combination of two separate sub-phases between 1090 and 1200 CE (2-a) and 1200 and 1400 CE (2-b). Both sub-phases are marked by a decrease in Ca concentrations (PC3), Ca/Ti shows a clear increase of Ca compared to lithogenic elements from ~1250 CE to ~1440 CE. However, the accumulation rate does not noticeably change. Schitteck reported an increase in Ca compared to Ti in the same period in sediments core from the Andes and explained this increase to result from shallow open water on the peatland surface [21]. Ise and Muller described the Ca increase of this phase as due to peat decomposition during drought phases [22,23]. However, this interpretation of droughts in this study during phase 2 is contrasted by other indicators. A slight increase of chemical weathering is suggested by the decreases of the K/Al ratio from sub-phase 2-a to sub-phase 2-b, although lithogenic inputs remained substantially low (PC1). The Mn/Fe ratio suggests anoxic conditions that contrast with lake mineralization during drought phases. Iron and Mn values significantly increase between 1200 CE and 1400 CE (see PC2) in conjunction with a minor increase in Fe/Al. Because coarser particles can be increased in Mn and Fe, an increase in the local mineral source can result in an increase in absolute levels of Mn and Fe; it also indicates a change in sediment transportation as it signifies more surface runoff compared to the previously

dominant aeolian transport. However, the PC2 within our record shows that processes discussed above may likely be secondary processes. The hypothesis of a more local and less partitioned source is supported by The lower $(La/Yb)_N$ values, closer to soil and rock composition. transition to wetter conditions in the lake can induce the bio-cycling of older Ca by plants in the lake, this explains the increase of Ca during this period. the enrichment of the Ca in the lake increased the Ca/Ti concentration, which was favored by the layering of the water table with increasingly anoxic conditions (and possible decrease of pH) while the lake was still undergoing reduced lithogenic inputs during this period. Phase 2 is suggested to be a transition period, a shift towards a wetter climate, this shift is highly documented in eastern island vegetation as vegetation changes. the LCH index from the n-alkane record indicates woodland and shrubs to closed forests around Rano Aroi, also with the emergence of semi-aquatic vegetation, suggesting a rise of the water table, this is also in accordance data's from Rull [3]. This phase also indicates low lithogenic inputs as indicated by PC1, because of reduced erosion due to improve pedogenetic processes and forest expansion.

Phase 3 (1400 -1520 CE)

Phase 3 is marked by signs of a clear shift to a wetter condition and a noticeable environmental change. Increased in (PC3) Ca (and Sr) is in correspondence with lithogenic input increases (PC1), while a significantly decreases K/Al suggest leaching and washout were accompanied by hydric erosion by most of the mobile elements and a significant intake of K for primary production. The input of more weathered sediments is also supported by the clear peak in $(La/Yb)_N$ in this phase. A minor shift to a less anoxic environment is suggested by Mn/Fe and δCe , and partially by Fe/Al. This phase has the lowest value of P/Al in our sediment record, indicating changes in lake vegetation as suggested by LHC and less anoxic/more oxic conditions. The sedimentation rate increased during this phase. An increase in water level may have supported the expansion of plant macrophytes, which enhanced the formation of the peat sediments.

The La Ni-na conditions dominated regional climate this phase 3 [18]. During this period, the equatorial convergence zone moved to its southernmost position of the last two millennia, possibly as a result of changes in hemispheric temperature gradients caused by a decline in solar irradiance [24,25].

Phase 4 (1520 - 1710 CE)

Phase 4 is characterized by a peak of Fe/Al, a ratio 10 to 20 times higher than the rest of the record; the exogenous coarser particles contribution cannot justify this increase in Fe/Al. However, as shown on PC2, Mn and Fe are possibly a marker of intense oxic conditions [93], which is supported by the Mn/Fe ratio. The input of (K/Al and (La/Yb)N) in PC1, weathered source material, ascribable to physical weathering coupled with the highest Ca/Ti concentration level, suggests a highly desiccated mire. These changes in the environment may be strongly related to a combination of the human activities around Rano Aroi and the natural shift to arid conditions

The early study of a soil profile close to Rano Aroi linked early horticulture with covering the garden soil with a pavement of carved basalt stones and cobbles [26]. Phase 4 corresponds with the middle of the LIA [2,27,28]., the LIA climatic period was characterized by droughts, social crises, and food scarcity, in some parts of tropical Asia, this has been attributed to a southern transition in the humid sub-tropical storm with corresponding stability of dry anticyclonic conditions over Easter island On a regional scale[29], this period is also marked by a transition towards high-intensity El Nino conditions that commenced earlier in the LIA [30]. In other Pacific Ocean locations, this period has been marked by a southward shift in the position of the equatorial convergence zone near the equator [31]. However, the internal processes of tropical Pacific hydro-climate on centennial scales during this period and the effects at the local scale are still not well understood [32].

Phase 5 (1710 -1790 CE)

phase V is characterized by a partial increase of hydroclimate systems like the early LIA. In phase 3, the climate was slightly wetter, with a high lithogenic input (PC1) but in oxic conditions (Fe/Al, Mn/Fe). This phase marked the end of the LIA droughts in Rano Aroi during the first half of 18th century CE [20], corresponding to the early movement of the equatorial convergence zone towards northern latitude between 1700 – 1870 CE [31]. [28].

Phase 6 (1790 - 1900 CE)

Phase VI is characterized by a marked mineral sediments input (PC1) which is visible in a lighter colored unit at the uppermost section of the sediment core (fig 4.2), and reduced concentration of organic compound, corresponding to the depletion in Ca, Sr (PC3) and the total REE (PC4), where the PC4 can be identified by more soluble elements (apart from Ce). Mn/Fe ratios suggest that the lake conditions are less oxic than in phase 4. The K/Al ratios indicate that the exogenous material is likely weathered, although there is no noticeable change in the value of $(La/Yb)_N$, this phase could be considered to mark the end to LIA due to the high rainfall, similar to phase 3 marked the beginning of LIA, the Rano Aroi record in this study, capture both climate transition, where limited individual information is provided by other records [28]

Phase 7 (1900 CE - Present)

Similar to the last phase of the biomarker record, this phase is characterized by heavy environmental modification, especially the creation of an earthen dike barrier, that affected water level oscillations and the transportation dynamics; the Rapanui was also impacted with different problems in the last century, such as slavery and diseases [33].

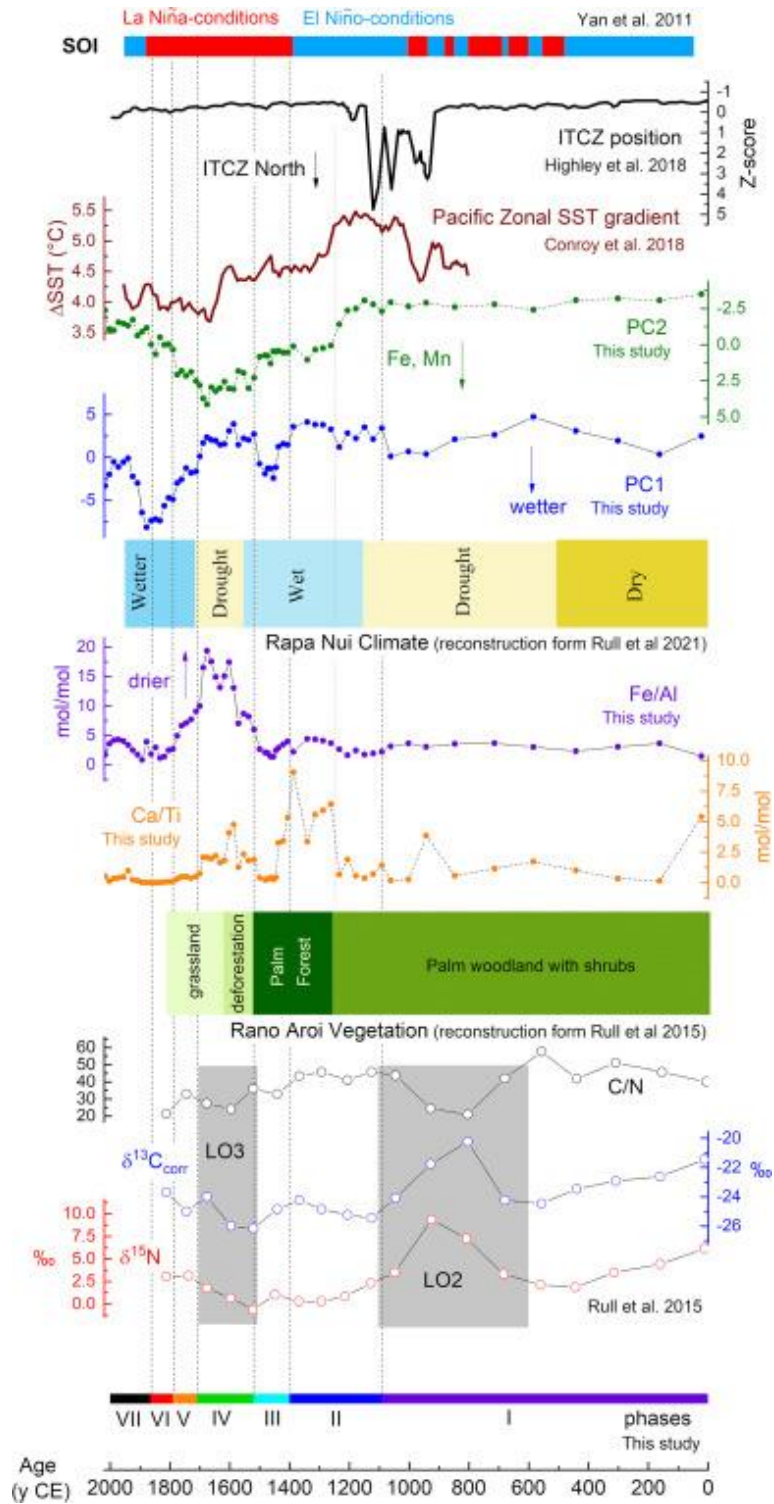


Figure 6.11. Summary of the key paleo-geochemical trends from trace elements in Rano Aroi covering the last 2000 years, compared to previous local geochemical/vegetational and regional climate reconstructions [8].

6.6 DISCUSSION

The Rano Aroi TE and REE records suggest several environmental changes in seven distinct phases around the mire for the past 2 millennian, while the biomaker records indicates 4 phases of environmetal changes in the last millemmian. This section will discuss the four phases of environmrtal changes around Rano Aroi mire as indicated by biomaker and charcoal records with the support of the TE and REE records.

Only three (coprostanol, levoglucosan and *n*-alkanes) out of four biomaker proxies analised in this recerch, were used alongside charcoal, for the reconstruction of human-environmrtal interaction. The PAH record was not suitable for fire reconstruction due to missing points and irregularities.

There is a correlation amongs mesured proxies in this reserch, which evidently indicate changes in the environment around Rano Aroi mire between 1463 and 1780 CE. These changes include fire occurrence and changes in vegetation, which correspond with the appearance of humans around the mire. Coprostanol concentration shows significant human impact in the lake system between 1470 and 1750 CE. During this time, Rano Aroi mire went through three major phases of environmental change. The first phase occurred Between 1463 and 1540 CE. This phase marked the first sign of human presence around the mire. Human presence was accompanied by fire occurrence and a shift in vegetation type, Charcoal record indicates a strong local fire occurrence and LHC data suggest forest recovery during the end of this phase. This record is consistent with the previous study of pollen record by Rull in 2019, indicating an expansion of palm forest between 1400 and 1500 CE [34]. Geochemical analysis indicates wet climate conditions around Rano Aroi mire during this phase, as suggested by increased lithological input alongside high level of K/Al between 1400 to 1520 CE. It is imperative to note that the appearance of humans around Rano Aroi mire between 1463 and 1540 CE does not signify the arrival date of Polynesians on the island, as other studies have suggest an earlier settlement date [35]. As a matter of fact, the Rapanui population may be as many as several thousands of people during this period, most of the islanders lived near the cultural center (near Rano Raraku crater) [2,36]. The second phase covers between 1536 to 1661 CE. This phase is characterized by a peak in Coprostanol flux, 3 times higher than that of the first phase, which is an indication of increased number of humans around the mire. LHC records suggest that deforestation between 1480 CE to 1600

CE, over the period of 100 years. Levoglucosan record indicates the presence of continuous fire, while charcoal record suggests that the fire occurrence during this period was low intensity fire, the combination of levoglucosan and charcoal record suggest that this phase had continuous fire with low intensity. The last ~ 80 years of this Phase also corresponds with intense drought as indicated by the high value of Fe/Al alongside K/Al and P/Al between 1520 to 1710 CE, the low water level during this drought period might be as a result of changes in climate or it might be caused by horticultural practice around the mire. The third phase of environmental change around Rano Aroi mire happened between 1665 and 1750, this phase is characterized by slight reduction in coprostanol flux which can be translated to fewer presence of humans, compared to the previous phase. However, the evidence of human activities was prominent, as deforestation had already happened between 1480 CE and 1600 CE. Levoglucosan and charcoal also show continuous fire during this phase, but the intensity was lower compared to previous phases. Most parts of this phase also fall within the drought period as seen in the TE and REE records. The fourth phase of environmental change occurred between 1750 CE and 1820 CE; this phase marked the lowest concentration of coprostanol compared to the three previous phases. The record shows human presence from 1750 CE to 1780 CE, after which the concentration reduces and then varies between $1000 \text{ ng cm}^{-2} \text{ yr}^{-1}$, which represents negligible presence of humans around the mire. Levoglucosan and charcoal record suggest fire activity during this phase. But it is possible the levoglucosan signal during this period is not from Rano Aroi mire. The fourth phase show the lowest activities of humans around the mire in comparison to the three previous phases.

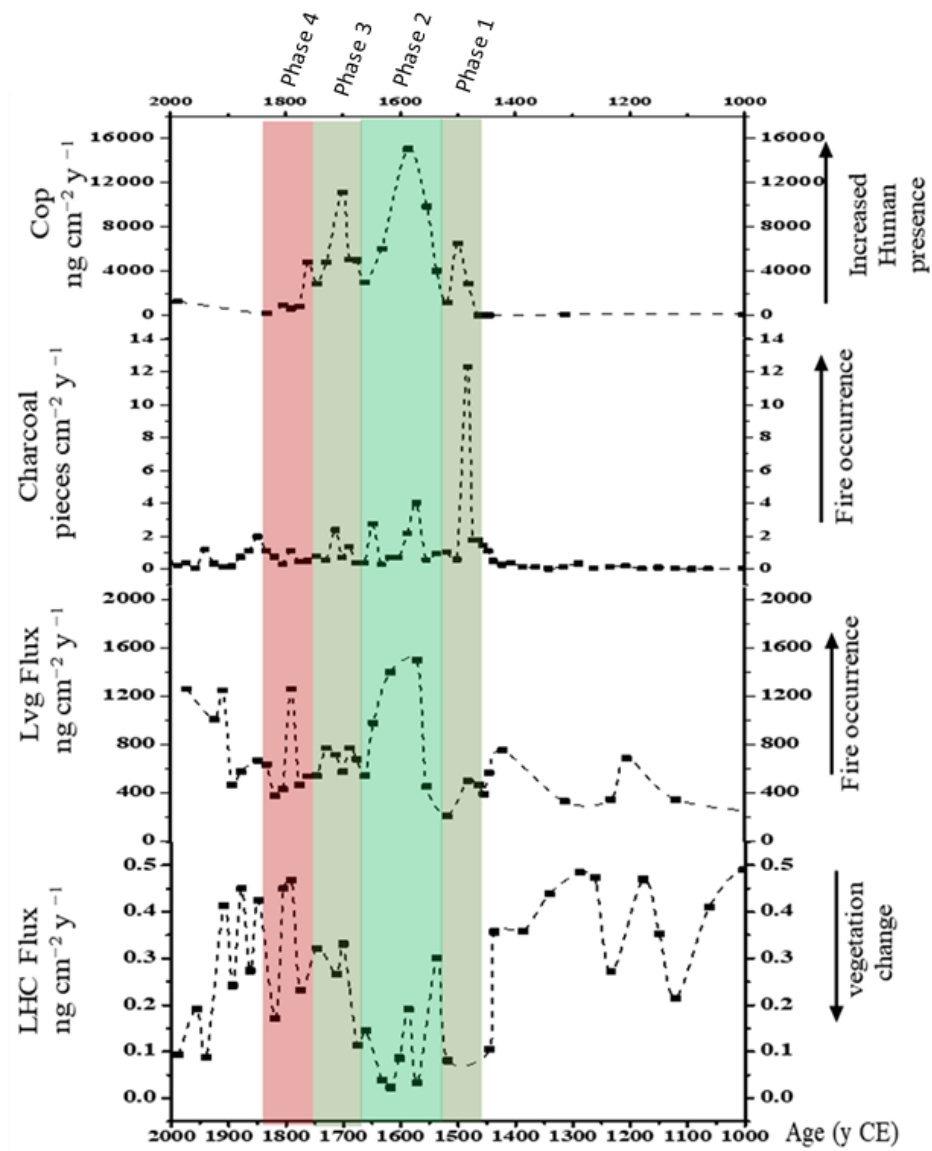


Figure 6.12 Biomarkers and charcoal flux from Rano Aroi sedimentary core, showing 4 phase of environmental changes

Conclusions:

The ongoing debate about the Rapa Nui environmental evolution is mainly caused by the occurrence of extended gaps in most sediment cores that have been studied till date, which prevents researchers to fully understand the cause-effect relationship between the natives of Rapa Nui and their immediate environment.

The Aim of this research was to archive a high-resolution palaeoecological data from Rano Raraku, Rano Aroi and Rano Kao in order to understand the palaeoecological evolution of Rapa Nui, such as colonization date and the possible cause-effect of the Rapa Nui deforestation. But sediment cores from Rano Raraku and Rano Kao could not be used for environmental reconstruction as Rano Kao core was unstratified and unconsolidated, and Rano Raraku core contain age inversion between 20 cm and 60 cm, which resulted in dating inconsistency. Just like many cores that have been retrieved from the island. However, Rano Aroi core was well dated with high resolution, which makes it suitable for climate reconstruction.

This is the first study that Implements a direct and specific human marker (coprostanol) to reconstruct human presence in Rapa Nui. The characterization of Rano Aroi through multiproxy approach (Biomarkers, and geochemical analysis) helps in understanding the complex interaction between the natives and their immediate environment.

The record reveals different environmental phases as discussed in chapter six. Coprostanol flux suggests significant human impact in the lake system between 1500 and 1750. The first Humans appearance around the lake between 1463 and 1540 CE did not have a significant impact on the environment, there was presence of fire and vegetation disturbance, this period also appears to be wet phase. This Rano Aroi record for this period, coincide consistent with the previous study of pollen record by Rull in 2019, indicating an expansion of palm forest between 1400 and 1500 CE [34].

The second phase 1536 to 1661 CE shows an increase in human presence, accompanied by frequent fire with low intensity, most of the deforestation or the removal of woody plants happened within this phase. The low intensity of fire during this period is an indication that fire was not used for the removal of woody plants around Rano Aroi mire. This is also evidenced in the charcoal concentration as it is significantly low. The mire experienced an intense drought during the last 80 years of this phase and the population/ human presence around the mire declined significantly.

Phase three 1665 and 1750 CE represents the third wave of human presence, The number of humans during this phase was significantly lower compared to the previous phase. LHC indicates reappearance of vegetation and some woody plants. This coincides with coincide consistent with the previous study of pollen record by Rull in 2021, indicating cultivation of plants and agricultural activities between 1670 and 1740 CE [20]. It is also important to indicate that this phase falls within the European contact which is dated to be 1722 CE.

Phase four 1750 CE and 1820 CE show the absence of humans around the mire.

Perspective and final remark

The data of the study mainly focuses on the environmental evolution around Rano Aroi mire; however, this record cannot be used to infer the deforestation rate and time across the island. colonization date of Rapa Nui cannot be inferred also, because the appearance of humans Rano Aroi mire does not represent the colonization date of Rapa Nui, several researchers have indicated that Rapa Nui was colonized before 1463 CE.

This is an indication that more multiproxy studies with the inclusion of fecal sterols need to be carried out on sediment cores with coherent age model, from Rano Raraku and Rano Kao. This can bring about the understanding of Rapa Nui colonization and deforestation dates.

Reference

- [1] M. Pérez-Rodríguez, O. Margalef, J.P. Corella, A. Saiz-Lopez, S. Pla-Rabes, S. Giralt, A.M. Cortizas, The role of climate: 71 ka of atmospheric mercury deposition in the southern hemisphere recorded by Rano Aroi Mire, Easter Island (Chile), *Geosci.* 8 (2018). <https://doi.org/10.3390/geosciences8100374>.
- [2] V. Rull, Natural and anthropogenic drivers of cultural change on Easter Island: Review and new insights, *Quat. Sci. Rev.* 150 (2016) 31–41. <https://doi.org/10.1016/j.quascirev.2016.08.015>.
- [3] V. Rull, N. Cañellas-Boltà, O. Margalef, A. Sáez, S. Pla-Rabes, S. Giralt, Late Holocene vegetation dynamics and deforestation in Rano Aroi: Implications for Easter Island's ecological and cultural history, *Quat. Sci. Rev.* 126 (2015) 219–226. <https://doi.org/10.1016/j.quascirev.2015.09.008>.
- [4] C. Herrera, E. Custodio, Conceptual hydrogeological model of volcanic Easter Island (Chile) after chemical and isotopic surveys, *Hydrogeol. J.* 16 (2008) 1329–1348. <https://doi.org/10.1007/s10040-008-0316-z>.
- [5] N. Cañellas-Boltà, V. Rull, A. Sáez, O. Margalef, R. Bao, S. Pla-Rabes, M. Blaauw, B. Valero-Garcés, S. Giralt, Vegetation changes and human settlement of Easter Island during the last millennia: A multiproxy study of the Lake Raraku sediments, *Quat. Sci. Rev.* 72 (2013) 36–48. <https://doi.org/10.1016/j.quascirev.2013.04.004>.
- [6] A.P. Grootjans, E. Adema, W. Bleuten, H. Joosten, Hydrological landscape settings of base-rich fen mires and fen meadows : An Hydrological landscape settings of base-rich fen mires and fen meadows : an overview, 2001 (2006). [https://doi.org/10.1658/1402-2001\(2006\)9](https://doi.org/10.1658/1402-2001(2006)9).
- [7] M. Blaauw, J.A. Christeny, Flexible paleoclimate age-depth models using an autoregressive gamma process, *Bayesian Anal.* 6 (2011) 457–474. <https://doi.org/10.1214/11-BA618>.
- [8] M. Roman, D.B. McWethy, N.M. Kehrwald, E.O. Erhenhi, A.E. Myrbo, J.M. Ramirez-Aliaga, A. Pauchard, C. Turetta, C. Barbante, M. Prebble, E. Argiriadis, D. Battistel, A multi-decadal geochemical record from Rano Aroi (Easter Island/Rapa Nui): Implications for the environment, climate and humans during the last two millennia, *Quat. Sci. Rev.* 268 (2021). <https://doi.org/10.1016/j.quascirev.2021.107115>.
- [9] W. Shotyk, Peat bog archives of atmospheric metal deposition: Geochemical evaluation of peat profiles, natural variations in metal concentrations, and metal enrichment factors, *Environ. Rev.* 4 (1996) 149–183. <https://doi.org/10.1139/a96-010>.
- [10] O. Margalef, A. Martínez Cortizas, M. Kylander, S. Pla-Rabes, N. Cañellas-Boltà, J.J. Pueyo, A. Sáez, B.L. Valero-Garcés, S. Giralt, Environmental processes in Rano Aroi (Easter Island) peat geochemistry forced by climate variability during the last 70kyr, *Palaeogeogr. Palaeoclimatol. Palaeoecol.* 414 (2014) 438–450. <https://doi.org/10.1016/j.palaeo.2014.09.025>.
- [11] D.S. Alibo, Y. Nozaki, Rare earth elements in seawater: Particle association, shale-normalization, and Ce oxidation, *Geochim. Cosmochim. Acta.* 63 (1999) 363–372. [https://doi.org/10.1016/S0016-7037\(98\)00279-8](https://doi.org/10.1016/S0016-7037(98)00279-8).
- [12] M. Zhang, Z. Liu, S. Xu, P. Sun, X. Hu, Element response to the ancient lake information and its evolution history of argillaceous source rocks in the Lucaogou Formation in Sangonghe area of southern margin of Junggar Basin, *J. Earth Sci.* 24 (2013) 987–996. <https://doi.org/10.1007/s12583-013-0392-4>.

- [13] O. Margalef, N. Cañellas-Boltà, S. Pla-Rabes, S. Giralt, J.J. Pueyo, H. Joosten, V. Rull, T. Buchaca, A. Hernández, B.L. Valero-Garcés, A. Moreno, A. Sáez, A 70,000 year multiproxy record of climatic and environmental change from Rano Aroi peatland (Easter Island), *Glob. Planet. Change*. 108 (2013) 72–84. <https://doi.org/10.1016/j.gloplacha.2013.05.016>.
- [14] P.D. Nunn, R. Hunter-Anderson, M.T. Carson, F. Thomas, S. Ulm, M.J. Rowland, Times of plenty, times of less: Last-millennium societal disruption in the Pacific Basin, *Hum. Ecol.* 35 (2007) 385–401. <https://doi.org/10.1007/s10745-006-9090-5>.
- [15] P.D.M. Hughes, D. Mauquoy, K.E. Barber, P.G. Langdon, Mire-development pathways and palaeoclimatic records from a full Holocene peat archive at Walton Moss, Cumbria, England, *Holocene*. 10 (2000) 465–479. <https://doi.org/10.1191/095968300675142023>.
- [16] N. Cañellas-Boltà, V. Rull, A. Sáez, O. Margalef, S. Pla-Rabes, B. Valero-Garcés, S. Giralt, Vegetation dynamics at Raraku Lake catchment (Easter Island) during the past 34,000years, *Palaeogeogr. Palaeoclimatol. Palaeoecol.* 446 (2016) 55–69. <https://doi.org/10.1016/j.palaeo.2016.01.019>.
- [17] J. Overpeck, J. Cole, El Niño/Southern Oscillation and changes in the zonal gradient of tropical Pacific sea surface temperature over the last 1.2 ka, *PAGES News*. 18 (2010) 32–34. <https://doi.org/10.22498/pages.18.1.32>.
- [18] H. Yan, L. Sun, Y. Wang, W. Huang, S. Qiu, C. Yang, A record of the Southern Oscillation Index for the past 2,000 years from precipitation proxies, *Nat. Geosci.* 4 (2011) 611–614. <https://doi.org/10.1038/ngeo1231>.
- [19] J.R. Flenley, S.M. King, Late Quaternary pollen records from Easter Island, *Nature*. 307 (1984) 47–50. <https://doi.org/10.1038/307047a0>.
- [20] V. Rull, Contributions of paleoecology to Easter Island’s prehistory: A thorough review, *Quat. Sci. Rev.* 252 (2021) 106751. <https://doi.org/10.1016/j.quascirev.2020.106751>.
- [21] K. Schitteck, S.T. Kock, A. Lücke, J. Hense, C. Ohlendorf, J.J. Kulemeyer, L.C. Lupo, F. Schäbitz, A high-altitude peatland record of environmental changes in the NW Argentine Andes (24 ° S) over the last 2100 years, *Clim. Past*. 12 (2016) 1165–1180. <https://doi.org/10.5194/cp-12-1165-2016>.
- [22] T. Ise, A.L. Dunn, S.C. Wofsy, P.R. Moorcroft, High sensitivity of peat decomposition to climate change through water-table feedback, *Nat. Geosci.* 1 (2008) 763–766. <https://doi.org/10.1038/ngeo331>.
- [23] J. Muller, M. Kylander, R.A.J. Wüst, D. Weiss, A. Martinez-Cortizas, A.N. LeGrande, T. Jennerjahn, H. Behling, W.T. Anderson, G. Jacobson, Possible evidence for wet Heinrich phases in tropical NE Australia: the Lynch’s Crater deposit, *Quat. Sci. Rev.* 27 (2008) 468–475. <https://doi.org/10.1016/j.quascirev.2007.11.006>.
- [24] D.A. Sear, M.S. Allen, J.D. Hassall, A.E. Maloney, P.G. Langdon, A.E. Morrison, A.C.G. Henderson, H. Mackay, I.W. Croudace, C. Clarke, J.P. Sachs, G. Macdonald, R.C. Chiverrell, M.J. Leng, L.M. Cisneros-Dozal, T. Fonville, E. Pearson, Erratum: Human settlement of East Polynesia earlier, incremental, and coincident with prolonged South Pacific drought (Proceedings of the National Academy of Sciences of the United States of America(2020)117(8813-8819)DOI: 10.1073/pnas.1920975117), *Proc. Natl. Acad. Sci. U. S. A.* 117 (2020) 13846. <https://doi.org/10.1073/pnas.2008788117>.
- [25] X. Wang, X. Huang, D. Sachse, W. Ding, J. Xue, Molecular paleoclimate reconstructions over the last 9 ka from a peat sequence in south China, *PLoS One*. 11 (2016).

<https://doi.org/10.1371/journal.pone.0160934>.

- [26] W.A. Out, A. Mieth, S. Pla-Rabés, M. Madella, S. Khamnueva-Wendt, C. Langan, S. Dreibrodt, S. Merseburger, H.R. Bork, Prehistoric pigment production on Rapa Nui (Easter Island), c. AD 1200–1650: New insights from Vaipú and Poike based on phytoliths, diatoms and 14C dating, *Holocene*. 31 (2021) 592–606. <https://doi.org/10.1177/0959683620981671>.
- [27] V. Rull, S. Giralt, PALEOECOLOGY OF EASTER ISLAND : NATURAL AND ANTHROPOGENIC DRIVERS OF ECOLOGICAL CHANGE EDITED BY : Valentí Rull and Santiago Giralt, 2018. <https://doi.org/10.3389/978-2-88945-562-1>.
- [28] L.G. Thompson, E. Mosley-Thompson, M.E. Davis, V.S. Zagorodnov, I.M. Howat, V.N. Mikhalenko, P.N. Lin, Annually resolved ice core records of tropical climate variability over the past ~1800 years, *Science* (80-.). 340 (2013) 945–950. <https://doi.org/10.1126/science.1234210>.
- [29] P.M. Medeiros, B.R.T. Simoneit, Analysis of sugars in environmental samples by gas chromatography-mass spectrometry, *J. Chromatogr. A*. 1141 (2007) 271–278. <https://doi.org/10.1016/j.chroma.2006.12.017>.
- [30] H. Yan, L. Sun, Y. Wang, W. Huang, S. Qiu, C. Yang, A record of the Southern Oscillation Index for the past 2,000 years from precipitation proxies, *Nat. Geosci.* 4 (2011) 611–614. <https://doi.org/10.1038/ngeo1231>.
- [31] J.P. Sachs, D. Sachse, R.H. Smittenberg, Z. Zhang, D.S. Battisti, S. Golubic, Southward movement of the Pacific intertropical convergence zone AD 1400-1850, *Nat. Geosci.* 2 (2009) 519–525. <https://doi.org/10.1038/ngeo554>.
- [32] M.C. Higley, J.L. Conroy, S. Schmitt, Last Millennium Meridional Shifts in Hydroclimate in the Central Tropical Pacific, *Paleoceanogr. Paleoclimatology*. 33 (2018) 354–366. <https://doi.org/10.1002/2017PA003233>.
- [33] H.J. Dumont, C. Cocquyt, M. Fontugne, M. Arnold, J.L. Reyss, J. Bloemendal, F. Oldfield, C.L.M. Steenbergen, H.J. Korthals, B.A. Zeeb, The end of moai quarrying and its effect on Lake Rano Raraku, Easter Island, *J. Paleolimnol.* 20 (1998) 409–422. <https://doi.org/10.1023/A:1008012720960>.
- [34] V. Rull, The deforestation of Easter Island, *Biol. Rev.* 95 (2020) 124–141. <https://doi.org/10.1111/brv.12556>.
- [35] C. Whitlock, *Tracking Environmental Change Using Lake Sediments*, (2001). <https://doi.org/10.1007/0-306-47668-1-5>.
- [36] G. Brandt, A. Merico, The slow demise of Easter Island: Insights from a modeling investigation, *Front. Ecol. Evol.* 3 (2015). <https://doi.org/10.3389/fevo.2015.00013>.

ABSTRACT

The fascinating history of the Easter Island's (Rapa Nui) environmental degradation and civilization collapse is a meaningful example of human-environment interaction and the management of natural resources. It has been a topic of interest to researchers since the Europeans firstly arrived on the island in 1722. Although several types of research have been carried out during the last decades, the history of Easter Island is still not well understood, as the existing knowledge has several interpretations due to lack of reliable information. The hypothesis that has dominates the island's narrative suggests that the deforestation and environmental degradation was a direct result of unsustainable anthropogenic land use, leading to civilization collapse and a significant reduction of the human population on the island. In this thesis, I reconstructed the past human environmental-interaction, changes in redox condition, and weathering process in Easter Island, through multiproxy analysis (biomarker, trace, and rare earth elements) in lake sediments to determine the causes of environmental degradation and the eventual civilization collapse of the Rapa Nui. Sediment cores from two lakes (Rano Aroi and Rano Raraku) were retrieved during an expedition in 2017. In these cores I analyzed a series of proxies using Gas chromatography-mass spectrometry (GC-MS) and inductively coupled plasma mass spectrometry (ICP-MS).

The elemental records indicate intense drought between ~1520 - 1710 CE. This drought is associated to a coheval vegetation change. The biomarker records mainly indicate that, during the period ~1510 - 1763 CE, the Rapanui people occupied more intensely the highlands rather than the coastal areas, where, in the former, the limited water resources were still available.

ABSTRACT (ITALIAN VERSION)

L'affascinante storia della degradazione ambientale e declino sociale avvenuta nell'Isola di Pasqua (Rapa Nui) rappresenta un significativo esempio di interazione uomo-ambiente e di utilizzo delle risorse naturali che ha interessato la comunità scientifica sin dai tempi in cui l'isola venne scoperta per la prima volta dagli Europei, nel 1722. Anche se diversi studi sono stati condotti negli ultimi decenni, i risultati ottenuti ha solo parzialmente descritto le dinamiche dei fenomeni ambientali associati alle attività antropiche. L'ipotesi che la deforestazione ed il degrado ambientale siano direttamente associati ad un utilizzo irresponsabile delle risorse naturali che ha causato a sua volta una riduzione della popolazione, ha dominato la narrativa degli ultimi decenni. In questa tesi, sono stati determinati dei proxy climatici ed ambientali quali composti organici e elementi in traccia in sedimenti lacustri. Questi proxy hanno permesso diversi processi geologici associati ad attività antropiche. In questo studio sono state indagate due carote di sedimento prelevate nei siti di Rano Aroi e Rano Raraku durante una spedizione condotta nel 2017. In queste carote sono stati analizzati i proxy mediante gascromatografia accoppiata a spettrometria di massa (GC-MS) e ICP-MS. Il record elementare ha indicato la presenza di sette distinte fasi cronologiche, demarcate da ben definite transizioni geochemiche che hanno evidenziato la presenza di un periodo siccitoso tra il 1520 ed il 1710 CE. Questo periodo secco è associato ad un cambiamento nel pattern di vegetazione dell'isola. Il record dei biomarcatori ha indicato che in questo periodo siccitoso, il popolo Rapa Nui ha occupato più intensamente la regione interna dell'isola in cui le limitate risorse idriche erano ancora limitate seppur disponibili, piuttosto che le aree costiere più sensibili al periodo secco. I risultati riportati in questa tesi suggeriscono che l'ipotesi della deforestazione e di un utilizzo insostenibile delle risorse dovrebbe essere rivista, valutando un ruolo determinante della componente climatica